THE UNIVERSITY OF CHICAGO

ORIGINS AND MIGRATION OF THE OCTAVOLATERAL EFFERENT AND FACIAL BRANCHIOMOTOR NEURONS IN ZEBRAFISH

A DISSERTATION SUBMITTED TO
THE FACULTY OF THE DIVISION OF THE BIOLOGICAL SCIENCES
AND THE PRITZKER SCHOOL OF MEDICINE
IN CANDIDACY FOR THE DEGREE OF
DOCTOR OF PHILOSOPHY

COMMITTEE ON DEVELOPMENT, REGENERATION, AND STEM CELL BIOLOGY

BY
ANASTASIA E. BEIRIGER

CHICAGO, ILLINOIS
JUNE 2020

For my family.

Table of Contents

List of Figures

ACKNOWLEDGMENTS

First and foremost, I would like to thank Vicky Prince for her mentorship. I could not have asked for a better thesis advisor, and I am deeply grateful to Vicky for supporting and challenging my ideas, as well as guiding my growth as a researcher. Thank you for trusting in my work ethic, and believing in my ability to carve out my own niche. I will miss our weekly meetings.

To my thesis committee - Sally Horne-Badovinac, Cliff Ragsdale, and Chip Ferguson - thank you for investing your time into my development as a scientist. Your questions and insights were essential in helping me refine the scope of this project over the years, and you helped me to find value in places where I did not always expect it. Thank you also to Robert Ho for insightful feedback during a great many lab meetings, and to the entire Ho Lab for making Culver Hall such a wonderful place to work. I am also immensely grateful to my MolBio cohort for their camaraderie during our tenure in grad school.

To past and present members of the Prince Lab: I owe Sarah Wanner a great debt for laying the foundation of my work in her pioneer neuron analyses, and for encouraging me to take ownership of my project from the very beginning. Also to Gökhan Dalgin, for countless conversations that helped me formulate my research goals (and career plans). I learned how to be a better scientist from both of you. Thank you to Anita Ng, too, for showing me how to make transgenic lines (and keep my fish happy). To Sweta Narayan, the other half of team hindbrain and a phenomenal mentee: your detailed approach and unending curiosity helped this study take shape. To Noor Singh, for her friendship, dedication, and hard work: you made coming into lab every day worthwhile, even on the days when nothing worked. To Manny Rocha, for many discussions in our RNAse Free Zone: thank you for reminding me that there are, in fact, benefits to cautious enthusiasm. To Vish and Elaine: the future is yours.

I would also like to thank Vytas Bindokas, Christine Labno, and Hari Shroff for their

expert advice on imaging methods, and Gordon Kindlmann for discussions on image processing. A special thank you to Teodora Szasz of the University of Chicago Research Computing Center, for many hours spent adapting and troubleshooting software on Midway. I would also like to acknowledge Clare Buckley for providing me with a Kaede construct, and Jon Clarke for helpful discussions on zebrafish neurogenesis. Additionally, thank you to Martha Bagnall, Ruth Anne Eatock, and Vicente Lumbreras for generously providing both advice and lab space for me to test single-neuron capture in the zebrafish.

I would be remiss not to also acknowledge the many individuals who helped me see this project through outside of the lab. First and foremost, to my husband Emre, for accompanying me on this grad school journey: your sense of humor and constant companionship brighten every single one of my days. Thank you for your unshakeable belief in my ability to do just about anything. To my Allen Hall family, who are a constant source of joy in my life: I would be much worse for wear without your love and friendship. Thank you to each and every one of you for helping me never to lose sight of the bigger picture. To my sister Alexandra, who was my first tutor and is my oldest friend: your drive, compassion, and curiosity are a constant source of inspiration to me. Thank you for being my biggest champion. And finally to my parents, Antonia and Gene, from whom I inherited my love of learning: thank you for encouraging my curiosity, supporting my interests, and always having my back. You have always believed in me, even in times when I did not believe in myself, and for that I am eternally grateful. I am so lucky to have you in my life.

ABSTRACT

The vertebrate hindbrain is a segmented structure that displays broad morphological and molecular conservation across vertebrate species. Efferent neurons within the hindbrain project to peripheral targets such as muscles and sensory organs, providing essential control over functions of the vertebrate head. Their axons project often along highly stereotyped routes, exiting the brainstem as the cranial nerves.

This thesis will focus on the development and migration of two types of cranial efferent neurons in zebrafish: the facial branchiomotor neurons (FBMNs) of the VIIth (facial) nerve and the octavolateral efferent neurons (OENs) of the VIIIth (vestibuloacoustic) nerve. Very little is known about the OENs, in part due to the lack of molecular markers which distinguish them from the better-characterized FBMNs. Two clusters of OENs have been identified in the hindbrain, consisting of the rostral efferent neurons (RENs) in r6 and the caudal efferent neurons (CENs) in r7. Both RENs and CENs migrate tangentially in a rostrocaudal manner along the same route as the FBMNs before clustering in r6 and r7. However, the segmental origins of the OENs, timing of their migration and axon outgrowth, and interactions with the FBMNs have not been characterized.

Here, I employ high-resolution imaging techniques to investigate early stages of OEN development. In Chapter 2, I use single-plane illumination microscopy (SPIM) to backtrack individual neurons to their birthplaces over 12 hours of developmental time. I demonstrate that OENs are born in the ventral neuroepithelium, close to the medial floor plate. RENs are born with the FBMNs in r4 between 11 and 16 hpf, but CENs have a more posterior origin within r5 and their births occur later, between 15 and 16 hpf. Both FBMNs and OENs generally remain ipsilateral to their mothers, while their sisters integrate contralaterally into the neuroepithelium. In Chapter 3, I use a new photoconvertible transgenic line to characterize the migration of the OENs and investigate their interactions with FBMNs. I find that OENs migrate alongside the FBMNs between 18 and 48 hpf. RENs rely on proper

function of *hoxb1a* to migrate caudally out of r4 and to innervate the otic vesicle, while CEN identity is independent of *hoxb1a*. Neither RENs nor CENs rely on the planar cell polarity molecule, Pk1b, to migrate, unlike the FBMNs which remain in r4 in its absence. In a series of cell ablation experiments, I also investigate interactions between the FBMNs, RENs, and CENs during their migration, determining that although FBMN/RENs make contact with CENs across the r4/5 border, CENs do not lead migration through r5.

These results uncover important differences between OEN and FBMN migration and suggest that the origins of OENs in the zebrafish may be more complex than previously assumed. Taken together, my findings offer a better understanding of this rarely studied cell type, and raise important questions about its relationship to other cranial efferent populations in the vertebrate brainstem.

CHAPTER 1

INTERTWINED ORIGINS: EFFERENT NEURONS OF THE FACIAL AND VESTIBULOACOUSTIC NERVES IN ZEBRAFISH

1.1 Abstract

The vertebrate hindbrain is a segmented structure that displays broad morphological and molecular conservation between species, and controls vital bodily processes such as respiration, circulation, and locomotion. This chapter starts with a discussion of neurulation in the zebrafish *Danio rerio* and examines how the neural tube is regionalized along the body axis. I explore how the segmental organization of the embryonic hindbrain prefigures segmental organization of adult neuroanatomical structures such as the cranial nerves. I then consider the role of the Hox code in establishing segmental identity in the hindbrain, paying special attention to the role of Hox paralogue group 1 genes in the development of hindbrain-derived efferent neurons contributing to the facial (VIIth) and vestibuloacoustic (VIIIth) cranial nerves. Finally, I examine what is known about the development and migration of these two efferent populations. This dissertation focuses on the intertwined origins and movements of these two cell types the facial branchiomotor neurons (FBMNs) of the VIIth nerve and the octavolateral efferent neurons (OENs) of the VIIIth nerve in the zebrafish.

1.2 Neurulation in the zebrafish, *Danio rerio*

The development of the central nervous system (CNS) is a complex process which commences with the formation of the three germ layers during gastrulation. The embryonic organizer - known as Spemann's organizer in amphibians, Hensen's node in chick, the node in mammals, and the embryonic shield in zebrafish - is a source of antagonists that inhibit

bone morphogenic protein (BMP) signaling in the surrounding tissue to induce the neural plate, a thickened region of ectoderm that will give rise to the future brain and spinal cord [10, 43]. First, however, the neural plate must undergo extensive morphological changes, transforming from a two-dimensional sheet into a bilaterally symmetric tube in a process known as neurulation.

In amniotes such as mouse and chick, neurulation occurs through two different morphogenic processes dependent on the axial level. Primary neurulation in the head and trunk begins with the organization of the neural plate into a columnar epithelium, which develops one or more hinge points that allow it to fold down the center, forming the neural groove. Upon closure, the neural groove becomes the central lumen of the neural tube. Secondary neurulation in the tail, on the other hand, begins with condensation of mesenchymal precursors into a neural rod that later undergoes cavitation at the midline [111].

In contrast, neurulation occurs similarly at all axial levels in the zebrafish (Figure 1.1) [86]. The neural plate starts as a multi-layered, epithelial-like structure which initially forms around 10 hpf. Rather than folding into a tube as in amniotes, the zebrafish neural plate thickens and sinks ventrally, driven by convergence movements to form the neural keel, a solid structure resembling the v-shaped hull of a ship. Fate-mapping experiments demonstrate that cells of the zebrafish neural plate retain their overall topology during keel formation, with medial cells internalizing to contribute to the ventral neural tube and lateral cells elongating towards the dorsal midline [147]. By 17 hpf, the neural keel has condensed into a cylindrical rod and separated from the overlying epidermis [37]. During these stages, cells within the keel and rod undergo organized divisions that help generate the mirror symmetry of the neural tube. Progenitors orient their mitotic spindles perpendicular to the main body axis of the animal, depositing one daughter on either side of the neural rod in a process known as crossing or C-division. Cumulatively, these highly stereotyped cell divisions rearrange the neuroectoderm into a pseudostratified epithelium with a distinct midline [38, 193, 222].

Eventually, cells on either side of the midline pull their apical endfeet apart, dividing the left and right sides of the nervous system and establishing the ventricle of the brain and spinal cord.

1.3 Patterning of the vertebrate hindbrain

Subsequent regionalization of the neural tube along the anteroposterior axis divides it into several domains: forebrain (prosencephalon), midbrain (mesencephalon), hindbrain (rhombencephalon), and spinal cord. The vertebrate hindbrain is a transiently segmented structure that displays morphological and molecular conservation between species and controls several higher-order behaviors such as respiration, circulation, and locomotion [76, 95, 135].

While much of what we know about hindbrain development is based on detailed studies in chick and mouse, the underlying mechanisms are typically conserved in zebrafish. During hindbrain development, the anteroposterior (AP) axis is patterned prior to and independently of the dorsoventral (DV) axis. Along the AP axis, signaling centers in the isthmus and pre-somitic mesoderm help pattern the neural tissue. The isthmus, a constriction in the neural tube at the midbrain-hindbrain boundary, organizes surrounding tissue through Fgf8 signaling and sets the anterior limit of homeodomain transcription factor, or Hox, expression in the hindbrain [94]. Posterior to the isthmus, nested domains of Hox gene expression prefigure the subdivision of the hindbrain into eight segments called rhombomeres (r) and influence the segmental organization of the cranial nerves and the cranial neural crest. At the posterior end of the hindbrain, the pre-somitic mesoderm acts as a source of retinoic acid (RA), which initiates rhombomere boundary formation and induces progressively more posterior segmental programs along a gradient of low-to-high RA signaling [50, 70, 77, 141]. This gradient is robustly regulated by the action of several RA-degradation enzymes within the Cyp26 class [1, 54, 89, 217]. Rhombomeres eventually become lineage-restricted, their boundaries reinforced by selective cell sorting that is driven in part by repulsive interactions

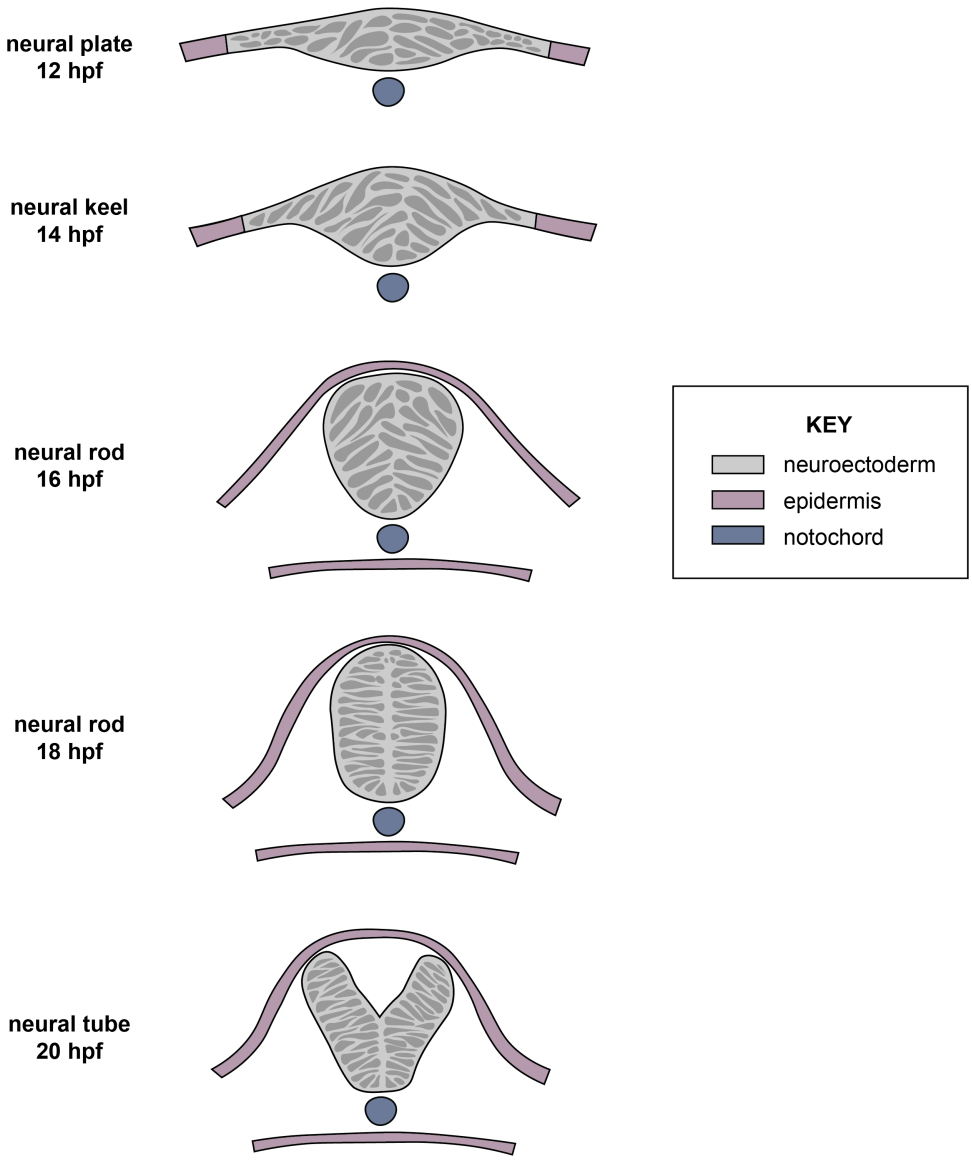

Figure 1.1: **Neurulation in the teleost hindbrain.**

between receptor/ligand pairs such as Ephs and Ephrins [39, 85, 112].

Dorsoventral (DV) patterning of the neural tube begins slightly later in development, starting with the induction of signaling centers in the roof and floor plates. In the dorsal neural tube, bone morphogenic protein (BMP) and Wnt signaling from the roof plate help pattern several classes of dorsal interneurons [35]. In mouse, Sonic Hedgehog (Shh) signaling from the underlying notochord ventralizes the closest neural progenitors and induces the differentiation of floor plate cells. A second period of Shh signaling from the floor plate itself is later needed to induce discrete neuronal fates in a concentration-dependent manner along the DV axis [57]. Progenitors directly adjacent to the floor plate become ventral interneurons, while those slightly further away from the Shh source differentiate into motor neurons. In zebrafish, which express multiple hedgehog genes during neurulation, mutation of shh alone is not sufficient to perturb motor neuron development [30, 177]. However, double knockdown of both *shh* and *tiggy-winkle hedgehog* (*twhh*) or physical removal of *hedgehog* sources such as the notochord and floor plate, does lead to a loss of motor neurons in the zebrafish [16, 19].

The motor neuron progenitor domain, which is located just dorsal to the floor plate, is demarcated by repression of Pax6 as well as upregulation of Nkx2.2 [44, 56, 153]. Post-mitotic ventral motor neurons and related sensory efferents will eventually express Islet1, a LIM-domain transcription factor, which helps distinguish them from more dorsal populations [58]. Many zebrafish transgenic lines, including several used in the following chapters, take advantage of Islet1 specificity to visualize these ventral efferent neuron populations [90, 120, 201].

While each axis of the neural tube is patterned independently, AP and DV signals must be integrated at the cellular level to achieve the full diversity of cell types in the CNS. In 1996, Lumsden and Krumlauf proposed that neurons are patterned along a kind of Cartesian grid of positional information, where local integration of AP and DV signals at each coordinate within the neural tube determines cell identity [114]. Indeed, numerous genetic

studies in mouse and chick have demonstrated that while DV signals broadly determine the class of a post-mitotic neuron, AP signals are needed to regulate its subtype identity [139, 24]. Exactly how these AP and DV signals are integrated is still an area of active research. The expression patterns of many Hox genes provide some insights: many of these AP patterning factors become progressively restricted along the DV axis in late neurulation, in a manner consistent with the Cartesian grid model [42, 68, 173]. Section 1.5 will discuss the integration of AP and DV patterning factors in the ventral part of hindbrain r4, a domain which gives rise to two neuronal subtypes central to this thesis: the facial branchiomotor neurons (FBMNs), which comprise the motor component of the VIIth (facial) nerve, and the octavolateral efferent neurons (OENs), which contribute sensory efferent projections to the VIIIth (vestibuloacoustic) nerve.

1.4 Segmental organization of the hindbrain

In the vertebrate hindbrain, early morphological segmentation into rhombomeres prefigures later neuroanatomical segmentation. The Hox code, which determines segmental identity across the vertebrate body plan, and is recruited within the hindbrain to pattern the rhombomeres. Vertebrate Hox genes are comprised of 13 paralogue groups, four of which are expressed within the hindbrain in overlapping domains. The combination of *hox* genes expressed within a given rhombomere confers its unique segmental identity and influences properties of the neurons that are specified within it.

Most tetrapods, including mouse, chick, and frog, have a total of 4 Hox clusters, reflecting ancestral genome duplications at the base of the vertebrate tree. Ray-finned fishes, however, have additional Hox clusters, as a consequence of a third genome duplication in the lineage leading to teleosts [160]. Although many of these duplicate genes were subsequently lost, some copies were preserved within the genome. Duplicate genes can be maintained in the genome as a consequence of subfunctionalization, where each copy takes on a part of the

ancestral gene's function, or neofunctionalization, in which one of the two copies takes on a novel role. In the zebrafish, these changes have resulted in a net total of 48 *hox* genes across 7 clusters, as compared with 39 in human and mouse [8]. 13 of these 48 genes are expressed in the zebrafish hindbrain, exhibiting patterns that are overall similar to those of their orthologues in amniotes [161]. Specific differences between zebrafish and amniote paralogue group 1 orthologues, which have a central role in hindbrain development, will be discussed in the Section 1.5.

Within each rhombomere, *Hox* genes help to establish specific populations of segmentally organized neurons, including reticulospinal interneurons and motor neurons. Several types of motor neurons exist, including somatomotor neurons, which control eye and tongue movements, and visceromotor neurons, which innervate glands and smooth muscles in a variety of organ systems [28]. The branchiomotor neurons (BMNs) are a subset of visceromotor neurons that are located in the hindbrain and project through stereotyped exit points to pharyngeal arch-derived muscles of the jaw, face, larynx, and pharynx. For the purposes of this thesis, I will focus on the role of *Hox* genes in patterning the branchiomotor neurons.

The broad organization of the cranial motor neurons is conserved in chick, mouse, and zebrafish, with a few notable differences. The locations of mature zebrafish BMNs are schematized in Figure 1.2. There are species-specific differences in the locations of mature BMNs, such as the facial branchiomotor neurons (FBMNs) of cranial nerve VII, which undergo a posterior migration into r6 in zebrafish and mouse, but remain more anterior in chick. However, the segmental origins of the BMNs are conserved such that each BMN subtype is under the control of orthologous *Hox* genes across species [28, 156, 139]. For example, projections of the r2/3-localized trigeminal BMNs are aberrantly located in *Hoxa2* mutants in mouse [71], while expression of *Hoxa2* in the anterior hindbrain of chick results in ectopic nV-like neurons [97]. Similarly, broad overexpression of *teashirt zinc finger homeobox 3b* (*tshz3b*), which normally represses paralogue group 1-4 gene expression in the zebrafish spinal cord,

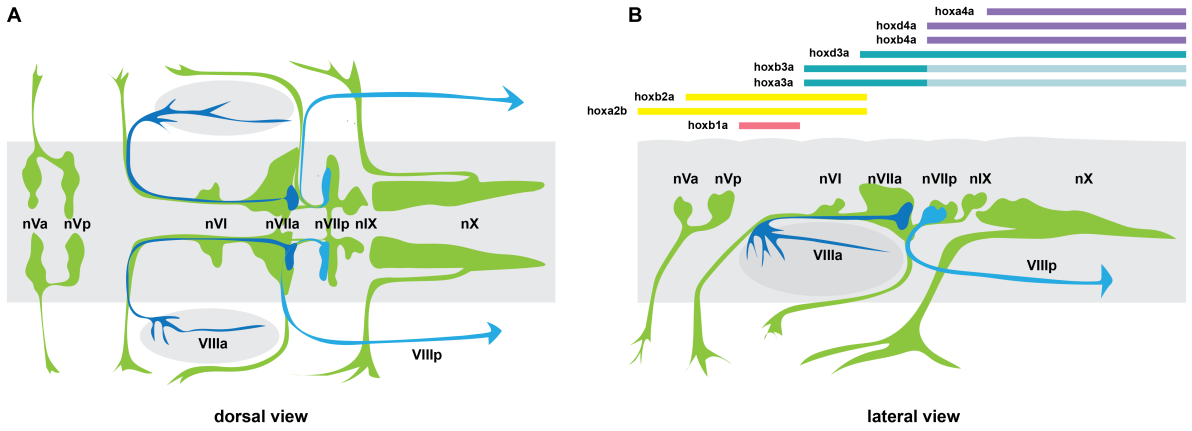

Figure 1.2: **Cranial nerves and *hox* gene expression in the zebrafish hindbrain.** (A) Dorsal view and (B) lateral view of cranial efferents in the zebrafish hindbrain. Cranial motor nuclei are shown in green, including FBMNs in r6 (nVIIa) and r7 (nVIIp). Sensory efferent nuclei, including rostral OENs (RENs) in r6 (VIIIa) and caudal OENs (CENs) in r7 (VIIIp), are shown in blue. Expression patterns of zebrafish *hox* genes are also depicted.

leads to downregulation of *hoxa2b* and mispatterning of nVI in r2 and r3 [55]. Roles of the paralogue group 3 genes appear to be similarly conserved in patterning the BMNs of r5 and r6. Knockout of *Hoxa3* in mouse leads to a truncation of the glossopharyngeal (nIX) BMNs and partial fusion with the vagal (nX) motor nucleus [215], while double knockdown of *Hoxa3/Hoxb3* causes ectopic expression of *Hoxb1* in r5 and r6 and transforms nIX into nVII-like neurons [69]. There is also some evidence for mis-routing of IX and X projections in *Hoxa3* knockdown chick embryos [216], although these experiments have yet to be replicated in zebrafish. Roles of the *Hox* paralogue group 1 genes in patterning the r4-derived FBMNs are also broadly conserved and will be discussed in detail in Section 1.5.

1.5 Intertwined origins: motor neurons and sensory efferents

1.5.1 Role of Hox paralogue group 1 genes in early hindbrain patterning

The mouse *Hox* paralogue group 1 genes, *Hoxa1* and *Hoxb1*, are the first to be expressed in the hindbrain [170, 189]. Their function is necessary to regulate a host of factors that are

necessary for proper hindbrain development, including Krox20, Fgf3 and Fgf8, Val/MafB, and several other Hox proteins [151]. The diversity of these interactions depends in large part on the cooperation of Hox proteins with other homeodomain transcription factors, such as Pbx and Meis, with which they can form heterodimeric complexes [159, 204, 36, 212]. In zebrafish, elimination of the early-acting Pbx proteins Lzr/Pbx4 and Pbx2 prevents the *Hox* paralogue group 1 genes from carrying out their function, resulting in a complete loss of hindbrain segmentation [213]. As such, *Hoxa1* and *Hoxb1* are thought to act at the top of the gene regulatory network (GRN) that controls hindbrain patterning and segmentation along the AP axis.

In mouse, *Hoxa1* is expressed broadly and transiently within the hindbrain, while *Hoxb1* exhibits two distinct phases of expression. The *Hoxb1* sequence is flanked by two RA-responsive regulatory elements (RAREs), one upstream and one downstream of the coding region, which appear to promote early and late expression patterns, respectively [143, 144]. Initially, *Hoxb1* is expressed broadly in the posterior half of the embryo, up to the level of r3/4 of the hindbrain [123]. Later, *Hoxb1* is restricted to r4 through auto- and cross-regulatory interactions which include repression by Krox20 and the Hox group 3 genes [191, 214, 219]. As would be expected, mouse *Hoxa1-/-;Hoxb1-/-* double mutants fail to specify r4 and exhibit general disorganization of the hindbrain [170, 189].

1.5.2 Role of Hoxb1 in FBMN and CVA development in amniotes

Hoxb1 is instrumental in patterning multiple cell types in mouse and chick. In mouse, Hoxb1 impacts development of the hyoid crest and its derivatives and specifies several neuronal subtypes in r4, including interneurons, motor neurons, and sensory efferents [13, 68]. In *Hoxb1* knockout mice, both the facial branchiomotor neurons (FBMNs) of the VIIth cranial nerve and the contralateral vestibuloacoustic efferents (CVA) of the VIIIth nerve are incorrectly specified and display atypical migration [78, 190]. Moreover, ectopic retroviral expression of

Hoxb1 in r2 of chick embryos causes FBMNs to be specified in the place of the trigeminal motor neurons [18].

Numerous studies in chick and mouse suggest that FBMNs and CVAs arise from a single progenitor population in ventral r4 [25, 154, 197, 185]. However, Hoxb1 helps specify different neuronal populations along the entire DV extent of r4 [68], raising questions about how it can induce distinct neuronal fates along the DV axis. Some insight can be gained from the regulatory region of *Phox2b*. Hoxb1 directly activates transcription of *Phox2b*, which regulates the cell cycle exit of neuronal precursors and is sufficient to initiate the differentiation of Islet1-positive efferent neurons, including the FBMNs and CVAs [48, 57, 154, 197].

In their study of the *Phox2b* regulatory region, Samad and colleagues identify a highly-conserved proximal enhancer that contains binding sites for Hox-Pbx (PH) and Prep/Meis (P/M). These conserved sites promote the formation of a Hox-Pbx-Prep ternary complex, which in turn drives high levels of Phox2b in r4 [173]. The DV patterning factor Nkx2.2 also contributes to regulation of the *Phox2b* enhancer, likely through the sequestration of a putative repressor [173]. The coordination of multiple transcription factors—here, the AP-restricted Hoxb1 and DV-restricted Nkx2.2—at a single enhancer region drives specification of certain AP-defined neuronal subtypes (FBMNs/CVAs) from a given DV-restricted class of neuron (ventral efferents). In this way, a discrete progenitor domain is defined at a specific coordinate within the neural tube, as would be predicted by Lumsden and Krumlauf's "Cartesian grid" model.

1.5.3 Subfunctionalization of hoxb1a and hoxb1b in zebrafish

As a result of genome duplication in the lineages leading to teleosts, there are two orthologues of amniote *Hoxb1* in zebrafish: *hoxb1a* and *hoxb1b*. Careful analysis of their cis-regulatory elements points to function-shuffling among the paralogue group 1 genes [127]. Specifically, loss of the 5' auto-regulatory sequence in *hoxb1b* and loss of the 3' RARE in *hoxb1a* are

hypothesized to have driven sub-functionalization of these duplicates from an ancestral paralogue group 1 gene [126]. Gene expression data and morpholino knockdown experiments both support this hypothesis: similar to mouse *Hoxa1*, zebrafish *hoxb1b* is expressed broadly in the hindbrain up to r3/4 and appears to be necessary for the activation of *hoxb1a* in r4. Meanwhile, zebrafish *hoxb1a* shares the r4-specific expression of mouse *Hoxb1*, as well as its role in motor neuron development [126, 127]. Consequently, in *hoxb1a* knockdown embryos, FBMNs lose their capacity for posterior migration and remain clustered in r4. Moreover, *hoxb1a* appears to be necessary for projection of octavolateral efferent neurons (OLe/OENs) across the ear [126]. However, the role of *hoxb1a* in OEN development cannot be fully understood without further characterization of cell migration and axon morphology in *hoxb1a*-deficient animals. Like amniote CVAs, zebrafish OENs contribute efferent innervation to the ear, but they also project to the lateral line, a sensory system in aquatic organisms that will be discussed in more detail in Section 1.7.

1.6 Current models of neuronal migration

After their specification in ventral r4, FBMNs in mouse and zebrafish migrate away from their rhombomere of origin to more caudal destinations within hindbrain, while CVAs in chick move contralaterally across the midline [28]. In general, the migration of neurons away from their birthplaces is essential to the proper wiring of the brain and peripheral nervous system, allowing cells with vastly different origins to come within proximity and form functional connections [87]. These connections depend on two separate but molecularly related processes: axon guidance, which lies largely outside the focus of this thesis, and neuronal migration, which will be discussed extensively in Chapter 3. Neuronal migration can be classified as either radial or tangential. During radial migration, neurons move away from their birthplaces in the sub-ventricular and ventricular zones towards the outer pial surface of the brain. Most radially migrating neurons move singly, often crawling along the

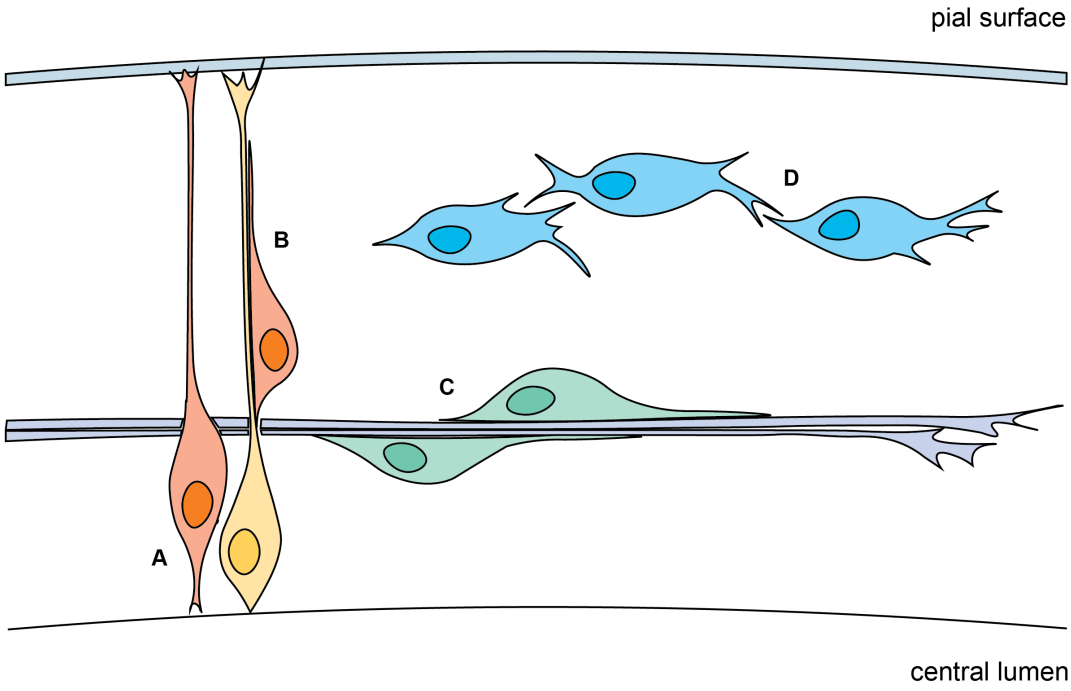

Figure 1.3: **Different modes of neuronal migration.** Radial migration occurs either (A) independently of glial fibers or (B) using glial fibers as a scaffold. Tangential migration can occur (C) along an existing axon tract or (D) through heterotypic contacts with other migrating neurons.

length of a glial fiber towards the pial surface. Interactions between neurons and glia depend on the action of adhesion molecules, with integrins and their ligands often keeping the two in contact during migration [49, 66, 73, 121]. However, other types of radial migration occur independently of glial fibers, with neurons extending a leading process towards the pial surface and translocating their soma behind it [138].

In contrast to radial migration, tangential migration occurs parallel to the ventricular surface of the brain and perpendicular to glial fibers. Tangentially migrating neurons often migrate in tandem, forming homotypic contacts with each other or heterotypic contacts with other structures [122]. In the mouse, olfactory bulb interneurons undergo long, chain-like tangential migrations that rely on homotypic cell-cell contacts mediated by NCAM, or neural cell adhesion molecule [218, 145]. These neurons then collectively follow attractive and

repulsive cues from prokineticin 2 (PK2) and Slit, respectively, which guide their movement into the olfactory bulb [124, 140].

Tangential migration can also occur through heterotypic interactions, such as the contact of migrating neurons with a preexisting axon tract or extracellular matrix components such as those found in the basement membrane. However, the signals which control these types of interactions and dictate the overall direction of tangentially migrating cell populations have been fairly elusive. Some chemoattractants have been identified in the tangential migration of certain neuronal populations, such as Sdf1/Cxcr4, which direct the migration of cortical interneurons and also appear to impact the caudal movements of FBMNs and OENs [41, 175, 198]. Chemorepellants such as Sema3A/Nrp1-2 also act on cortical interneurons to prevent them from mis-migrating, while Nrp1 uses an alternate ligand (VEGF164) in guidance of tangentially migrating FBMNs [122, 179]. A more in-depth discussion about the heterotypic interactions formed by FBMNs and OENs/CVAs will follow in the sections below.

1.7 Development and migration of the octavolateral efferent neurons (OENs)

In amniotes such as chick and mouse, CVAs innervate structures of the inner ear, helping to regulate both vestibular and auditory functions. In anamniotes such as fish and amphibians, efferent innervation is shared between the ear and the lateral line, with single efferent neurons often projecting to both sensory systems [17, 21, 132, 88]. Often referred to collectively as the octavolateralis system, the ear and lateral line are derived from adjacent epithelial placodes during development, display common afferent projection patterns, and contain the same type of mechanosensory hair cells [20, 183, 27]. The ability of zebrafish to regenerate mechanosensory hair cells of the lateral line has made them an unlikely but powerful model for research on repair of cochlear hair cells in mammals [15, 96, 102, 210].

The lateral line system (LLS) gives anamniote vertebrates, such as fish and aquatic am-

phibians, the ability to detect disruptions in the aquatic environment. This sense of distant touch is essential for a host of behaviors, including prey detection, predator avoidance, schooling activities, and orientation within the surrounding environment. While the anatomy of the LLS varies between species, its fundamental sensory organ, the neuromast, is conserved. Neuromasts contain an inner core of mechanosensory hair cells which are surrounded by non-sensory support cells that secrete a flexible, jellylike cupula. Each hair cell has a ciliated apical surface that detects displacement of the cupula and transmits this information to the CNS via basally located nerve termini [74].

Every neuromast is supplied by a pair of afferent neurons which terminate directly on the mechanosensory hair cells [60]. Patterns of efferent innervation are less consistent. Between species, the number of efferent neurons can vary widely, but low ratios between efferents and their target hair cells are common, from 1:400 in the small-spotted catshark (*Scyliorhinus canicula*) to 1:900 in the European eel (*Anguilla anguilla*) [131, 130]. As a result, single efferent neurons often branch extensively, projecting to multiple end organs [17, 21, 132, 88]. Despite the extensive arborization of individual efferents, however, it is uncommon for every hair cell within an individual animal to receive efferent innervation [20]. Collectively, these findings imply a relatively crude level of efferent control over signal processing in the octavolateralis system.

Initial experiments performed in *S. canicular* suggested that the octavolateral efferent neurons (OENs) were part of a single nucleus within the hindbrain [130]. However, subsequent work established the presence of three separate nuclei, including two within the hindbrain and one more anteriorly within the forebrain, in zebrafish, goldfish, and catfish [17, 21, 132]. This anatomical division may reflect differences in function. The two rhombencephalic OENs are cholinergic and likely to perform an inhibitory role [131], whereas the single diencephalic nucleus is likely catecholaminergic and may perform an excitatory role [23]. Consequently, it has been hypothesized that the rhombencephalic nuclei may repress

activation of the LLS based on activity of the Mauthner neuron, while the diencephalic nucleus may sensitize the LLS to increase responsiveness when visual inputs are low [23].

Very little is known about OEN development and migration in fish, although some hints can be gained through comparison to the CVAs in amniotes. As previously mentioned, CVAs are specified by Hoxb1 in amniotes, as are the FBMNs [18, 79, 190]. Backlabeling experiments in mouse support a common embryological origin for CVAs and FBMNs, although the two cell populations later separate from each other through differential migration [64]. Their axons also take divergent routes in the periphery, with CVAs branching away from the VIIth cranial nerve to join up with the VIIIth nerve tract [184]. The molecular basis of this divergence is unclear, although the GATA family of transcription factors does appear to play a role in proper migration and axon routing of CVAs [18, 98]. In contrast, rhombencephalic OENs and FBMNs appear to migrate along similar pathways within the zebrafish hindbrain, although their projection patterns diverge in the periphery [132, 175]. It is unknown whether rhombencephalic OENs and FBMNs share a developmental origin. Zebrafish morphants deficient for *hoxb1a* show defects in OEN projection across the ear, but additional work is needed to determine whether this reflects a defect in axon routing in the periphery or a more general mis-specification of OENs [126]. In Chapter 2, I present live imaging data to visualize the birthplaces of rhombencephalic OENs and FBMNs, tracking them back through time to map ventral efferent progenitors in space and time. Chapter 3 expands on this work with an exploration of *Hox* gene function in OEN development.

1.8 Development and migration of the facial branchiomotor neurons (FBMNs)

Facial branchiomotor neurons (FBMNs) form the motor neuron component of the VIIth cranial nerve, which innervates second pharyngeal arch derivatives including muscles of the face and jaw. In humans, disorders of the VIIth cranial nerve, such as Bell's palsy and

Moebius syndrome, are typified by weakness or paralysis of the facial muscles [75, 195], and several cases of hereditary congenital facial palsy and paralysis have been linked to mutation of HOXB1 [171, 202, 205]. As discussed above, FBMNs are specified in the ventral half of r4 and require function of Hoxb1 for proper development and migration.

After their birth in r4, FBMNs in humans, mice, and zebrafish migrate caudally through the hindbrain [28]. In chick, FBMNs are largely stationary, although transplantation of mouse r5 into the chick hindbrain causes the neurons to undergo ectopic migration and demonstrates that they are competent to move in the presence of a conducive signaling environment [188]. Interestingly, recent work has shown that FBMNs are functionally resilient to positional shifts of their soma and exhibit wild-type firing patterns in the presence of genetic perturbations that stall their migration in r4 [125]. These results may partly explain the variation in FBMN soma placement between species. Additionally, they suggest that other aspects of FBMN development, such as proper axon routing into the second pharyngeal arch, are more essential to their functional role.

Nevertheless, the extensive migration of the FBMNs in many model organisms makes them an ideal system for studying mechanisms of cell motility. In zebrafish, FBMNs migrate in two parallel streams, translocating their cell bodies caudally while leaving a trailing axon near the r4 exit point [28]. The first stage of this migration is a chain-like tangential migration into r6/7. After reaching r6/7, FBMNs turn laterally away from the midline and undergo a short radial migration towards the dorsal roof plate, using glial fibers as a scaffold (Beiriger, unpublished data). Subsequently, FBMNs cluster into two bilateral nuclei: a major nucleus located in r6 and a minor nucleus in r7.

The tangential migration of FBMNs is characterized by both homotypic and heterotypic interactions. Late-born FBMNs appear to physically contact the trailing axon of early-born FBMNs as they migrate behind them through the neuroepithelium. In zebrafish, ablation of either the first FBMN or its trailing axon causes severe migration defects, indicating that 1)

the first FBMN to migrate acts as a pioneer and 2) homotypic contacts between the pioneer and its followers are necessary for proper caudal movement [208]. These contacts appear to rely on cell-autonomous function of the neural cadherin Cdh2 [165], although depletion of Cdh2 in the environment also disrupts neuroepithelial cohesion and causes mis-migration of FBMNs into the midline [187, 208]. Heterotypic interactions also facilitate FBMN migration. FBMNs move slowly in r4, but lateral views of the hindbrain demonstrate that their velocity increases once they make contact with the basement membrane at the r4/5 boundary [80]. Later, as they near the r5/6 boundary, migrating FBMNs are overtaken by the rapidly extending growth cone of the medial longitudinal fasciculus (MLF), a major axon tract within the hindbrain. Cutting the MLF before it enters the hindbrain causes FBMNs to stall in r5, demonstrating that they use the MLF as yet another substrate to complete their tangential migration into r6/7 [208].

Numerous studies have also revealed that planar cell polarity (PCP) signaling influences the caudal and lateral migrations of the FBMNs. Several PCP molecules, including Frizzled3a, Celsr2, Vangl2 and Scrib, are required non-cell autonomously in the neuroepithelium for proper migration of the FBMNs [209]. Additionally, function of Pk1b, a downstream effector of Hoxb1a, is required by migrating FBMNs [120, 169]. While Pk1b may act partly through the classical PCP pathway, it is also required cell-autonomously within FBMNs to localize RE1-silencing transcription factor (Rest) to the nucleus in a farnesylation-dependent manner [119]. Rest is a transcriptional repressor which regulates a host of neuron-specific terminal maturation genes, and it is required to keep FBMNs in an immature state during their migration [110]. Interestingly, transplantation of PCP-deficient cells into wild-type fish reveals that zebrafish FBMNs can migrate collectively, as wild-type FBMNs are able to pull mutant FBMNs with them into r6/7 [207]. Whether OENs can also migrate collectively with the FBMNs is unknown. I explore this question, as well as the role of Pk1b in each cell type, in Chapter 3.

1.9 Thesis overview

In this chapter, I have described two populations of efferent neurons the facial branchiomotor neurons (FBMNs) and contralateral vestibuloacoustic efferents (CVAs) which appear to have common origins within the vertebrate hindbrain. Although a wealth of research in multiple animal models has contributed to our understanding of FBMN development and migration, comparatively little is known about the CVAs and their zebrafish equivalents, the octavolateral efferent neurons (OENs). The optical clarity of the zebrafish embryo, coupled with the ease of making transgenic lines and the availability of advanced light microscope techniques, makes it a particularly appealing model for the investigation of neuronal specification and migration. Accordingly, this thesis aims to broaden our understanding of OENs and their relationship to the FBMNs by focusing on the origins and movements of both cell types in the zebrafish hindbrain.

In Chapter 2, I describe the birthplaces of OENs and FBMNs, and explore how differences in the spatial origins of these two cell types may contribute to their acquisition of different cell fates. My work in this chapter relies on the interpretation of single-plane illumination microscopy (SPIM) data, and as such will contain a discussion of the technical challenges inherent in manually reconstructing individual cell lineages. Chapter 3 contains an extensive description of OEN migration, as well as an exploration of the molecular differences underlying their migration and that of the FBMNs. I employ a single-cell labeling technique to identify and describe early morphological markers of OEN fate, such as characteristic lateral projections in r5. Additionally, I test whether interactions between OENs and FBMNs are necessary for the migration of either cell type into r6/7.

Taken together, my findings indicate that FBMNs are specified in ventral r4 alongside the rostral population of OENs, while caudal OENs are born more posteriorly within ventral r5. As such, rostral OENs rely on function of Hoxb1a in r4 for proper specification and migration: in hoxb1a morphants, rostral OENs are unable to migrate posteriorly and do

not properly innervate the ear. Caudal OENs, however, are unaffected in the absence of hoxb1a. Both cell types arise largely from divisions at the apical midline which give rise to one Islet1(+) efferent neuron and one Islet1(-) daughter cell.

Once specified within r4, FBMNs and rostral OENs migrate together towards the posterior hindbrain, making contact with caudal OENs as they cross the r4/5 border. Ablation experiments reveal that these contacts are not necessary for the migration of either cell type, but may instead represent one of many heterotypic interactions made by the FBMNs during their migration into r6/7. Caudal OENs do not appear to need a pioneer neuron to complete their migration into r7, and both OEN populations can move independently of Pk1b. Taken together, these results indicate that there are significant differences in the mechanisms that FBMNs and OENs use to migrate, and suggest that the two cell populations are unable to migrate collectively despite their intertwined origins within the neural tube. I will discuss these findings in more depth and offer ideas for future investigations in Chapter 4.

CHAPTER 2

SCOPING OUT THE ORIGINS OF CRANIAL EFFERENTS: A LIGHTSHEET-BASED APPROACH

2.1 Abstract

In the zebrafish, efferent neurons of the facial (VIIth) and vestibuloacoustic (VIIIth) cranial nerves migrate posteriorly through the hindbrain between 18 and 48 hours post-fertilization (hpf). These efferent populations are thought to arise from the same progenitor domain within the ventral half of rhombomere (r)4 before migrating into r6 and r7. While numerous genetic experiments have helped piece together the spatial origins of these cell types, limitations in traditional microscopy techniques have made direct visualization of their birthplaces difficult. Here, I use single-plane illumination microscopy (SPIM) to perform cell lineage reconstruction on these two efferent populations in live zebrafish. I demonstrate that facial branchiomotor neurons (FBMNs) and octavolateral efferent neurons (OENs) have more than one segmental origin, suggesting a possible mechanism for cell type specification. FBMNs are born continuously throughout neural plate, keel, and rod stages, while OENs are born over a shorter temporal window within the neural rod. The vast majority of sister cells do not appear to develop into cranial efferents, but rather integrate back into the neuroepithelium and occasionally migrate dorsally from their birthplaces. Finally, I find that both FBMNs and OENs are overwhelmingly born at the nascent apical plane of the neuroepithelium through crossing, or c-divisions.

2.2 Introduction

Over the course of embryonic development, neurons are born from stem and progenitor cells in a process known as neurogenesis. Our current understanding of the cellular mechanisms

underlying neurogenesis comes largely from the study of cortex development in the mouse [11, 149, 59, 181, 61]. The cortex begins as a single-layered epithelium, which undergoes multiple rounds of cell proliferation and migration to transform into a complex, six-layered structure. In the ventricular zone, apical progenitors (APs) divide near the central lumen of the neural tube, while subapical progenitors (SAPs) undergo mitosis a short distance away but remain anchored to the lumen with an apical process. As the cortex thickens, basal progenitors (BPs) in the sub-ventricular zone also give rise to a variety of renewing and non-renewing cell types. The polarity of these progenitors influences the diversity of cell types to which they give rise: their placement along the apicobasal axis exposes them to different types of signals [182, 107], while asymmetric distribution of subcellular components within them influences the fate of their daughter cells. Broadly speaking, inheritance of the apical membrane generally correlates with differentiation into a neuron [105], while inheritance of the basal process typically directs daughters to replenish the progenitor pool [200, 180, 104].

The cellular basis of neurogenesis in the zebrafish is less well understood. The zebrafish neuroepithelium is less polarized than its mammalian counterpart, and may be better described as epithelial-like than fully epithelial during plate, keel, and rod stages [194, 37, 93, 26, 222]. Much of what is known about zebrafish neurogenesis comes from late neural rod stages and beyond, after a clear apical plane has been established at the midline. In the zebrafish hindbrain, symmetric divisions appear to predominate after 15 hpf: one set of lineage analyses found that 84% of neurons were born from symmetric divisions, and 68% of lineages contained no asymmetric divisions [115]. Instead, symmetric divisions give rise either to two new progenitors or two neurons, with a clear bias towards differentiation of both daughters into neurons after the second round of division [115]. When asymmetric divisions do occur in the zebrafish hindbrain and spinal cord, mechanisms of cell fate specification more closely resemble those in mouse. Apical daughters are more likely to become neurons, and inheritance of Par3, a marker of apical membranes, correlates strongly with

neuronal fate [5]. While most neurons appear to be born apically in the zebrafish, small populations of non-apical progenitors (NAPs) are present at all axial levels. NAPs tend to divide symmetrically, often giving rise to two neurons [128].

Notably, Notch-Delta signaling, which has been implicated broadly in cell fate decisions during neurogenesis, is also linked to renewal of the progenitor pool in zebrafish [81, 106]. The Notch-DeltaD complex is internalized into cells via endosomes expressing the protein Sara, or Smad anchor for receptor activation. Asymmetric partitioning of Sara endosomes between daughters correlates with asymmetric fate in a wide variety of stem cell lineages: daughters receiving more endosomes tend to replenish the progenitor pool, while those receiving fewer endosomes differentiate [40, 136]. Accordingly, during zebrafish neurogenesis, Sara endosomes containing DeltaD ligand and membranes containing the apical protein Par3 segregate into opposite daughter cells [106]. Daughters that received Par3 were more likely to differentiate. These patterns held true for all stages examined, including neural plate and rod stages [106]. The asymmetric partitioning of Sara endosomes is therefore one of the few known mechanisms of cell fate selection in progenitors that divide prior to the establishment of an apical midline in the zebrafish neural tube.

These studies have gone a long way towards improving our understanding of zebrafish neurogenesis. However, they have mostly identified mechanisms governing cell fate specification at the population level. Here, I investigate the neurogenesis of a specific sub-population of neurons: namely, the cranial efferents that migrate through r4 and r5 of the zebrafish hindbrain [28]. Though the vast majority of cranial efferents are motor neurons, sensory efferent neurons also send their axons into the periphery while their soma lie within the central nervous system (CNS). In zebrafish, the octavolateral efferent neurons (OENs) of the VIIIth nerve, which provide sensory efferent innervation to the ear and lateral line, migrate alongside the more numerous facial branchiomotor neurons (FBMNs) of the VIIth nerve [175]. Comparatively little is known about thier specification. In chick and mouse, genetic

studies have provided evidence that both of these efferent populations arise from the same progenitor population in r4 [154, 197, 18, 173], but these studies have not been replicated in zebrafish. Furthermore, an investigation of the developmental mechanisms that might influence selection of FBMN versus OEN fate has not been performed in any species.

However, linking mechanisms of neurogenesis to specific neuronal fates presents significant technical challenges, since several hours often elapse between the birth of a neuron and its expression of cell type specific markers. Here, I leverage the availability of non-specific cell labels in the zebrafish, such as nuclear localized EGFP [155], to reconstruct the lineages of FBMNs and OENs prior to the expression of cell type specific markers such as Islet1 [90, 201, 120]. I employ a dual transgenic method to track FBMNs and OENs back through time to their birthplaces in the developing hindbrain. This study relies on the temporal resolution and gentle illumination of single-plane illumination microscopy (SPIM) [174] to capture rapid cell divisions over nearly 12 hours of developmental time. To date, other optical lineage reconstructions in zebrafish have relied on standard confocal imaging, which does not offer the temporal resolution required for a study of this nature [3, 187].

Using this technique, I am able to reconstruct the birthplaces of over 30 FBMNs and OENs. I find that the vast majority of divisions give rise to only one cranial efferent neuron. I describe behavioral differences between cranial efferents and their sister cells: the latter tend to remain in their rhombomere of origin and often move dorsally, in marked contrast to the tangential migration of FBMNs and OENs along the ventral surface of the hindbrain. Furthermore, I identify two distinct spatiotemporal origins for my neurons of interest. The majority of tracked neurons arose in r4, as would be expected of the FBMNs. These r4-derived efferents were born continuously between 11 and 16 hpf, with a clear peak in the rate of births during early neural keel stages. A smaller number of tracked neurons were born in r5 between 14 and 15 hpf. These r5-derived efferents display morphology characteristic of caudal OENs and will be discussed in greater depth in Chapter 3. Finally, I demonstrate

that FBMNs and OENs are predominantly born at the nascent apical plane of the neural keel through midline crossing, or c-divisions. The vast majority of them arise from the more basally located daughter, remaining ipsilateral to their mother cell while their sisters cross the midline contralaterally. Despite these large-scale trends, I am limited in my ability to draw conclusions about more rare events, such as the contribution of non-apical progenitors to the FBMN and OEN efferent populations. These limitations reflect technical challenges inherent to this technique, which will be discussed in in Section 2.4 and Chapter 4.

2.3 Results

2.3.1 Double transgenic line permits reconstruction of cell lineages prior to expression of cell type specific markers

To date, analyses of FBMN development and migration in the zebrafish have relied on the availability of transgenic lines that specifically label cranial efferent neuron populations [90, 201, 120]. However, these lines are limited by the spatiotemporal expression patterns of Islet1 in post-mitotic motor neurons. Generally, *islet1* transgene expression is not visible until 17 hpf, when FBMN migration is already underway. Therefore, I crossed *Tg(en.crest1-hsp70l:mRFP)* [120], which uses the *zCREST1* enhancer element from the *islet1* locus to drive RFP in cranial efferent neurons, with the pan-nuclear *Tg(h2afva:h2afva-GFP)* [155], which labels chromatin through fusion of GFP with histone 2B. Using this double transgenic line, I am able to identify FBMNs and OENs by mRFP expression after 18 hpf and use their nuclear GFP expression to track them back through time to their birthplaces. I will refer to these two efferent cell types collectively as Isl1(+) neurons for most of this chapter.

To visualize the births of Isl1(+) neurons, I used single-plane illumination microscopy (SPIM) to image zebrafish embryos for 12 hours, starting from early neural plate stages (12 hpf) and continuing until Isl1(+) neurons could be seen migrating posteriorly through

the hindbrain (Figure 2.1, Panels A-B). Embryos were positioned with anterior towards the top of the microscope chamber and the developing hindbrain oriented towards the detection objective (Figure 2.1, Panels C-D). To position embryos correctly within the field of view, I used the anterior tip of the notochord as a morphological landmark since it lies ventral to r4 and is visible prior to most other structures, including the otic vesicles. Embryos were imaged every 90 seconds to catch rapid cell movements, particularly at the start of the time-lapse when medial cells of the neural plate are internalizing rapidly to form the neural keel.

To reconstruct cell lineages, I backtracked individual Isl1(+) neurons to their birthplaces. Sisters of Isl1(+) neurons were also tracked. A plot of all cell tracks from a single embryo is shown in Figure 2.2, Panel A, with each lineage indicated by a different color. Selected lineages from this data set are shown in 2.2, Panel B, including one lineage producing two Isl1(+) neurons (purple tracks) and one producing both an Isl1(+) neuron and an Isl1(-) sister cell (yellow tracks). Across all lineages, only a small minority of divisions produced two Isl1(+) neurons (n=2/29), while the rest resulted in the birth of one Isl1(+) neuron and one Isl1(-) sister cell (n=27/29) (2.2, Panel C). However, this study is limited in that it uses only one marker of neural fate and cannot reveal whether Isl1(-) sister cells do or do not become neurons. Therefore, these divisions may not be asymmetrically fated in the classical sense of giving rise to one neuron and one neural progenitor.

In total, 64 cells were tracked across three embryos. Of these, 37 were Isl1(+) neurons and 27 were Isl1(-) sister cells (Figure 2.2, Panel D). For 6 of the 37 Isl1(+) neurons, I was unable to find a birthplace. These 6 tracks are likely to be false negatives, reflecting the technical challenges inherent in tracking a cell population that migrates close to the opaque, light-scattering zebrafish yolk (see Box 1). Tracks for an additional 8 cells were discarded due to low confidence in cell position at two or more time points (Box 1). However, 31 Isl1(+) neurons were successfully tracked back to a division. All other tracked cells were

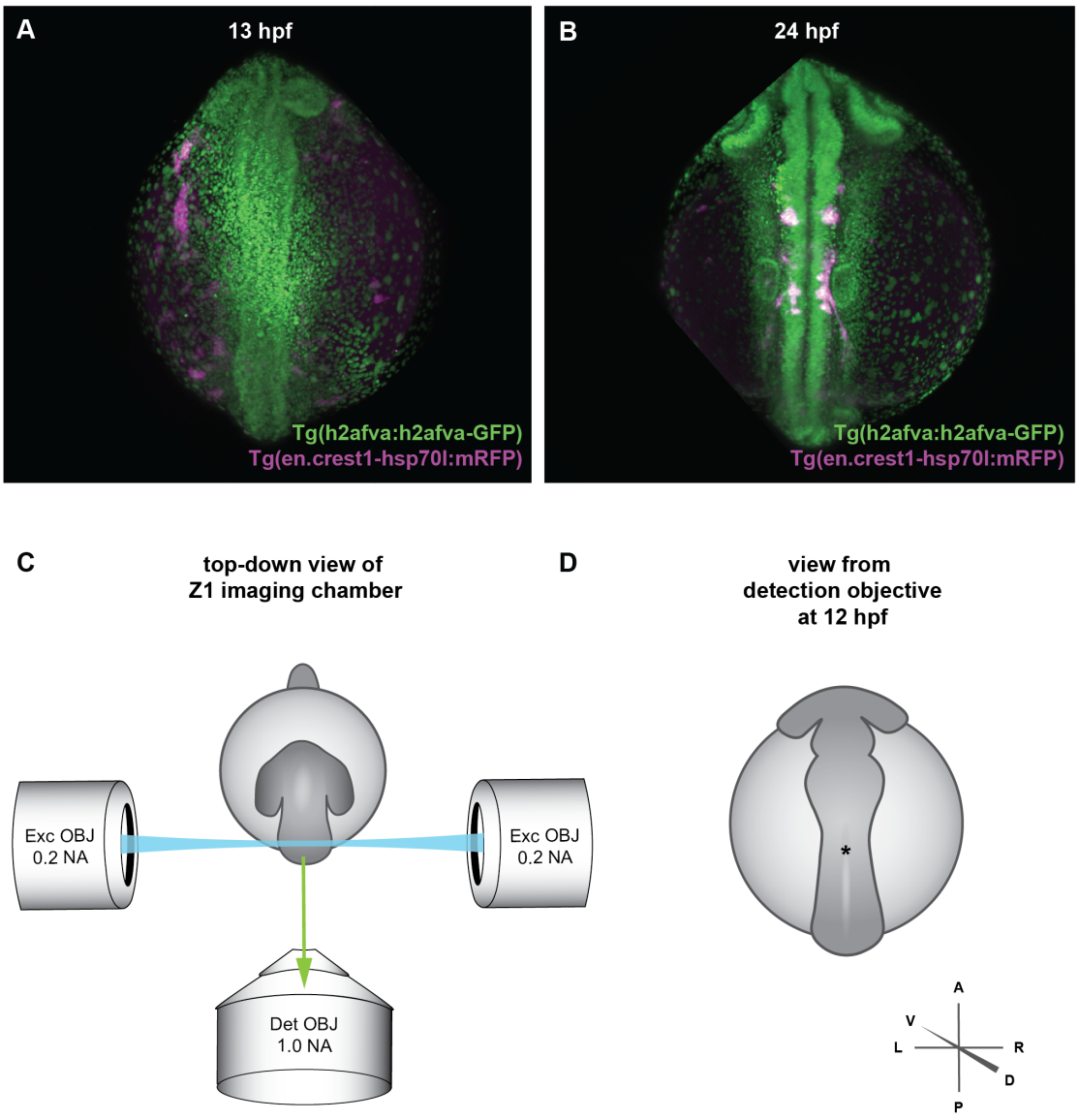

Figure 2.1: **Orientation of zebrafish embryo within the imaging chamber.** (A) Movie still of double transgenic embryo at 13 hpf and (B) 24 hpf. (C) Schematic showing 90 degree orientation of detection objective relative to illumination objectives. Size of embryo is exaggerated for clarity. (D) View of 13 hpf embryo from detection objective. Specimens mounted with midbrain-hindbrain boundary oriented towards the objective to account for movement of ROI during axis elongation.

Isl(-) sister cells (n=27).

2.3.2 Behaviors of Isl1(-) sister cells differ significantly from Isl1(+) efferent neurons

By following the movements of both Isl1(+) neurons and Isl1(-) sisters, I identified several behavioral differences evident in their trajectories. All Isl1(+) neurons behave as expected from previously published studies, undergoing a tangential migration through r4 and r5 near the ventral surface of the brain [80]. As they reach r6, some Isl1(+) neurons begin to move dorsally, possibly in preparation for their radial migration in r6 and r7. However, the total distance covered by Isl1(+) neurons along the dorsoventral axis is no more than 20 μm (Figure 2.3, Panels A and B), reflecting use of the ventral basement membrane as a substrate by migrating FBMNs and, ostensibly, OENs [80].

Isl1(-) sister cells, on the other hand, tend to behave as would be expected of neuroepithelial progenitors. Rather than undergoing a directed tangential migration, the vast majority of them remain in their rhombomere of origin. They tend to move freely along the dorsoventral axis, covering a much wider range of depths within the neuroepithelium and often moving up to 40 μm dorsally from their birthplaces (Figure 2.3, Panels A' and B', arrowheads). Moreover, the nuclei of several Isl1(-) sisters move cyclically along the nascent apicobasal axis, as would be expected of neural progenitors [192]. However, the vast majority of Isl1(-) sisters do not divide again within the duration of the time-lapse (n=26/27, data not shown).

2.3.3 Isl1(+) neurons have two distinct segmental origins

Examining the anteroposterior and dorsoventral spread of Isl1(+) birthplaces reveals distinct trends in the segmental origins of these neurons. Along the dorsoventral axis, all Isl1(+) neurons are born within a 20 μm-wide section of the ventral neuroepithelium, a short distance away from the floor plate. The spread of Isl1(+) birthplaces along the anteroposterior axis

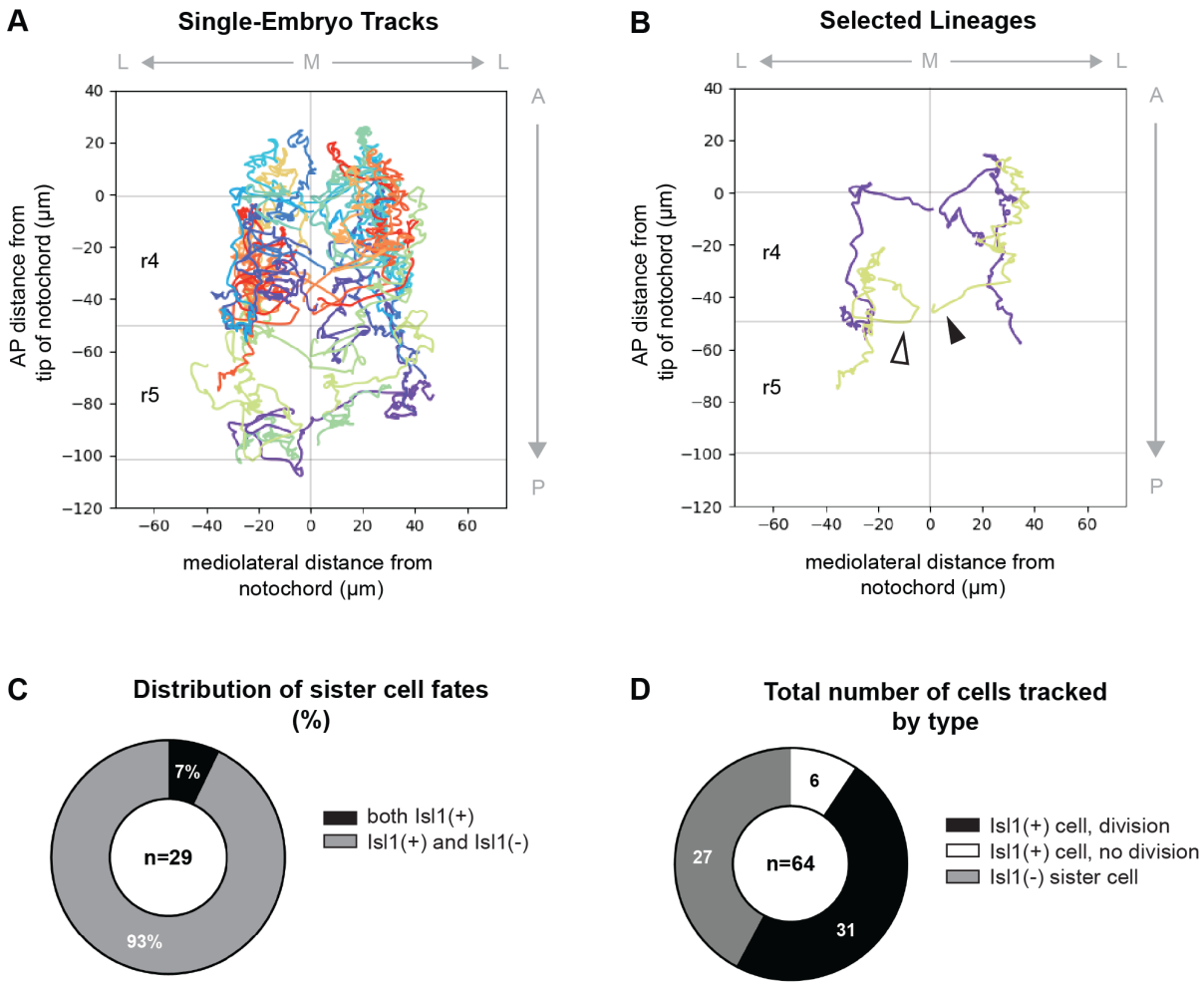

Figure 2.2: **Overview of tracked cells.** (A) Anatomical plot of cell tracks from a single embryo, including both Isl1(+) neurons and sister cells. Tracks are color-coded by lineage. Cell positions are registered to the anterior tip of the notochord (origin) at every time point. Mediolateral and anteroposterior axes are indicated. Presumptive rhombomere boundaries are denoted by grey lines. (B) Selected tracks isolated from A. Purple tracks indicate two Isl1(+) neurons arising from a single mother cell. Yellow tracks indicate one Isl1(+) neuron (open arrowhead) and one Isl1(-) sister cell (closed arrowhead) arising from a single mother cell. (C) Distribution of cell fates resulting from 29 progenitor divisions. Symmetric (n=2/29) indicates division giving rise to two Isl1(+) neurons, while asymmetric (n=27/29) indicates division giving rise to one Isl1(+) neuron and one Isl1(-) neuroepithelial cell. (D) Plot indicating number of cells tracked by type.

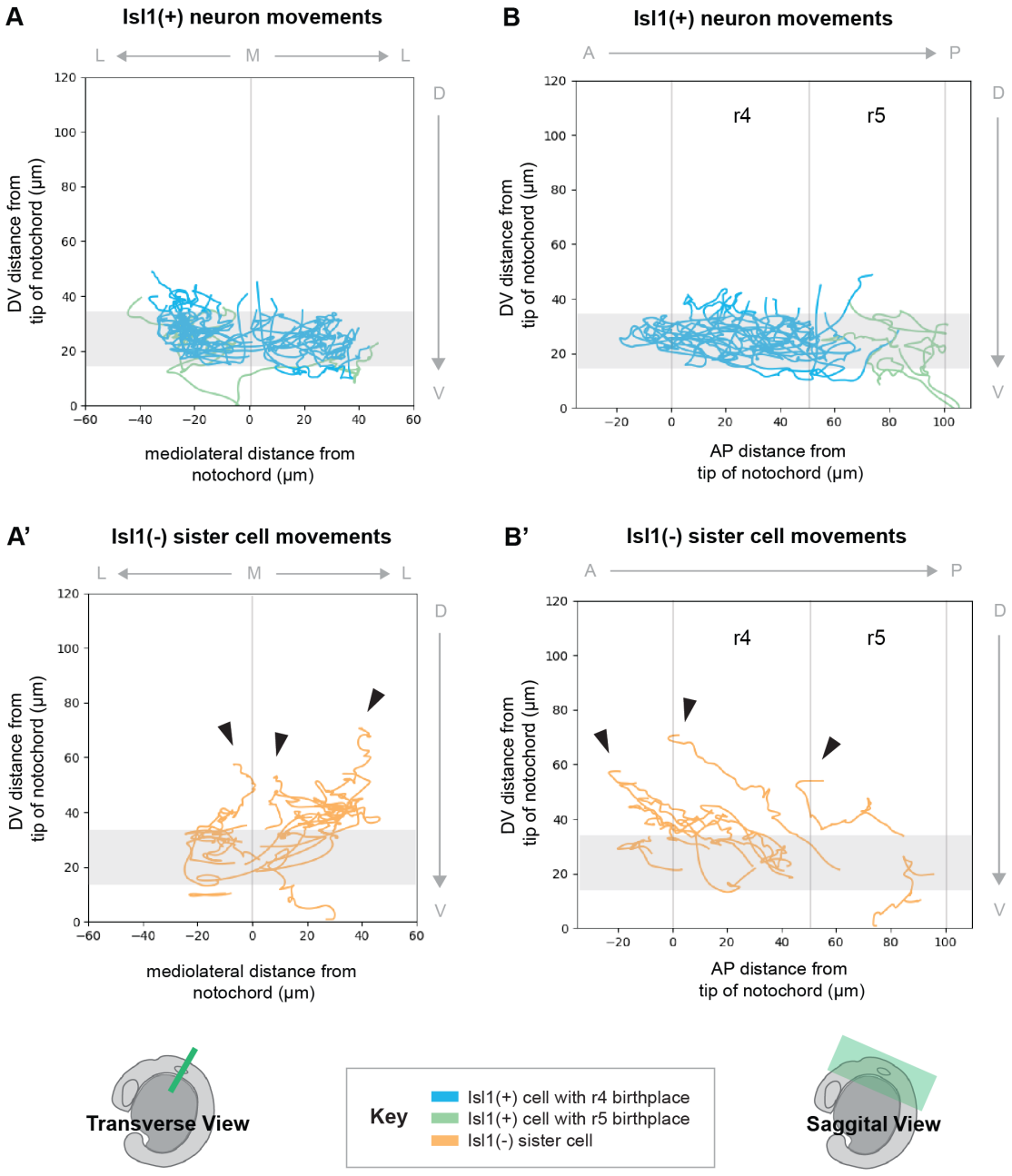

Figure 2.3: **Dorsoventral (DV) plots of cell movements by fate.** (A-A') Transverse (X, Z) and (B-B') sagittal (Y, Z) plots of cell tracks from a single embryo. Tracks of Isl1(+) neurons (blue, green) are separated from tracks of Isl1(-) sister cells (orange). Isl1(+) neurons migrate within a narrow domain of around 20 μm, shown in grey, in the ventral neural tube. Tracks of Isl1(-) sister cells (orange) encompass a wider area along the DV axis, with many Isl1(-) cells appearing to migrate dorsally (arrowheads) by the end of the time-lapse.

is much wider. The vast majority of Isl1(+) neurons are born in r4 (n=26/31), as would be expected of the *hoxb1a*-specified FBMNs [126, 127]. However, a second, more posteriorly-derived population of Isl1(+) neurons is also evident (n=5/31). Plotting the birth times of these two Isl1(+) populations reveals that the r5-derived population is born later, and within a narrower temporal window, than the r4-derived population. Specifically, all r5-derived Isl1(+) neurons tracked across three embryos arose between 14-15 hpf, while r4-derived Isl1(+) neurons were born continuously between 10-16 hpf. Based on lateral projections characterized more fully in Chapter 3, I suspect that the r5-derived Isl1(+) neurons are caudal OENs.

2.3.4 Isl1(+) neurons are predominantly born near the developing midline

Through these backtracking experiments, I also identified two types of Isl1(+) birthplaces along the mediolateral axis. The first occurs medially, near the nascent apical plane (arrowheads, Figure 2.5, Panel A) while the second occurs close to the ventral surface of the brain (insets, Figure 2.5, Panel A'). Of these two types of divisions, medial ones predominate (n=26/29). In almost all medial divisions, the mother cell orients its mitotic spindle perpendicular to the presumptive midline, depositing one daughter on either side of the brain as would be expected from a midline-crossing, or c-division (n=25/26) [194].

Visualizing the birthplaces of Isl1(+) neurons and their Isl1(-) sisters relative to the nascent apical plane reveals interesting trends in cell fate. In particular, Isl1(+) neurons tend to arise from the more lateral daughter, while Isl1(-) sisters are born more medially (Figure 2.5, Panel C). Accordingly, the daughter that stays ipsilateral to the mother tends to become an Isl1(+) neuron, whereas the daughter that crosses contralaterally is generally Isl1(-) (n=19/27; Figure 2.5, Panel E).

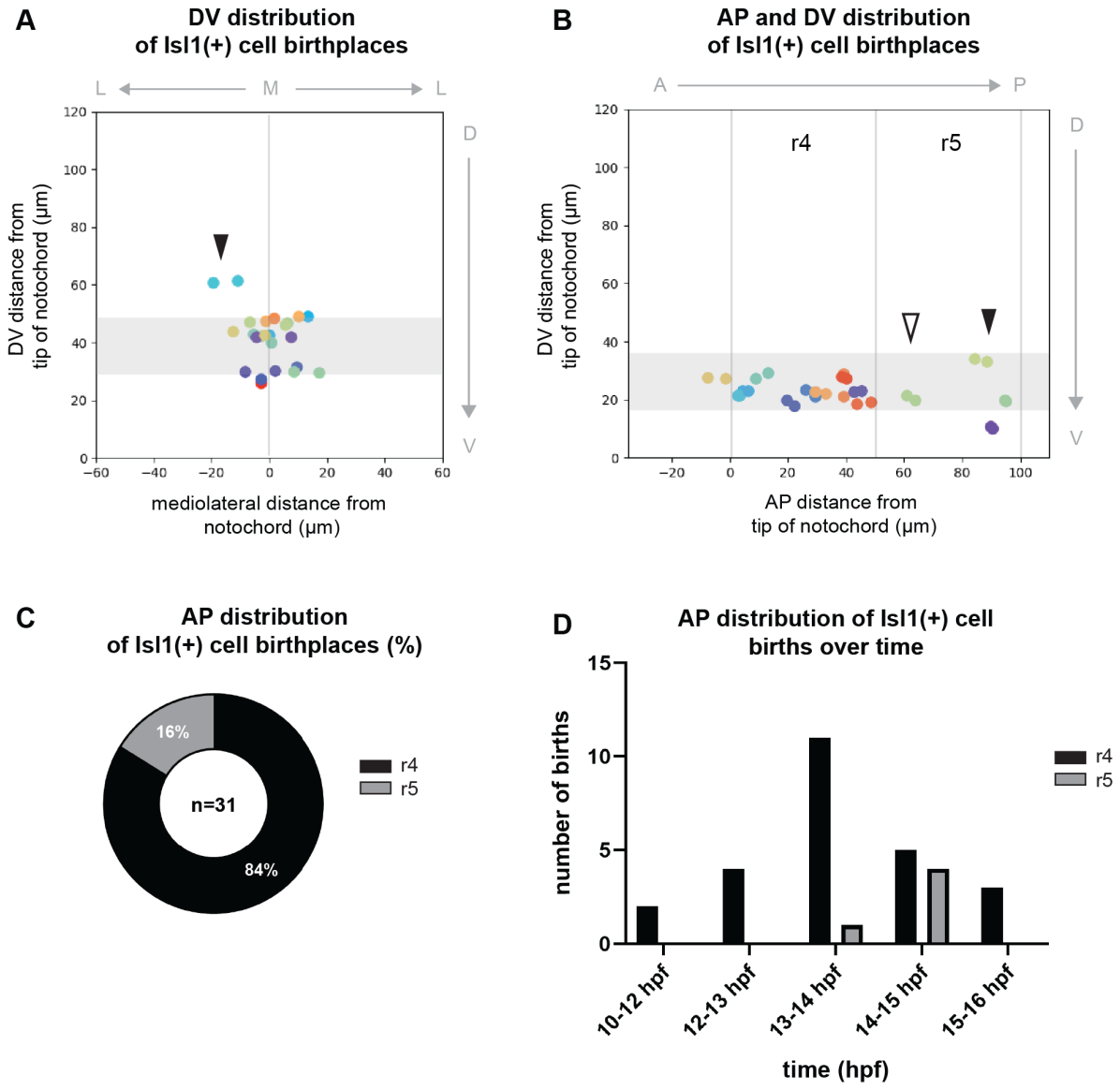

Figure 2.4: **Distinct clusters of Isl1(+) birthplaces exist along the AP, but not DV, axis.** (A) Transverse (X, Z) plot of birthplaces from a single embryo. Sister cells are color-coded by lineage and their location at the first time point after division is plotted. 90% of Isl1(+) neurons are born in a 20 μm stripe of tissue in the ventral neural tube. Outlier is indicated with an arrowhead. (B) Sagittal (Y, Z) plot of birthplaces from a different embryo. Clustering of birthplaces in DV and AP is evident. Several Isl1(+) neurons (arrowheads) are born in a distinct posterior zone lying outside of r4. (C) Distribution of all Isl1(+) birthplaces along the AP axis (r4=26/31; r5=5/31). (D) Plot of birthplace location over time. Isl1(+) neurons arising in r5 are born over a narrower temporal window than those arising in r4.

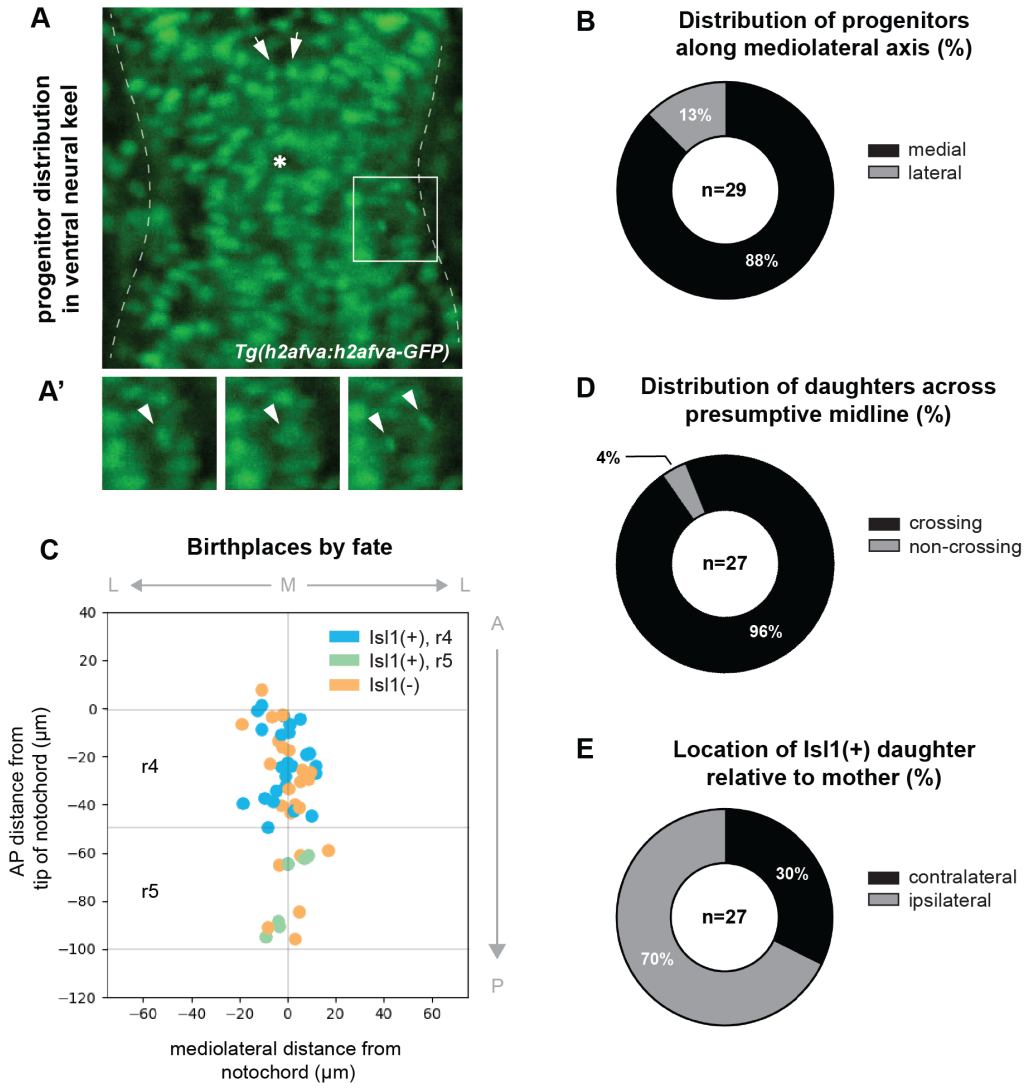

Figure 2.5: **Isl1(+) neurons are overwhelmingly born from divisions near the presumptive midline.**(A) Single z-slice from a 13 hpf embryo showing GFP expression in cell nuclei. One cell division at the presumptive midline (arrowheads) is visible. Location of anterior tip of notochord is indicated (asterisk). Boxed area indicates a second division near the pial surface of the brain. (A') Three time points from inset area show division of laterally located progenitor (arrowheads). (B) Distribution of birthplaces along the mediolateral axis. Isl1(+) neurons are generally born from medially located progenitors (n=26/29). (C) Anatomical plot of all cell birthplaces. Isl1(+) neurons (blue, r4; green, r5) tend to arise from the lateral daughter, whereas Isl1(-) sisters (orange) are born more medially. (D) Mothers of Isl1(+) neurons almost always send one daughter to either side of the brain (crossing, n=28/29). (E) Plot of asymmetrically fated divisions. The Isl1(+) daughter stays ipsilateral to its mother in a majority of cases (n=19/27).

2.4 Discussion

This study provides the first comprehensive description of FBMN and OEN birthplaces. To date, only one other study has performed backtracking on FBMNs; however, its focus was on the mediolateral distribution of migratory FBMNs in Cdh2-deficient embryos rather than their birthplaces [187]. Here, I use backtracking to identify spatiotemporal relationships between FBMN and OEN progenitors and provide a glimpse into the cellular basis of neurogenesis in cranial efferents. All tracked neurons were born between neural plate and rod stages, with the highest proportion of Isl1(+) births occurring between 13 and 14 hpf. Isl1(+) neurons arise from a discrete 20 μm domain in the ventral neural tube, but appear to have two separate origins along the anteroposterior axis: 84% of Isl1(+) neurons are born in r4, whereas 16% are born in r5. Isl1(+) neurons derived from r5 tended to be born later, between 15 and 16 hpf. Finally, FBMNs and OENs are overwhelmingly born at the nascent apical plane of the neural tube. About 70% of FBMNs and OENs remain ipsilateral to their mother cell, whereas Isl1(-) sisters cross contralaterally to integrate into the neuroepithelium.

Isl1(+) neurons are born continuously over a wide temporal window, beginning at 11 hpf and continuing until at least 16 hpf. While Isl1(+) neurons may continue to be born in later stages, these younger neurons may not have accrued enough *islet1* transgene to be visible before the end of my time-lapse experiments. The early births of some Isl1(+) neurons are not entirely unexpected when taken in context with work on the genetic basis of neurogenesis in the zebrafish. By 9 hpf, *in situ* hybridization reveals that distinct columns of *neurog1* expressing cells are already present in the zebrafish neural plate. In the hindbrain and spinal cord, the most medial of these columns corresponds to the nascent motor neuron domain [31]. There is some evidence that a subset of these zebrafish motor neurons undergo their last round of DNA replication shortly after 9 hpf, making early specification of Isl1(+) neurons not wholly unprecedented [137]. However, I find that the greatest number of Isl1(+) neurons

are born between 13 and 14 hpf, consistent with the timing of FBMN precursor divisions previously reported by Stockinger and colleagues [187].

Development of motor neurons additionally relies on two periods of *hedgehog* signaling, the first from the ventrally positioned notochord and the second from the floor plate of the neural tube [30, 19, 177]. In mouse, specification of visceromotor neurons such as the FBMNs relies on Hedgehog-mediated repression of the transcription factor Pax6 and upregulation of both Nkx6.1 and Nkx2.2 in the ventral neural tube [44, 56, 153]. Collectively, these transcription factors delineate a motor neuron progenitor domain that lies just dorsal to the floor plate. Later, the expression of Phox2b within the same domain will be required to pattern the FBMNs [173, 48, 47]. In zebrafish, the expression patterns of these transcription factors match their amniote counterparts, again defining a domain of motor neuron progenitors adjacent to the floor plate [203, 4, 84, 108, 32, 196]. Here, my reconstruction of FBMN birthplaces confirms that the majority emerge from a distinct 20 μm section of the ventral neural tube which matches this previously described motor neuron progenitor domain. Notably, OENs also appear to be born within this domain, indicating that sensory efferents can be patterned at the same dorsoventral level of the neural tube as motor neurons. Implications for the development and evolution of OENs will be discussed more completely in Chapters 3 and 4.

While all tracked Isl1(+) neurons were born within the same dorsoventral domain, their distribution along the anteroposterior axis is wider than expected. Proper development of FBMNs is contingent upon expression of *hoxb1a* in r4, but a small group of Isl1(+) neurons appears to be born more posteriorly in r5. These findings are reproducible between specimens, with 1-3 Isl1(+) neurons per embryo exhibiting this more posterior origin. These numbers correlate with the low number of OENs expected per embryo [175, 132, 23]. Notably, there are two types of OENs in the zebrafish hindbrain, each of which sends its axon along a markedly different route: rostral OENs fasciculate with the FBMNs and project their

axons out of r4, while caudal OENs send lateral projections posteriorly towards the r6 exit point. Isl1(+) neurons that are born in r5 display lateral projections characteristic of caudal OENs (Figure 2.1, Panel B). Imaging experiments detailed in Chapter 3 further support this separate segmental origin for the caudal OENs. Interestingly, the births of these caudal OENs are temporally distinct, occurring over a short period of time between 14 and 15 hpf. These findings raise the question of whether rostral OEN births are also temporally distinct, as similar numbers of Isl1(+) neurons are born in r4 between 14 and 15 hpf (1-3 per embryo). However, due to the morphological similarities between rostral OENs and FBMNs, their birth times cannot be separated without a specific marker of OEN fate.

The birth of caudal OENs in r5 suggests that they develop from a separate group of motor neuron progenitors - in this case, likely those that give rise to the abducens (nVI). It is worth noting here that the abducens are somatomotor neurons rather than visceromotor neurons like the FBMNs. Therefore, their development depends on the action of Olig2, a transcription factor that, like Nkx2.2, functions downstream of the *hedgehog* genes [150]. At neural plate stages, Olig2 is expressed in a single broad column near the presumptive midline. These cells are later internalized into the ventral neural keel, forming a discrete stripe of Olig2-expressing progenitors close to the medial floor plate [150, 224]. This domain correlates roughly with the dorsoventral distribution of caudal OEN birthplaces discussed above. Possible connections between the abducens and the caudal OENs will be discussed further in Chapters 3 and 4.

Both r4- and r5-derived Isl1(+) neurons are born from divisions that overwhelmingly give rise to only one cranial efferent neuron. Given that this study uses only one marker of neuronal fate, it is possible that Isl1(-) sister cells are also neurons. However, divisions that give rise to two neurons appear to be very rare at neural plate and rod stages, at least in the zebrafish spinal cord [106]. If this trend also holds in the hindbrain, then Isl1(-) sisters are more likely to contribute to maintaining the progenitor pool rather than

differentiating into neurons. The behavior of some Isl1(-) sister cells appears to confirm this, as their nuclei often cycle along the developing apicobasal axis. These movements resemble the interkinetic nuclear migration that is typical of proliferative neuroepithelial cells and is thought to correlate nuclear position with cell cycle to help maximize the number of apical divisions [192, 133, 178]. However, other Isl1(-) sister cells can be seen migrating dorsally between 18 and 24 hpf, as would be expected of neurons migrating along radial glial cells [138]. If Isl1(-) sisters do eventually take on a neural fate, their dorsal movement may help explain why they do not become motor neurons. Neural progenitors retain a "memory" of Hedgehog signaling, with progenitors requiring a longer duration of Hedgehog signaling to take on ventral identities, including motor neuron fate [45, 45, 14]. After division, however, Isl1(-) sisters move away from sources of Hedgehog signaling in the floor plate and notochord and may be exposed to a lower total dose of Hedgehog signaling as a result. However, further conclusions about the identity of Isl1(-) sisters cannot be drawn without additional molecular or morphological information.

Notably, the vast majority of Isl1(+) births occur before the apical midline of the neuroepithelium has been established. As such, traditional mechanisms of cell fate specification through asymmetric inheritance of apical components are unlikely to determine the identity of daughter cells at this stage. The vast majority of Isl1(+) neurons are nevertheless born at the nascent apical plane through divisions that closely resemble the c, or crossing, divisions which establish mirror symmetry of the neural tube in keel and rod stages [194]. Mothers of Isl1(+) neurons orient their mitotic spindles perpendicular to the developing midline, depositing one daughter on either side of the brain. Par3, a marker of apical membranes, is localized to the cleavage furrow during c-division [194, 26]. Whether asymmetric partitioning of Par3 between daughters influences their fate at these early stages is unknown, but inheritance of Par3 has been linked to neuronal fate in daughters born after 20 hpf [5]. In contrast, inheritance of the basal process by the non-apical daughter is correlated with re-

plenishment of the progenitor population at these later stages [5]. However, my backtracking experiments reveal that Isl1(+) neurons almost always arise from the more basally-located daughter. This would suggest that mechanisms of cell fate specification differ significantly during early stages of neurogenesis. Additional studies will be needed to clarify the mechanisms of cell fate specification that determine daughter cell identity prior to the establishment of apicobasal polarity within the neuroepithelium.

To date, one of the only mechanisms of cell fate determination that has been examined at neural plate and rod stages relates to Notch-DeltaD signaling between dividing sister cells. Sara endosomes carrying internalized DeltaD ligand partition asymmetrically into the daughter that retains proliferative capabilities, even at these early stages [106]. However, evidence indicates that lineages are already biased towards symmetric or asymmetric division upstream of endosome partitioning [106]. The mechanism that establishes this bias is unknown. Several recent studies have provided evidence that biomechanical forces within the zebrafish neuroepithelium can prompt neural progenitors to switch between asymmetric and symmetric fates. In 24 hpf embryos, tight packing of neuroepithelial cells causes the displacement of progenitor nuclei away from the midline, leading to an increase in neural fates [91]. Furthermore, boundary cells appear to use Yap/Taz-TEAD activity as a sensor of mechanical signals generated by actinomyosin activity during hindbrain segmentation. When Yap/Taz-TEAD is upregulated, boundary cells remain proliferative, but in the absence of signal they differentiate symmetrically into neurons [206]. A similar kind of coupling between tissue mechanics and cell fate decisions could act on Isl1(+) efferents and their sisters, given that they are born during stages when neural plate cells are actively rearranging to form the neural keel [12].

Taken together, these findings uncover interesting trends in the neurogenesis of FBMNs and OENs and provide a compelling example of lineage reconstruction using SPIM. However, this study is also limited by technical drawbacks inherent to imaging in a ventral population

of cells in the zebrafish. Specifically, I am unable to draw conclusions about the biological relevance of several rare events identified through these experiments. For example, three Isl1(+) efferents are born from non-apical progenitors (NAPs), a particularly compelling finding given that Olig2-expressing NAPs have been described in later stages of hindbrain development [128]. Similarly, one Isl1(-) sister cell undergoes a second round of division around 10 hours after its first. Whether these rare events accurately represent the biology of cranial efferent progenitors or not hinges on my ability to reconstruct cell tracks with accuracy. While superficially-located cell populations in the zebrafish such as the lateral plate mesoderm can generally be tracked without issue [163], image quality close to the zebrafish yolk degrades significantly, preventing this technique from being successfully applied to more ventral cell populations. As detailed in Box 1, I employed rigorous parameters during the construction of cell tracks, but some amount of error must still be taken into account. Moving forward, studies of this nature can benefit from multi-color or scatter-labeling of cell nuclei, as well as newer deconvolution techniques (see Chapter 4). With these modifications, use of SPIM has the potential to provide insights into the spatiotemporal origins of an almost limitless array of cell types.

2.5 Methods

2.5.1 Transgenic lines and fish husbandry

Two existing trangenic lines were incrossed to generate a stable double transgenic that expresses RFP in the membranes of cranial efferent neurons *Tg(en.crest1-hsp70l:mRFP, ch100)* [120] and GFP in all cell nuclei *Tg(h2afva:h2afva-GFP)* [155]. Embryos were raised at 31.5°C to accelerate development and staged to 10 hpf following standard morphological criteria [101].

2.5.2 Embryo mounting and microscopy

At 10 hpf, Zebrafish embryos were mounted in Fluorostore Fractional FEP Tubing (F018153-5) using a modified multilayer technique [99]. Embryos were immobilized using 0.3% agarose (Invitrogen UltraPure Agarose #16500) dissolved in E3 medium and 0.2 mg/ml tricaine, and the FEP tubing was capped with a 1.2% agarose plug. Embryos were incubated at 28.5C during data collection. Images were captured with a Zeiss Lightsheet Z.1 Selective Plane Illumination microscope (Carl Zeiss Microscopy, Thornwood, NY) with tandem PCO.edge sCMOS cameras (PCO.Imaging, Kelheim, Germany) and Zeiss Zen imaging software. A 20x/1.0 long working distance detection objective was used alongside a pair of 10x/0.2 dry illumination objectives, and the excitation sheet was narrowed to 2.0 μm. Volumes were acquired every two minutes between 12-24 hpf, with 10 ms exposure per slice for both green (488 nm, 7.5%) and red (561 nm, 7.0%) channels.

2.5.3 Data analysis and code availability

Acquired images were cropped to a smaller region of interest and converted from .czi to .tif for use with a variety of processing modules. Individual FBMNs were identified by expression of *Tg(en.crest1-hsp70l:mRFP, ch100)* at 18.5 hpf, shortly after the transgene becomes visible, and tracked back through time using *Tg(h2afva:h2afva-GFP)* to identify Isl1(+) neuron birthplaces. Cell tracks were manually reconstructed using the mTrackJ plugin in FIJI [129]. A detailed explanation of tracking criteria is included in Box 1.

Data were exported to a custom Python script for plotting of cell movements and birthplaces. The code is open-source and available for download from https://github. com/aebeiriger/plot-tracks. This script includes functions to plot tracking data and cell birthplaces, smooth random cell movements, and register cell locations to the tip of the notochord. The anterior limit of the notochord lies under r4, providing an anatomical landmark that allows for birthplace comparisons between embryos. Rhombomere widths are plotted based on published

expression patterns of Krox20 [162, 116], a marker of r3 and r5, in 14 hpf embryos. This particular stage was chosen because the greatest number of Isl1(+) progenitor divisions occur at 14 hpf. As such, the rhombomere boundaries plotted here will not be exact at all cell birth times due to morphological changes during neurulation. All tracks shown are smoothed over a window of three time points.

Box 1: Constructing Cell Tracks. The conclusions from this study must be viewed in light of data quality issues that impact my ability to identify a "true" cell track. At most time points, there is sufficient separation between nuclei to determine cell tracks. However, FBMNs and OENs migrate ventrally within the neural tube, close to the opaque, light-scattering zebrafish yolk. As a result, data quality tends to degrade along the dorsoventral axis, reflecting limitations inherent in the biology of the zebrafish model as well as the optics of the microscope. Therefore, close movements of two nuclei relative to one another within the ventral neural tube can present challenges in the reconstruction of cell trajectories. Below, I detail the criteria used to reconstruct cell movements, and discuss how these decisions were informed by the biology FBMNs and OENs.

1. Persistence: A given nucleus is more likely to keep moving in the same direction from one time point to the next, rather than switching direction.
2. Spatial constraints: The centers of two nuclei crossing through the same XY coordinates must be at least 10 μm apart along the Z axis.
3. Conservative movement: The center of a given nucleus is likely to stay within 10 μm over two consecutive time points, unless one of the time points contains a cell division.
4. Addressing gaps: If a track is lost for one time point but regained in the next, this gap is tracked over. If a track is lost for more than one time point, the track is re-evaluated.
5. Confidence: Two or more gaps resulted in a given track being discarded. In this study, 8 tracks were discarded due to low confidence.
6. Tracking in triplicate: three independent tracks were created for each cell. If two or more tracks were identical, this was chosen as the "correct" track, increasing confidence in the final outcome.
7. Biological hints: The neuroepithelial basement membrane acts as a substrate for tangentially migrating FBMNs [80]. Therefore, FBMN nuclei should localize to the ventral surface of the brain during the majority of their migration.

CHAPTER 3

DEVELOPMENT AND MIGRATION OF THE ZEBRAFISH RHOMBENCEPHALIC OCTAVOLATERAL EFFERENT NEURONS

3.1 Abstract

In vertebrate animals, motor and sensory efferent neurons carry information from the central nervous system (CNS) to peripheral targets. These two types of efferent systems sometimes bear a close resemblance, sharing common segmental organization, axon pathways, and chemical messengers. Here, we focus on the development of the octavolateral efferent neurons (OENs) and their interactions with the closely-related facial branchiomotor neurons (FBMNs) in zebrafish. Using live-imaging approaches, we investigate the birth, migration, and projection patterns of OENs and examine their interactions with the better-studied FBMNs. We find that OENs are born in two distinct groups: a rostral group that arises in the fourth segment, or rhombomere (r4), of the hindbrain and a caudal group that arises in r5. Both rostral and caudal OENs then migrate posteriorly through the hindbrain between 18 and 48 hours post-fertilization, alongside the r4-derived FBMNs. Like the FBMNs, migration of the r4-derived rostral OENs depends upon *hoxb1a* function. Unlike the FBMNs, however, both OEN populations move independently of *pk1b*, and the r5-derived caudal OENs do not rely on the action of a single pioneer neuron to migrate. Together, these results indicate that the mechanisms OENs use to navigate the hindbrain differ significantly from those employed by FBMNs.

3.2 Preface

This work was completed in collaboration with Sweta Narayan, an undergraduate in the lab, who performed photoconversion experiments (Figure 3.1, Panels D, E, F; Figure 3.5, Panels A, C) and our technician, Noor Singh, who performed *pk1b* knockdown experiments (Figure 3.3, Panel C').

3.3 Introduction

Integration of the central nervous system (CNS) with peripheral targets is achieved through the projections of afferent and efferent neurons, which carry information towards and away from the CNS, respectively. Most efferent neurons are motor neurons, although sensory efferents also localize their somas in the CNS, sending their axon termini to the periphery to provide an important level of regulatory control over sensory inputs. Occasionally these two classes of efferents display a close relationship, as is the case with the facial branchiomotor neurons (FBMNs) of the VIIth cranial nerve and octavolateral efferent neurons (OENs) of the VIIIth cranial nerve. Shared attributes between these two efferent populations, including the position of their somas, close coupling of their projections, and reliance on common neurotransmitters have led some researchers to consider the OENs a subset of the branchiomotor column, albeit one that innervates sensory structures rather than muscle [166].

There has been significant focus on the specification and migration of the FBMNs, aided in the zebrafish by the development of transgenic lines driven by the *islet1* (*isl1*) regulatory sequences [90, 120, 201]. However, the *islet1* transgenes also label the closely associated but comparatively understudied OENs. Here, we set out to describe OEN development and migration, with special attention to the qualities that set OENs apart from FBMNs.

FBMNs are specified in the fourth segment, or rhombomere (r), of the vertebrate hindbrain with input from the homeodomain transcription factor Hoxb1, encoded by *hoxb1a* in

zebrafish [78, 126, 169, 190]. In zebrafish, mice, and humans, the FBMNs migrate posteriorly from r4 in two parallel streams, leaving a trailing axon behind them that exits the hindbrain from r4 to innervate second pharyngeal arch derivatives [29]. Time-lapse microscopy in zebrafish has shown that FBMNs migrate tangentially along the medial floor plate through r5, after which they undergo a short radial migration before clustering into bilateral nuclei in r6 and r7 [80, 209]. Previously, we demonstrated that the initial migration of FBMNs across the r4/r5 border is led by a pioneer neuron, and that ablation of the pioneer results in a partial or complete block to FBMN migration [208]. FBMNs rely on several additional mechanisms to migrate, including contacts with the medial longitudinal fasciculus (MLF) [208], function of several PCP factors such as Scrib, Vangl2, and Pk1b [119, 207, 209, 223], and activity of the transcriptional repressor Rest, which is required to keep FBMNs in an immature and migratory state [103, 110]. Furthermore, FBMN migration is a collective process in which cell-cell contacts between neurons are partially mediated by Cadherin-2 [165, 187, 208].

Comparatively little is known about the OENs. In zebrafish and most other anamniote vertebrates, OENs project to the lateral line system (LLS), forming part of a sensory circuit that provides information on the surrounding aquatic environment [20, 166]. While the anatomy of the LLS varies between species, the fundamental sensory organ, the neuromast, is conserved. Neuromasts contain mechanosensory hair cells that transmit information to the central nervous system via basally located afferent nerve termini [60]. The neuromasts are also supplied by the OENs, which are thought to provide both excitatory and inhibitory roles, modulating hair cell sensitivity based on the behavioral state of the animal [23, 131]. Single OENs generally innervate multiple neuromasts; however, not every neuromast within an individual animal receives efferent innervation [20]. Furthermore, in many species including catfish, goldfish, and zebrafish, single OENs often supply not only the LLS but also the inner ear. As such, they are often considered analogous to the vestibulocochlear efferents of amniotes, which make up the efferent component of the VIIIth cranial nerve [17, 21, 132, 63].

In zebrafish, three octavolateral efferent nuclei have been characterized by backfilling from the periphery at 24 hours post-fertilization (hpf) and beyond [23, 132]. The most anteriorly-located of the OENs comprise the diencephalic efferents to the lateral line (DELL). Typically, there are only 2-3 DELL on each side of the brain, although each neuron possesses an extensive axonal arbor that includes multiple branch points and terminates on several sensory end organs. Bricaud and colleagues [23] posit that individual DELL are likely to project to both the anterior and posterior LLS, while Metcalfe and colleagues [132] have demonstrated that the DELL also innervate the ear. In addition, two separate nuclei of rhombencephalic OENs have been described, the rostral and caudal efferent neurons (RENs and CENs, respectively). Our study is focused on the rhombencephalic OENs (schematized in Figure 3.1, Panel A).

The rostral efferent neurons (RENs) are located in r6 and project their axons anteriorly to r4 where they exit the hindbrain together with the main fascicle of the FBMNs. The caudal efferent neurons (CENs) cluster loosely in r7 and project their axons anteriorly to r6, where they turn laterally and exit the hindbrain together with the glossopharyngeal nerve (nIX) [28, 90]. Although both groups of rhombencephalic efferents cluster into larger nuclei with the FBMNs, zebrafish OENs are a fairly rare cell type: there are 1-3 RENs on each side of the brain, and the CENs are only slightly more numerous at 3-5 per hemibrain [132]. Unlike the DELLs, single hindbrain OENs usually project either to the anterior or posterior LLS, with RENs displaying a preference for innervating the anterior LLS and CENs more commonly projecting to the posterior LLS [23].

Despite their well-characterized morphology, few studies have examined the development of zebrafish OENs. Experiments in mouse have shown that *Hoxb1* specifies the vestibulocochlear efferent neurons alongside the FBMNs in r4 [78, 152, 190]. However, the timing of their birth and the mechanisms driving their molecular divergence from FBMNs is unknown. Several studies have examined the function of zebrafish *hoxb1a* [126, 169], but a role for the

hox genes in OEN development has not been established due to the absence of molecular markers that distinguish OENs from FBMNs. Additionally, little is known about the migration of the OENs. RENs do migrate from r4 to r6 with the FBMNs, but the exact timing of this migration is unclear [175]. There is indirect evidence that CENs migrate from r6 to r7 after 24 hpf, but whether they perform additional movements before 24 hpf is unknown [175].

In this study, we provide an in depth analysis of the development of zebrafish rhombencephalic OENs, allowing comparison of their properties with those of the better described FBMNs. As both these types of efferent neuron express *isl1*, our study was facilitated by establishment of a new *Tg(en.crest1-hsp70l:mKaede)* transgenic line, which allows labeling of single efferent neurons and their projections in the absence of cell-type specific markers. We used this line in a series of photoconversion experiments to provide the first comprehensive description of OEN migration in zebrafish. We find that OENs migrate concurrently with FBMNs beginning at 18 hpf, and they reach their final destinations by 48 hpf. Using time-lapse microscopy and cell tracking methods, we demonstrate that the CENs are born in r5, in a region spatially distinct from the more anterior origin of RENs and FBMNs. We also demonstrate that similar to FBMNs, migration of RENs depends upon function of the r4-expressed *hox* gene, *hoxb1a*. However, while FBMN migration is additionally dependent on the function of the Hoxb1a downstream effector gene *pk1b*, REN migration is *pk1b*-independent. This finding reveals that RENs and FBMNs are subject to distinct molecular control. Finally, we investigate physical interactions between FBMNs and OENs during their migration. We show that r4-derived FBMN/RENs and r5-derived CENs can make contact across the r4/r5 border. However, neuron ablation experiments suggest that these interactions are not necessary for successful migration of FBMNs or OENs.

3.4 Results

3.4.1 A new Kaede transgenic line allows visualization of single efferent neurons and their projections

We began our analysis of the zebrafish rhombencephalic octavolateral efferent neurons (OENs) by developing a new transgenic tool that facilitates single cell labeling of Islet1-positive (Isl1(+)) neurons. The new line, *Tg(en.crest1-hsp70l:mKaede) ch104*, uses the *zCREST1* enhancer element from the *islet1* locus [201] to drive a membrane-targeted variant of the Kaede fluorophore in zebrafish cranial efferent neurons (Figure 3.1, Panel B). Exposure to UV light cleaves Kaede protein, converting it from green to red fluorescence. A CaaX motif was added at the C-terminal end of the molecule, ensuring the red fluorescent variant of the protein remains membrane bound and permitting visualization of fine cellular projections from individual neurons (Figure 3.1, Panel B'-B'). Moreover, the red fluorescent form of the protein perdures for around 3 days, allowing us to identify the same cell through multiple developmental stages.

Importantly, the *Tg(en.crest1-hsp70l:mKaede)* line is extremely bright and accrues fluorescence earlier than the *Tg(en.crest1-hsp70:mRFP)* and *Tg(isl1:GFP)* lines used in our previous studies [90, 120]. As a consequence, cranial efferent neurons become visible at slightly earlier stages in the *Tg(en.crest1-hsp70l:mKaede)* line. This includes the facial branchiomotor neurons (FBMNs), which we can reliably detect by 17 hpf, an hour earlier than with the previous transgenic lines. We will return to this point as we compare findings in this study with those reported previously.

3.4.2 OENs migrate concurrently with FBMNs through the hindbrain

We first sought to establish the when OENs migrate relative to the FBMNs. Using our new *Tg(en.crest1-hsp70l:mKaede)* line, we investigated the Isl1(+) neurons that migrate

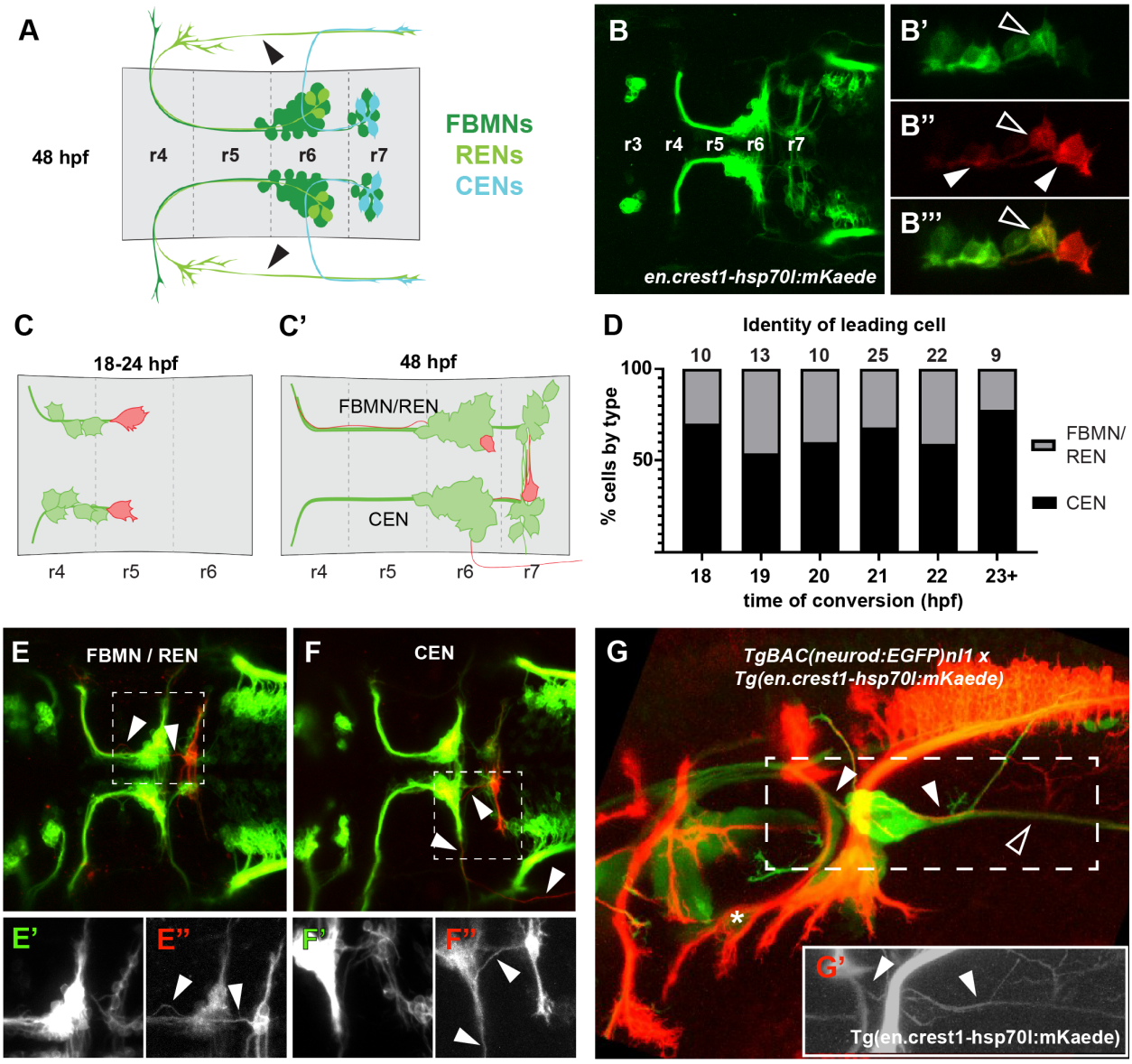

Figure 3.1: **Single-cell photoconversions reveal that OENs migrate concurrently with FBMNs.** (A) Schematic of FBMN, REN, and CEN somas and axon morphologies at 48 hpf. The REN projection crossing the otic vesicle (arrowheads) is not visible in all embryos. (B) The newly-generated *Tg(en.crest1-hsp70l:mKaede)* line uses the *islet1 zCREST1* enhancer [201] to drive expression of the photoconvertible protein Kaede in a subset of cranial efferent neurons. (B'-B'''') Single-cell labeling via photoconversion of Kaede from green to red. A fully converted leading cell and its trailing axon (closed arrowheads) are identified by the presence of red and absence of green protein. Contrast with partial conversion of a follower, in which green protein remains (open arrowheads). (C) Schematic of photoconversion experiments targeting leading mKaede-expressing neurons between 18-24 hpf and (C') screening criteria for axon morphology of different cell types at 48 hpf. (D) CENs are present

Figure 3.1, continued: in the leading position in over 50% of embryos at every time point between 18-24 hpf. (E) Axon morphology typical of FBMN/RENs (arrowheads); (E'-E'') insets of boxed area show separated green and red channels, respectively. (F) Axon morphology typical of CENs (arrowheads); (F'-F'') insets of boxed area show separated green and red channels, respectively. (G-G') Double transgenic line with converted *Tg(en.crest1-hsp70l:mKaede)* and *Tg-BAC(neurod:EGFP)nl1* demonstrates that efferent projections leaving r6 (red; closed arrowheads) fasciculate with the sensory afferent projections to the lateral line (green; open arrowheads). Glossopharyngeal motor neurons (nIX) are indicated by an asterisk.

through r5 and r6 in a chain-like manner. In a series of experiments, we photoconverted individual leading (most posteriorly located) neurons, in embryos staged between 18 and 24 hpf (Figure 3.1, Panel C). We then screened for red fluorescence at 48 hpf, scoring the identity of converted cells in each hemibrain based on their axon morphology (Figure 3.1, Panel C').

Morphological features typical of the FBMNs and the REN population of OENs are shown in Figure 3.1, Panel E-E'', where a converted cell projects its axon anteriorly to exit the hindbrain from r4. Conversely, axons of the CEN population of OENs project anteriorly for a shorter distance, before exiting the hindbrain from r6 (Figure 3.1, Panels F-F''). For the purposes of quantitative analysis, FBMNs and RENs were grouped into a single category, since individual RENs displayed considerable variation in their axon branch points and therefore could not be reliably distinguished from FBMNs. We found that the leading neurons ultimately displayed CEN morphology in more than 50% of the hemibrains assayed (Figure 3.1, Panel D), independent of the stage at which photoconversion was performed.

Other cell populations are known to use the r6 exit point, namely the glossopharyngeal (nIX) motor neurons. Projections of the nIX are also labeled by *Tg(en.crest1-hsp70l:mKaede)*, but these turn rostrally and route under the otic vesicle after leaving r6 (asterisk; Figure 1G) rather than projecting caudally down the tail of the fish as is typical for the CENs. To affirm that caudally projecting Isl1(+) neurons are indeed CENs, we crossed fish carrying *Tg(en.crest1-hsp70l:mKaede)* with fish of the *TgBAC(neurod:EGFP)*^{nl1} line.

TgBAC(neurod:EGFP)^{nl1} labels sensory afferent projections, including those of the posterior lateral line (PLL) [142]. We carried out whole-embryo photoconversions so that all Isl1(+) efferents were labeled in red. In double-transgenic embryos, a subset of Isl1(+) axons using the r6 exit point (converted, red) fasciculate with Nrd(+) sensory afferent projections (green) of the PLL (closed arrowhead). This common axon routing pattern confirms that the Isl1(+) neurons projecting posteriorly from the r6 exit point are indeed CENs (arrowheads; Figure 1G-1G).

Together, these results demonstrate that OENs migrate concurrently with FBMNs beginning as early as 18 hpf. Additionally, the leading, or most posteriorly-located, Isl1(+) cell is often a CEN rather than an FBMN or REN. This finding raises the intriguing question of whether the previously described 'pioneer' neuron [208] could be a CEN rather than an FBMN, a topic we return to below. Finally, CEN axons have established their characteristic morphology by 48 hpf, using the r6 exit point and sending their growth cones posteriorly along the same axon tract as sensory projections of the PLL.

3.4.3 CENs do not share a common spatial origin with FBMNs

To examine the initial birthplaces of OENs, we performed a series of backtracking experiments designed to visualize OEN and FBMN progenitor divisions. We crossed fish of the *Tg(en.crest1-hsp70l:mRFP)* line with fish carrying the pan-nuclear label *Tg(h2az2a:h2az2a-GFP)* [155] to generate a double transgenic line for single-plane illumination microscopy (SPIM). Time-lapse movies were acquired starting at 11.5 hpf, during early stages of neurulation, and ending close to 24 hpf, after Isl1(+) neurons had begun to migrate into r6. Because expression of *Tg(en.crest1-hsp70l:mRFP)* cannot be detected until about 18 hpf, we identified FBMNs and OENs at the end of the time-lapse movie and used nuclear *Tg(h2az2a:h2az2a-GFP)* to backtrack the cells through time to their birthplace.

In Figure 3.2, we provide an overview of cell tracks and birthplaces. As expected, the

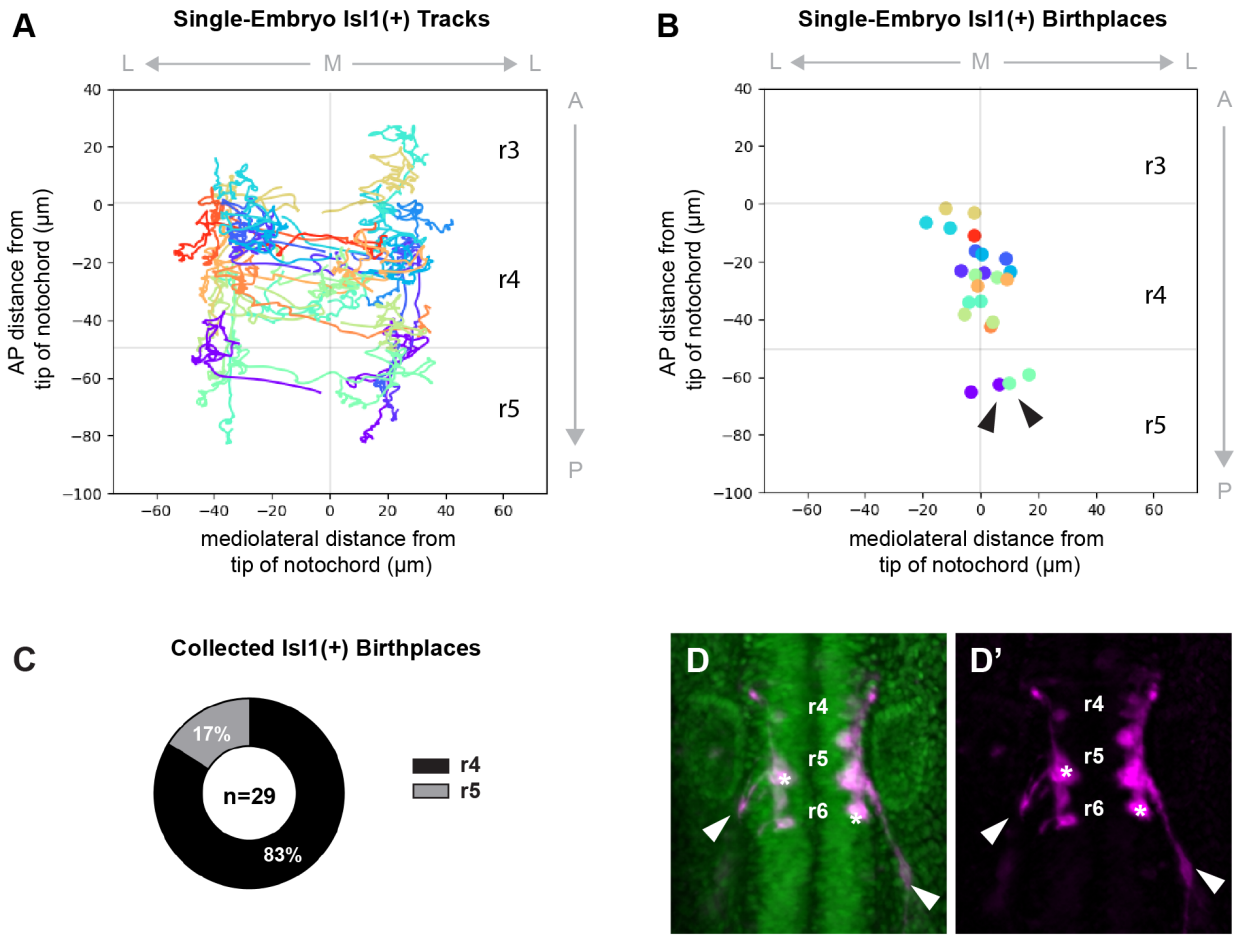

Figure 3.2: **Caudal efferent neurons (CENs) do not share a common developmental origin with FBMNs.** Cell lineages were reconstructed by tracking the nuclei of neurons carrying both *Tg(h2az2a:h2az2a-GFP)* and *Tg(en.crestl1-hsp70l:mRFP)*. (A) Cell tracks from one specimen are graphed on an anatomical plot, where the origin is placed at the tip of the notochord. Rhombomere boundaries (grey lines) are based on average segmental width during Isl1(+) neuron births at 14 hpf. Each Isl1(+) cell track is represented by a different color, and circles indicate cell position at the start of the time-lapse. (B) Birthplaces of all tracked neurons from the same specimen are plotted; sister cells are color-coded by lineage. Two progenitor divisions occur close to the midline in r5 rather than r4, giving rise to Isl1(+) CENs (arrowheads). (C) Aggregated data from three embryos show that 17% of all cells tracked between 13-24 hpf time are born in r5. (D) Movie still from a lightsheet time-lapse showing that neurons born in r5 (asterisks) eventually send out projections characteristic of CENs (arrowheads).

vast majority of tracks begin in r4, where *hoxb1a* function has been shown to confer FBMN identity [126]. Furthermore, most tracks end in r6, reflecting the well-described tangential migration of these neurons (Figure 3.2, Panel A). However, in each specimen a subset of Isl1(+) neurons was born in r5 (Figure 3.2, Panel B), posterior to the domain of elevated *hoxb1a* expression. Across two time-lapse movies, r5-derived neurons made up 17% of all tracked cells (Figure 3.2, Panel C). After 22 hpf, the r5-derived neurons consistently displayed cellular projections near the r6 exit point (Figure 3.2, Panel D, arrowheads), as would be expected of CENs. Taken together, these results indicate that CENs have a more posterior segmental origin in comparison to the FBMNs and RENs.

Despite their different segmental origins, all three cell types are born at similar developmental stages. Neurons arising from r4, comprising both FBMNs and RENs, were born continuously during neural plate and keel stages, between 11 and 16 hpf (n=24). The r5-derived CENs were born closer to 15 hpf (n=5). These data reflect only a subset of Isl1(+) neurons in each fish, since some later-born neurons do not accrue enough fluorescent protein to be detectable at 24 hpf. However, we can conclude that the divisions from which FBMNs and OENs arise occur during early neurulation, and while their birthdates are very similar, the r5-derived CENs are born slightly later than the earliest born r4-derived efferents.

3.4.4 Hoxb1a function is required for REN but not CEN migration

We next investigated the role of the *hoxb1a* gene, which is expressed at high levels in a characteristic r4 'stripe', as well as at much lower levels more posteriorly [162]. When Hoxb1a function is disrupted, the FBMNs fail to migrate out of r4 and instead display characteristics reminiscent of the r2-derived trigeminal (nV) motor neurons, a phenotype consistent with a classic anteriorizing homeotic transformation [126]. Our backtracking data have indicated that the CENs originate in r5, spatially distinct from the origin of FBMNs. As Hoxb1a is not expressed at significant levels in r5, we expect CEN development to be

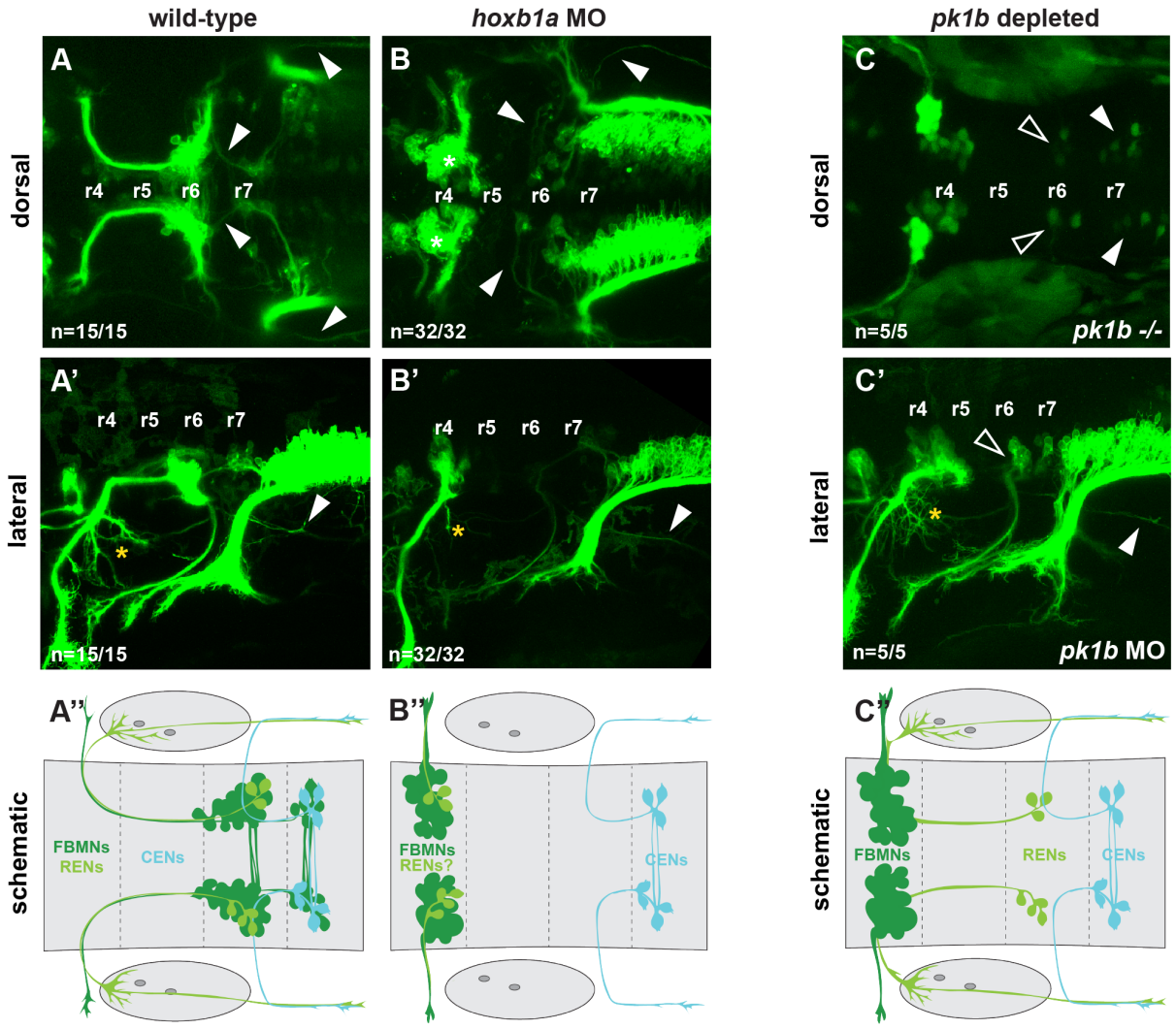

Figure 3.3: **Rostral efferent neurons (RENs) are specified by *hoxb1a* in r4, but do not need *pk1b* to migrate.** (A-A') Wild-type embryos showing characteristic projections of RENs (yellow asterisk) and CENs (arrowheads) in dorsal and lateral views. (A'') Schematic indicates wild-type cell soma locations. (B-B'') Morpholino knockdown of *hoxb1a* results in a complete block to FBMN migration (asterisks); notably, RENs are absent from r6 but CENs still migrate successfully (arrowheads). (C) In *pk1b* homozygous mutants, RENs (open arrowheads) and CENs (closed arrowheads) are still able to migrate. Transgenic background is *Tg(isl1:GFP)*. (C') Morpholino knockdown of *pk1b* in *Tg(en.crest1-hsp70l:mKaede)* fish demonstrates that projections of RENs (asterisk) and CENs (closed arrowhead) are undisturbed in the absence of Pk1b. (C'') Schematic indicates soma and projection locations of all three cell types in Pk1b-depleted embryos.

independent of Hoxb1a function. We predict that in Hoxb1a-deficient embryos, the CENs should migrate normally to reach their typical r7 location by 48 hpf. To test this model, we performed Hoxb1a morpholino knockdown experiments as previously described [126]. As we expected, in Hoxb1a-deficient embryos the CENs appear undisturbed, migrating normally to r7 and successfully routing their axons towards the lateral line (Figure 3.3, Panels B-B'; n=32/32). Meanwhile, as we previously reported [126], r4-derived Isl1(+) neurons fail to migrate posteriorly (Figure 3.3, Panels B-B'; n=32/32). Interestingly, in Hoxb1a morphants no RENs were found in r6, providing additional support for a model in which RENs share characteristics with FBMNs. Not only do FBMNs and RENs arise together in r4, but both cell types require Hoxb1a function in order to migrate.

3.4.5 OEN migration is independent of Pk1b function

In previous studies, we showed that *pk1b* functions downstream of Hoxb1a [169]. Not only is *pk1b* expressed specifically in the FBMNs, but it also functions cell-autonomously within these neurons to facilitate their migration [120, 119, 169]. Since our knockdown results demonstrated that CEN migration is independent of Hoxb1a, we predicted that CEN migration was similarly unlikely to rely on Pk1b function. To test this prediction, we examined *pk1b*$^{fh122/fh122}$ homozygous mutants in the *Tg(isl1:GFP)* background, which provides a cytoplasmic label of Isl1(+) neurons. We found that in *pk1b* mutant embryos, r6 and r7 each contained 6-10 Isl1(+) cells. The neurons in r7 likely correspond to CENs, while the r6 cells are likely to be RENs (Figure 3.3, Panel C, n=5/5), suggesting that both classes of hindbrain OENs migrate independently of Pk1b. Consistent with this interpretation, *pk1b* morpholino knockdown in *Tg(en.crest1-hsp70l:mKaede)* embryos confirms that neurons localized in r6 and r7 display axon morphology characteristic of the REN and CEN classes of OENs (Figure 3.3, Panel C', n=5/5). The successful migration of RENs in the absence of Pk1b function indicates that despite sharing a spatial origin with FBMNs, they nevertheless

rely on different molecular mechanisms to migrate. Moreover, the migration of RENs and CENs does not depend on the posterior movement of FBMNs.

3.4.6 The leading CEN does not act as a pioneer neuron

In a previous study, we described the unique ability of the leading FBMN to pioneer a route through the neuroepithelium for its followers [208]. Here, we revisit the pioneer hypothesis in light of the experimental findings presented above on OEN birth and migration. Our original pioneer ablation experiments demonstrated that the pioneer performs its function at 18 hpf, around the time that migrating FBMNs first cross the r4/5 border [208]. Given our new evidence that CENs begin migrating as early as 18 hpf and are often found leading the migrating chain of Isl1(+) neurons, we sought to investigate whether the pioneer neuron might be a CEN. Similarly, we wanted to address whether contact between an r4-derived FBMN/REN and an r5-derived CEN might provide a mechanism for pioneer activity.

We first sought to confirm whether we could reliably identify CENs prior to 48 hpf based on early lateral projections in r5. We photoconverted these lateral projections in 20 hpf *Tg(en.crest1-hsp70l:mKaede)* embryos, allowing the converted Kaede protein to diffuse back into the cell soma (Figure 3.4, Panels A-A'). Every cell converted in this manner displayed CEN-like morphology at 48 hpf, sending contralateral projections across the midline in r7 and projecting an axon through the r6 exit point and posteriorly towards the lateral line (Figure 3.4, Panel A'', n=8/8). However, there appears to be variation between hemibrains on the timing of CEN axon outgrowth (Figure 3.4, Panel B-B''). With this information on early CEN axon morphology, we analyzed time-lapse videos of *Tg(en.crest1-hsp70l:mKaede)* embryos to determine when contact first occurs between FBMN/RENs and CENs. Our data reveal that r4-derived FBMN/RENs make transient contacts with r5-localized CENs at 18 hpf. Eventually, these contacts appear to be stabilized, with FBMN/REN protrusions contacting branches of the CEN axonal arbor across the r4/5 border by 19.5 hpf (Figure 3.4,

Panels C-C''').

If contact between these two cell types is necessary for FBMN/RENs to cross the r4/5 border, we would expect to find FBMN/RENs and CENs consistently localizing together at the leading position at 18 hpf. We selected 18 hpf embryos in which neurons carrying *Tg(en.crest1-hsp70l:mKaede)* had reached or just crossed the r4/5 border and photoconverted two leading migratory neurons per hemibrain. Two rounds of photoconversion were performed: the first at 18 hpf, when Kaede protein had just begun to accrue, and the second at 20 hpf, when each red-labeled neuron was again exposed to UV light to boost the red fluorescent signal (Figure 3.4, Panel D). At 48 hpf, we observed that a majority of hemibrains displayed one converted FBMN/REN and one converted CEN (53%, n=34, Figure 3.4, Panel D'). These results leave open the possibility of a mechanism in which observed pioneer activity is influenced by the leading FBMN/REN reaching across the r4/5 boundary to contact a CEN.

To test whether this contact is necessary for migration, we next performed a series of ablation experiments, similar in design to those we previously reported [208]. In 18 hpf embryos, we ablated cells based on their precise location in the hindbrain, which varies between embryos and between hemibrains at the equivalent stage (schematized in Figure 3.5, Panels A-C). In embryos where all observable Isl1(+) neurons were still localized in r4, and thus had not yet migrated across the r4/5 boundary, we ablated a single leading neuron (Figure 3.5, Panel A). Based on our photoconversion analyses, in this experimental paradigm the ablated neuron was either an FBMN or a REN. As shown in Figure 3.5, Panel A', and summarized in Panel D, the ablation of a single r4-localized FBMN/REN significantly abrogated migration ($P<0.05$), consistent with our previously reported findings [208]. In embryos where one Isl1(+) neuron was located in r5, we ablated either one or two leading neurons (Figure 3.5, Panels B, C). In these experiments, the leading neuron could be an r4-derived FMBN/REN that had just crossed the r4/5 boundary, or an r5-derived

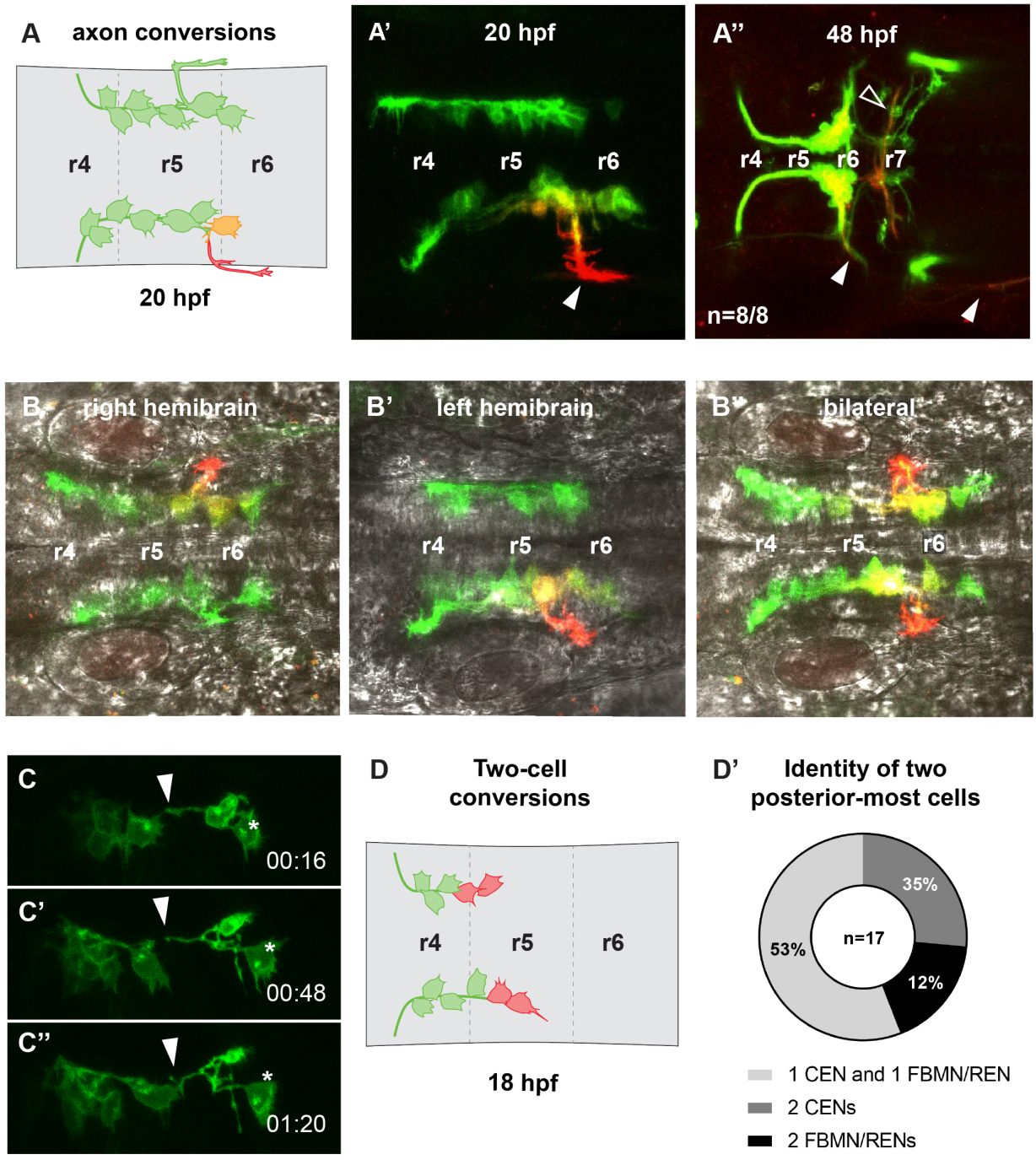

Figure 3.4: **CEN axons begin their lateral outgrowth early and are contacted by leading FBMN/RENs.** (A-A') Photoconversion of lateral projections (closed arrowhead) at 20 hpf allows converted protein to diffuse back into the cell soma. (A'') Neurons that send out lateral projections at 20 hpf display CEN morphology at 48 hpf, including contralateral dendritic projections (open arrowhead) and posteriorly-routed axons (closed arrowhead; n=8/8). (B-B''') The timing of CEN axon outgrowth is variable between hemibrains.

Figure 3.4, continued: Embryos staged to 20 hpf can exhibit CEN axon outgrowth on either one or both sides of the brain. (C-C'') Time-lapse stills of embryos carrying *Tg(en.crest1-hsp70l:mKaede)*, with time points as indicated in minutes. Time-lapse analysis begins at 18hpf. FBMN/RENs make transient contacts (arrowheads) with CENs (asterisks) during migration which are later stabilized. (D) Schematic and (D') quantification of two-cell conversions. One CEN and one FBMN/REN typically occupy the leading position together at 18 hpf.

CEN. As shown in Figure 3.5, Panel B' and summarized in Panel D the ablation of a single neuron in r5 had no discernible effect on migration, with the resulting range of phenotypes resembling those of unablated control animals (P=0.89). Interestingly, in those cases where we ablated two leading neurons in a single hemibrain we found significant abrogation of migration (Figure 3.5, Panels C', D) in comparison to controls (P<0.0005). However, this effect was not significantly different from the outcome of ablation of a single r4-localized neuron.

We must note that the ablations performed in this study resulted in a less severe phenotype (i.e. more Isl1(+) neurons visible in r6) than our previously published 18 hpf ablation experiments [208]. We suspect that this discrepancy is related to use of the new *Tg(en.crest1-hsp70l:mKaede)* transgene, which is brighter than the *Tg(islet1:GFP)* and *Tg(en.crest1-hsp70l:mRFP)* transgenes we used previously [208]. The 'extra' r6-localized cells present in the ablation experiments we report here (Figure 3.5, Panels D) are likely to be CENs. Interestingly, if we account for r6-localized CENs in all ablation conditions reported here (Figure 3.5, Panels D'), the resulting phenotypes more closely resemble those described in our previously published work [208]. These adjustments were made as described in Section 3.6.5.

These experiments clarify and extend our previously published work on pioneer activity [208]. Our results confirm that the pioneer is 1) active at 18 hpf and 2) r4-derived, from which we conclude that the pioneer is an FBMN or REN. Since ablation of a single r5-localized neuron had no measurable consequence for migration, and at least in some cases

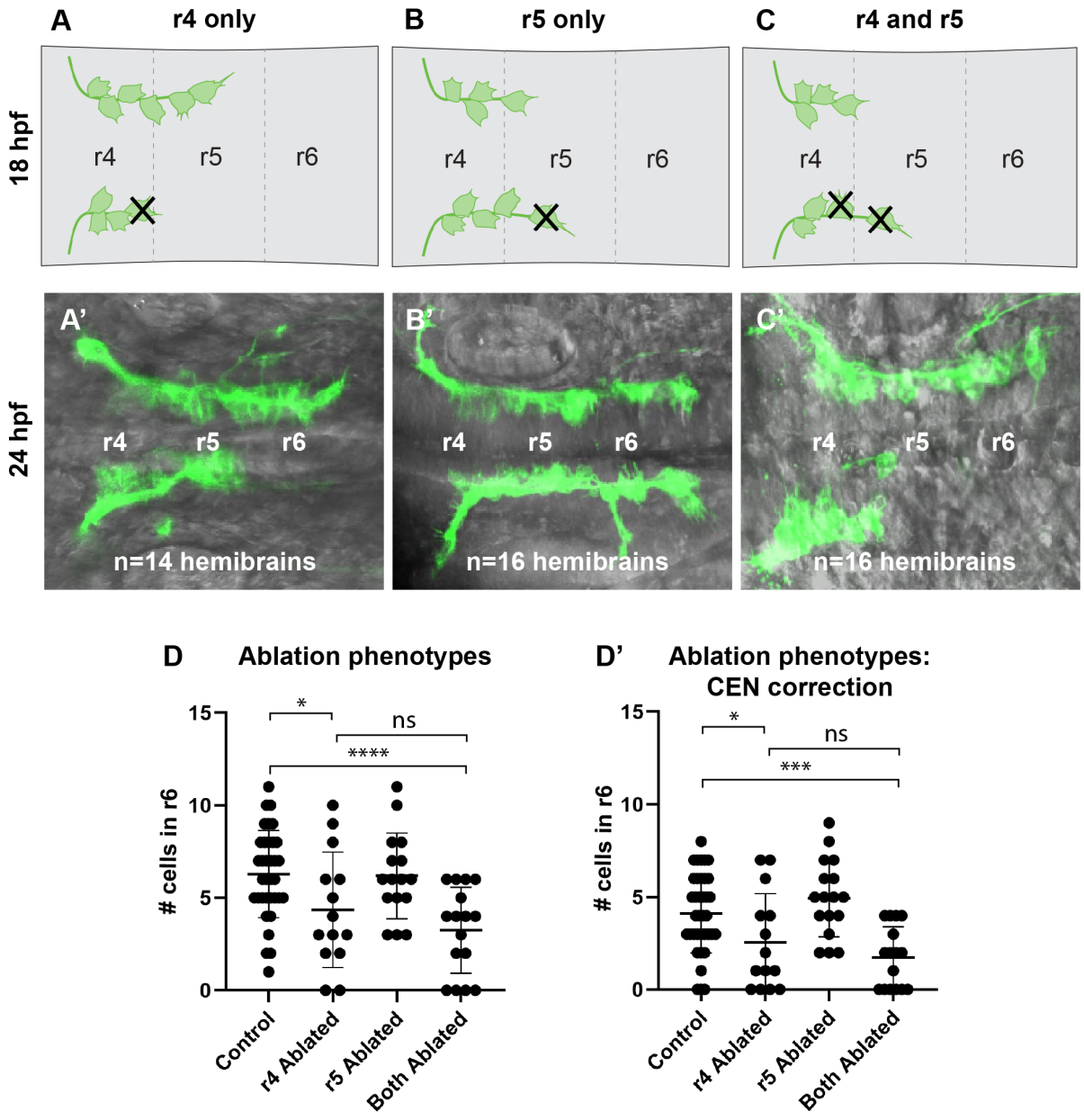

Figure 3.5: **Interactions between neuron classes and their impact on neuronal migration.** (A-A') Ablation of a leading neuron localized in r4 was performed at 18 hpf, and neuronal migration assayed at 24 hpf. (B-B') Ablation of a leading neuron localized in r5 was performed at 18 hpf, and neuronal migration assayed at 24 hpf. (C-C') Ablation of two leading neurons - one localized in r4 and one in r5 - was performed at 18 hpf, and neuronal migration assayed at 24 hpf. (D) Number of neurons located in r6 after each class of ablation. Ablation of single leading neurons in r4 led to a significant decrease in the number

Figure 3.5of neurons reaching r6 in comparison to unablated controls (*P<0.05, n=14), while ablation of a pair of leading neurons led to a highly significant block in migration in comparison to unablated controls (****P<0.0001, n=16). There is not a statistically significant difference between the number of neurons reaching r6 in single r4-localized ablations and double r4/r5-localized ablations. (D') Number of neurons located in r6 after correcting for the presence of CENs (***P<0.0005).

that neuron will have been a FBMN/REN, we conclude that the pioneer neuron becomes dispensable for posterior movement once it has crossed the r4/5 border. In other cases the single r5 neuron will have been a CEN, allowing us to conclude further that the first CEN to migrate in r5 does not have pioneer function. However, the results of our two-neuron ablation experiments leave open the possibility that the presence of a CEN has some influence on FBMN/REN migration. While two-cell ablations result in a severe block to migration, the bulk of this effect likely stems from removal of an r4-derived pioneer rather than an r5-localized CEN. Instead of requiring contact with a CEN to migrate, we suggest that the FBMN/REN pioneer may use such contacts as just one of several mechanisms that enable it to cross the r4/5 border.

3.5 Discussion

In this study, we have shown that rhombencephalic OENs arise in two distinct locations. RENs are born in r4 with the FBMNs, while CENs are born in r5. The same *hox* genes that influence the segmental identity of motor neuron populations in the hindbrain also govern aspects of OEN identity, with REN soma location and axon morphology depending on expression of *hoxb1a* in r4. We observe that the migration of both OEN populations occurs between 18 and 48 hpf, concurrent with migration of the FBMNs. Unlike the FBMNs, however, neither RENs nor CENs need Pk1b function to migrate, and CENs also appear to migrate independently of the pioneer neuron. Together, these results suggest that OENs migrate through the hindbrain using a different set of mechanisms than those employed by

FBMNs.

To our knowledge, this study provides the first comprehensive description of the birthplaces and early movements of rhombencephalic OENs. While this group of sensory efferents has been examined in a variety of aquatic organisms [20], previous studies were limited by a lack of specific markers for OENs. Consequently, researchers identified OENs via backfilling from the periphery, restricting observation of this cell type to the developmental stages after its projections have reached terminal end organs [23, 132, 175]. Here, we circumvent this limitation by photoconverting single Isl1(+) neurons starting at 18 hpf and using the persistent red form of Kaede to identify OENs based on axon morphology. We demonstrate that RENs and CENs both begin their posterior migration by 18 hpf, making their tangential migration into r6 and r7 concurrent with that of the FBMNs. As previously observed, RENs form a tight cluster with the major motor nucleus of the FBMNs upon reaching r6, while CENs cluster with the minor motor nucleus of the FBMNs in anterior r7 [23, 132]. Crucially, we are able to photoconvert CENs in r5, placing the origin of this OEN population further anterior than previously postulated [175].

Our reconstructions of Isl1(+) cell birthplaces from time-lapse data also support an r5 origin for CENs. Isl1(+) cells have been backtracked in only one other study to date, which focused on the mediolateral rather than anteroposterior spread of FBMN birthplaces in Cdh2-deficient embryos [187]. Insights into the segmental origins of Isl1(+) neurons have otherwise been gained largely through genetic manipulations [72, 97, 126] or extrapolated from backfilling experiments [175]. Interestingly, Sapède and colleagues do posit that RENs and CENs have separate segmental origins, using cell soma locations at 24 and 72 hpf to conclude that CENs are born in r6 and later migrate to r7 [175]. Here, we are able to gain more insight into the early movements of CENs and directly visualize their birth in r5 at 13-14 hpf. We also find that migratory CENs begin sending projections laterally while still in r5, despite the fact that mature CENs use the r6 exit point. This implies some level of

axon remodeling between 18 and 48 hpf, likely influenced by the position of the developing ear as well as the r6 exit point already in use by the glossopharyngeal motor neurons (nIX).

These separate segmental origins are also corroborated by our knockdown experiments, in which we demonstrate that disruption of *hoxb1a* in r4 impacts REN, but not CEN, development. Experiments in multiple species including chick, mouse, and zebrafish have previously shown that Hoxb1 function is required both for the migration of FBMNs and the proper fasciculation of their projections [72, 78, 97, 126]. Of particular relevance to our study is the observation that Hoxb1 also impacts development of the vestibulocochlear efferent neurons in both chick and mouse [18, 78]. Our hoxb1a knockdowns in zebrafish support a model in which RENs, like vestibulocochlear efferents in amniotes, rely on *hoxb1a* to migrate.

To date, many authors have speculated that OENs are evolutionarily derived from FBMNs [25, 65, 130, 197]. Indeed, ablation of the inner ear afferents in mouse causes prospective efferents to re-route their axons in an FBMN-like manner [64, 117]. While our *hoxb1a* knockdowns and backtracking results support this interpretation of REN origins, CENs are likely derived from a different population of neurons within the branchiomotor column. Recent studies have lent credence to the idea that FBMNs are not the only motor neurons capable of routing to sensory hair cells, as motor neuron populations in the spinal cord and trunk can also re-route to innervate ectopic ears in *Xenopus laevis* embryos [51, 52]. Sapède and colleagues [175] argue that CENs may have arisen as a subset of the glossopharyngeal motor neurons (nIX), which migrate from r6 to r7. Based on our OEN birthplace reconstructions, we can instead suggest that the CENs may have arisen as a subset of the r5-derived abducens motor neurons (nVI), which despite being somatic motor neurons are cholinergic like the FBMNs [168]. While nVI are not labeled by available Islet1 transgenes, they do express Islet1 protein as assayed by immunolabeling [29]. Additional work will be needed to establish the relationship between these r5 and r6 motor neuron populations and the CENs.

Despite their common origins, our analysis of Pk1b-deficient embryos suggests that important differences exist between the migration of FBMNs and RENs. Pk1b is a core component of the planar cell polarity (PCP) pathway that also acts as a nuclear translocator of RE1-silencing transcription factor, or Rest [120, 119]. In FBMNs, Rest is required to repress terminal maturation genes during migration, keeping the neurons in an immature state until they reach r6 and r7 [110]. Here, we show that unlike FBMNs, both RENs and CENs migrate successfully in the absence of Pk1b. Pk1b-deficient FBMNs, however, are unable to follow RENs and CENs into r6. These results are particularly interesting when taken in context with the different birth times of CENs and FBMNs, described in Chapter 2. CENs are born later than most FBMNs, and the same may hold true for RENs. If all OENs are in fact younger than FBMNs, they may not yet need Rest—or Pk1b—to maintain them in an immature state during their migration. Our findings also concur with studies in mouse which show that FBMN, but not CVA, migration is perturbed in *Pk1b* homozygous mutants [221]. However, the contralateral projections of CVAs were occasionally lost in *Pk1b* mutants, suggesting that mouse CVAs may depend on the PCP functions of Pk1b for axon pathfinding [221]. In contrast, projections of RENs and CENs appear undisturbed in *pk1b*-deficient zebrafish. Conditional knockdowns and cell transplantation experiments may further clarify whether Pk1b is needed cell-autonomously or non-autonomously in each of these cell types.

Additional differences between FBMN and OEN migration are evident in their reliance on a pioneer. In a previous study, we demonstrated that the first Isl1(+) neuron to cross the r4/5 border acts as a pioneer neuron and is necessary to lead initial posterior migration of the FBMNs. Further, we established that the role of the pioneer is time-dependent, since leading cell ablations performed after 19 hpf did not impact FBMN migration [208]. Here, we add a spatial dimension to our understanding of the pioneer: ablation of a single neuron in r4 results in a severe migration defect, while ablation of a single neuron in r5 has no

significant effect. We consider these conditions comparable to our earlier 18 hpf and 19 hpf ablations, respectively. These results demonstrate that only an r4-derived neuron can act as a pioneer. Although it is possible that one of the RENs can fulfill this role, we consider it more likely that the pioneer is an FBMN. The *pk1b*-knockdown experiments we describe here support this conclusion: if the pioneer were a REN, we would expect the FBMNs to follow it into r6 even in the absence of *pk1b*. However, FBMNs remain clustered in r4 in *pk1b*-deficient embryos despite the successful posterior migration of the RENs.

While our two-cell ablations suggest that contacts between FBMN/RENs and CENs across the r4/5 border may not be essential to migration, our approach is limited by the lack of CEN-specific markers. Our membrane-targeted transgene allows us to identify CENs based on their placement in r5 and their lateral axon projections, but this distinction becomes much harder to make once FBMN/RENs reach r5 and begin to migrate alongside the CENs. As a result, we are unable to ablate all CENs and therefore cannot rule out the possibility that FBMN/RENs establish contact with CENs that begin their migration after our ablations have taken place. Moreover, the tracking data in Chapter 2 demonstrates that CENs are present in r5 starting at 14-15 hpf, even though they do not express *Tg(en.crest1-hsp70l:mKaede)* transgene until 18 hpf. Therefore, we also cannot rule out the possibility that FBMN/RENs are able to derive a migratory cue from CENs in these early stages, before our ablations take place.

Interestingly, the contacts we have documented between FBMN/RENs and CENs may help explain "escaper" phenotypes in Cdh2-deficient embryos. In wild-type embryos, Cdh2 is necessary for neuroepithelial cohesion, and it also appears to stabilize contacts between Isl1(+) neurons during their migration. Loss of these cell-cell interactions after global knockdown of Cdh2 causes FBMNs to cluster aberrantly in r4 and r5 [208, 187]. However, small groups of Isl(+) neurons can occasionally escape to r6 in Cdh2-deficient embryos [187, 208]. Our present study suggests that the transient contacts FBMN/RENs make with CENs across

the r4/5 border may, if stabilized, allow small numbers of r4-derived neurons escape with the CENs into r6. Alternately, all of these "escaper" neurons could be r5-derived CENs that migrate into r6 independently of Cdh2. In a recent study, Rebman and colleagues [165] also observed escaper cells after expression of a dominant-negative Cdh2 construct specifically in Isl(+) neurons. Replication of these results in embryos expressing a membrane-targeted transgene would provide insight into the projection patterns of escapers, and clarify whether CENs do indeed migrate independently of Cdh2.

The molecular mechanisms that guide OEN migration and axon routing remain incompletely understood. In this study, however, we have identified significant differences between the disposition and migration of FBMNs and OENs. We confirm that RENs are born alongside FBMNs in r4 and are specified by *hoxb1a*. In contrast, CENs arise in r5 from a different population of progenitors. Both RENs and CENs migrate independently of Pk1b, and their posterior movement also occurs independently from that of the FBMNs. Furthermore, CENs migrate independent of a pioneer. Taken together, our findings uncover several unique qualities of the OENs, and move us towards a better understanding of this rare cell type.

3.6 Methods

3.6.1 Transgenic lines and fish husbandry

Zebrafish (*Danio rerio*) were maintained according to IACUC-approved protocols. Embryos were raised in E3 solution (in mM: 5.0 NaCl, 0.17 KCl, 0.33 $CaCl_2$, 0.33 $MgSO_4$) at 21.5-28.5 °C and staged following standard morphological criteria [101]. Embryos analyzed at stages later than 24 hours post-fertilization (hpf) were treated with 0.2 mM 1-phenyl 2-thiourea (PTU; Sigma) to inhibit melanin synthesis. Transgenic and mutant lines used in this study include *Tg(en.crest1-hsp70l:mRFP, ch102)* [120], *Tg(h2az2a:h2az2a-GFP)* [155], *TgBAC(neurod:EGFP)nl1* [142], *Tg(isl1:GFP)* [90], and *pk1bf122* [119].

A new transgenic line, *Tg(en.crest1-hsp70l:mKaede, ch104)*, was established as follows: Primers containing SalI (FOR 5' TTAGTCGACATGAGTCTGATTAAACC AGAAAT 3') and BamHI (REV 5' TTC**ACACACGAGAGG**ACTGGATCCATT 3') restriction sites were used to PCR amplify a CaaX-modified variant of the photoconvertible protein Kaede [9], kindly provided by Drs. Clare Buckley and Jon Clarke. The part of the primer sequence complementary to the CaaX motif is indicated in bold. The resulting sequence was cloned downstream of the *zCREST1* enhancer (a subset of the *isl1* regulatory sequence) and hsp70l minimal promoter in a plasmid containing Tol2 transposon sequences [100, 119, 201]. We injected this construct as circular DNA into single-cell *AB embryos at a concentration of 80 ng/ul, together with 80 ng/ul of capped Tol2 transposase mRNA transcribed using the MEGAscript SP6 Kit (Ambion) according to manufacturer's instructions. Injected embryos were raised to adulthood. The progeny of these fish were screened for fluorescence and a single adult founder, selected for bright transgene expression, was outcrossed to generate a stable transgenic line.

3.6.2 3D-printed embryo molds

Three separate molds were designed to hold 8-10 embryos at the 18, 24, or 48 hpf stages, using TinkerCad and rendered in MeshLab. They were then 3D printed using acrylonitrile butadiene styrene (ABS) at the Polsky Exchange Fabrication Lab. Imprints of these molds were made with 3% agarose dissolved in E3, providing a semi-rigid structure that enabled rapid and reproducible orientation of embryos with the hindbrain in dorsal view for photoconversion experiments. Cast designs are open-source and hosted for download at the NIH 3D Print Exchange, accessible via https://3dprint.nih.gov/users/beiriger.

3.6.3 Photoconversions and data analysis

Photoconversions were performed on a Zeiss LSM 710 upright confocal microscope (Carl Zeiss Microscopy, Thornwood, NY) using a 40x/1.0 W Plan-Apochromat objective. A region of interest (ROI) was selected and repeatedly scanned with 405 nm light until the majority of green fluorescent Kaede protein in a given structure had been converted by photo-cleavage to the red fluorescent form [9]. It should be noted that despite careful ROI selection, the close proximity of individual neurons can on occasion lead to partial photoconversion of Kaede in adjacent neurons, due to scattering of UV light within the tissue. For these reasons, converted neurons were identified not only based on the strength of signal in the red channel, but also the absence of signal in the green channel. At 48 hpf, confocal stacks were collected from converted embryos, and the location and morphology of red-labelled neurons was recorded.

3.6.4 Single-plane illumination microscopy and cell tracking

Zebrafish embryos were staged to 10 hpf and mounted in Fluorostore Fractional FEP Tubing (F018153-5) using a modified multilayer technique [99]. Embryos were immobilized using 0.3% agarose (Invitrogen UltraPure Agarose #16500) dissolved in E3 medium and 0.2 mg/ml tricaine, and the FEP tubing was capped with a 1.2% agarose plug. Embryos were incubated at 28.5°C during data collection. Images were captured with a Zeiss Lightsheet Z.1 Selective Plane Illumination microscope (Carl Zeiss Microscopy, Thornwood, NY) with tandem PCO.edge sCMOS cameras (PCO.Imaging, Kelheim, Germany) and Zeiss Zen imaging software. A 20x/1.0 long working distance detection objective was used alongside a pair of 10x/0.2 dry illumination objectives, and the excitation sheet was narrowed to 2.0 μm. Volumes were acquired every two minutes between 11-23 hpf, with 10 ms exposure per slice for both green (488 nm, 7.5%) and red (561 nm, 7.0%) channels.

Cell tracks were manually reconstructed using the mTrackJ plugin in FIJI [129]. Data were exported to a custom Python script which is described at length in Chapter 2, Section

2.5.3.

3.6.5 Cell ablation experiments

Cell ablation experiments were performed as previously described [208], using an inverted Leica SP5 Tandem Scanner Spectral 2-photon confocal microscope (Leica Microsystems, Inc., Buffalo Grove, IL). Phenotypes were scored on a Zeiss LSM 710 upright confocal microscope (Carl Zeiss Microscopy, Thornwood, NY) using a 40x/1.0 W Plan-Apochromat objective. We note that the configurations of these particular microscopes produce mirror images; thus care was taken to ensure phenotypes were correctly assigned to right- and left-hand sides of the specimen before quantification. Ablation phenotypes were quantified with one-way ANOVA tests performed using GraphPad Prism version 7.00 for Windows, GraphPad Software, La Jolla California USA, www.graphpad.com.

Corrections for the number of CENs in r6 were made as follows: in each embryo with no ablation or an r4-only ablation, 2-3 cells were subtracted from the r6 totals; in each embryo with an r5-only or two-cell ablation, 1-2 cells were subtracted from r6 totals. The higher number was subtracted only in rare cases where 10 or more neurons were visible in r6. These corrections are based on the number of r5-derived CENs visible per hemibrain at 22-24 hpf (see Chapter 2) and assume that a single CEN was ablated in the r5-only and two-cell ablation conditions.

3.6.6 Morpholino injections

Morpholino oligonucleotides (MOs) used in this study have been previously described. These include start-codon targeting morpholinos to *hoxb1a* [126] and splice-blocking morpholinos targeting *pk1b* [169]. All morpholinos were synthesized by Genetools, LLC and solubilized in water to a stock concentration of 10 ng/nl. Single-cell embryos were injected at a concentration of 4 ng/embryo for *hoxb1a* knockdowns and 2.5 ng/embryo for *pk1b* knockdowns.

We did not observe any off-target phenotypes in morpholino-injected embryos.

CHAPTER 4

CONCLUSIONS AND FUTURE DIRECTIONS

4.1 Conclusions

In the last two chapters, I have presented findings on the developmental relationship between the facial branchiomotor neurons (FBMNs) and octavolateral efferent neurons (OENs) in zebrafish hindbrain. In this section, I will summarize the conclusions that can be drawn from my work.

In mouse and chick, sensory efferents of the VIIIth nerve, known as the contralateral vestibuloacoustic efferents (CVAs), are specified together with the FBMNs in r4 by the homeodomain transcription factor Hoxb1 [25, 154, 197, 185, 173]. Consistent with these reports, the rostral (REN) group of OENs in zebrafish is born in the ventral part of r4 alongside the more numerous FBMNs, beginning at 11 hpf and continuing until at least 16 hpf. Perturbing Hoxb1a function prevents them from migrating posteriorly into r6, and it also causes them to dramatically reduce their innervation of the ear. In contrast, the caudal (CEN) group of OENs has a spatially, temporally, and molecularly distinct origin. CENs are born in r5 between 15 and 16 hpf, and as such are unaffected by knockdown of *hoxb1a*.

The divisions that give rise to FBMNs and OENs occur almost exclusively at the developing apical plane of the hindbrain, with the more basally-located daughter generally taking on an efferent fate. Sisters of FBMNs and OENs cross the midline and integrate contralaterally into the neuroepithelium through a process known as c-division [193, 26]. These results provide more evidence that in addition to driving morphogenesis of the neural tube and expanding the progenitor pool, c-divisions at neural plate and keel stages can also be neurogenic in nature.

After their births in r4 and r5, RENs and CENs migrate tangentially alongside the FBMNs between 18 and 48 hpf. Previous work has indicated that a pioneer neuron leads

the migration of FBMNs across the r4/5 border [209]. Here, I show that the pioneer makes contact with the axonal arbor of a CEN across the r4/5 border, but this contact does not appear to be necessary for successful migration of the FBMNs into r5. Regardless, CENs often take the leading position during migration through r5 and r6. Between 20 and 24 hpf, CENs begin routing their axons towards the r6 exit point, although there is significant bilateral asymmetry in the timing of this outgrowth. Unlike the FBMNs, neither RENs nor CENs rely on the PCP factor Prickle1b to migrate. These findings indicate that FBMNs and OENs are molecularly distinct before they begin their migration, and provide additional evidence that these two cell populations are unable to migrate collectively.

4.2 Future Directions

4.2.1 Origins of the CENs

The data that I have presented in Chapters 2 and 3 demonstrate that CENs are born more posteriorly than FBMNs and RENs. Both my backtracking experiments and photoconversions suggest that CENs arise from r5. If we assume that CENs, similar to RENs, were re-routed from an ancestral motoneuron population, the most likely candidate appears to be the abducens motoneurons (nVI) which arise in both r5 and r6 in the zebrafish. The cholinergic nature of the nVI lends credence to this hypothesis [168], especially given that across taxa the vast majority of efferent neurons terminating on mechanosensory hair cells use acetylcholine as a primary neurotransmitter [183, 65].

However, several important caveats exist to this line of reasoning. The nVI are somatomotor neurons, and as such their projections exit the brain near the floor plate. CEN axons, on the other hand, leave the brain using the same dorsally located r6 exit point as the glossopharyngeal motor neurons (nIX). Additionally, the nVI do not perform a caudal migration, instead remaining in their rhombomere of origin [29]. The nIX, on the other hand, appear

to undergo a caudal migration into r7 [28]. As such, the CENs behave more similarly to the nIX than the nVI.

A re-examination of the literature on nIX development in zebrafish reveals that very little is known about their caudal migration. Unsurprisingly, there is not a detailed analysis of their migration in live embryos, given that existing transgenic lines which label the nIX also label the far more numerous nVII that migrate along the same pathway. Instead, the migration of the nIX is surmised based on the genu formed by their axons, which is characteristic of caudally migrating cell types such as the FBMNs [29, 28]. They are widely considered to arise in r6 in zebrafish, based on analysis of the *valentino* mutant [29]. However, *valentino* disrupts patterning in both r5 and r6 [162, 134]. Could it be, then, that the CENs arise together with the nIX in r5, and both migrate caudally into r7? While this deviates from the expected two-segment periodicity of cranial motor neuron development in the hindbrain [135], it is not without precedent, as chick r7 gives rise to both nIX and vagal (nX) motor neurons [113].

Visualizing the origins of the nIX would provide the same challenges that we encountered in our OEN studies, but insights could be gained by using the *Tg(en.crest1-hsp70l:mKaede)* line in a manner similar to that described in 3. Isl1(+) cells would be photoconverted in either r5 or r6, creating a snapshot of cell identities within that rhombomere at a given developmental stage. These identities would then be interpreted by analysis of cell projection patterns at 48 hpf. In a similar manner, molecular data might provide clues into the connections between various Isl1(+) cell types residing in r7: in zebrafish, the cell adhesion molecule TAG-1 has been shown to label nVII, while Dm-Grasp (recognized by the Zn5 antibody in zebrafish) and and the tyrosine kinase receptor Met label nVI [211, 53]. A combination of *in situ* hybridization and antibody staining using these and other markers may help identify similarities between CENs and other cranial motor neuron populations.

4.2.2 Specification of the CENs

Recent work has shown that the development of vestibulocochlear efferent sub-populations in amniotes is impacted by several segmental identity genes in addition to Hoxb1. Specifically, Hoxa2 and Hoxb2 in mouse help specify distinct auditory derivatives in r2-r5, such as the cochlear nuclear complex and superior olivary complex [46]. The data presented in Chapter 3 suggests that the two sub-populations of rhombencephalic zebrafish OENs are also differentially regulated by *hox* gene expression. Whereas RENs are impacted by *hoxb1a* knockdown, CENs are undisturbed. How is CEN identity genetically controlled within r5? Reasonable candidates for the specification of CENs would be the *hox* group 3 genes, *hoxa3a/hoxb3a*. In zebrafish, both of these genes are expressed strongly in r5 and r6 [162, 196], whereas the anterior limit of *hoxd3a* lies in r6 [162, 196, 116]. In mouse, knocking out *Hoxa3* leads to truncation of the glossopharyngeal (IX) nerve, while knocking out both *Hoxa3* and *Hoxb3* also leads to loss of the abducens (nVI) motor neurons and the Olig2+ precursors from which they develop [69]. Moreover, ectopic expression of *Hoxa3* in the anterior hindbrain of the chick is sufficient to specify nVI in r1-4 [82].

To test the hypothesis that *hoxa3a* and *hoxb3a* may also control the specification of CENs, I performed a series of preliminary experiments using anti-sense morpholinos to knockdown both transcripts in line with previously published parameters [92]. However, while double morphants exhibited significant disorganization of the motor column, CEN axons were still visible exiting the brain laterally from r6 (data not shown). These results are perhaps unsurprising when taken in context with work showing that oculomotor circuitry, including nVI function, is unperturbed in *hox* group 3 deficient embryos [116]. This study did not examine nIX phenotypes. However, it does indicate that the roles of the *hox* group 3 genes in patterning the nVI may differ between zebrafish and mouse. The aforementioned study also examines zebrafish *valentino* mutants, noting that nVI appear to develop normally [116], in contrast to previous reports [134]. Further work will be needed to clarify whether *valentino*

or other genes segmentally expressed in r5, such as *krox20*, play a role in CEN development.

4.2.3 Molecular differences between RENs and FBMNs

In mammals, studies suggest that CVAs and FBMNs may be molecularly distinct by the time they become post-mitotic, as they begin to segregate from each other through differential migration early in embryonic development [184, 25, 62]. Mouse CVAs migrate laterally within the brain, whereas FBMNs migrate tangentially towards the posterior. Zebrafish RENs are unique from CVAs in this respect, migrating tangentially alongside the FBMNs into r6 and segregating from the main fascicle of the FBMNs only after their axons exit the hindbrain together in r4. Regardless, RENs display some early molecular differences from FBMNs. Namely, they do not appear to need function of Pk1b to migrate: in its absence, RENs can still move tangentially through the hindbrain, whereas FBMNs are aberrantly confined to r4. Other molecular differences between the two populations in zebrafish are unknown.

In fact, very little is known about the molecular differences that underlie the differential migration and projection patterns of these two cell populations in any species [65]. One of the few candidates is the GATA family of transcription factors. In amniotes, several studies have implicated the GATA proteins in CVA development: GATA-3 is necessary for proper axon pathfinding of mouse efferents, as well as the lateral migration of their cell bodies within the hindbrain [98, 152]. Meanwhile, GATA-2 is expressed by chick efferents that translocate across the midline to project contralaterally to their targets [18]. The basic heix-loop-helix gene *Ascl1* also plays a role in CVA pathfinding in mouse, and in its absence CVAs fail to project contralaterally [197]. In preliminary experiments using a Gata3 antibody in zebrafish, I did not observe OEN-specific labeling at 24 or 48 hpf. However, the potential roles of the GATA transcription factors and Ascl1 in zebrafish OEN development are worth more complete investigation.

In addition to taking this kind of candidate-based approach, a more comprehensive un-

derstanding of the molecular differences between these cell types could be gained through RNA sequencing. The lack of markers specific for otic and lateral line efferents complicates a study of this nature, but strategic backfilling from the periphery could provide different fluorescent labels for the sensory efferents and FBMNs. This type of approach will limit temporal sampling of the CVAs/OENs to stages when they have already integrated with their targets, but may still provide interesting insights. In zebrafish, the low numbers of OENs per specimen also create complications for sequencing. However, low input RNA-seq has become more accessible in recent years [2, 226, 157, 158], and could be used to amplify material from this rare cell type. Low-input RNA-seq is not without significant drawbacks [164, 22, 148, 172], but a cleverly designed study of this nature could provide unparalleled insights into the biology of CVAs/OENs.

4.2.4 Recruitment of OENs from motoneuron populations

The developmental connections between the FBMNs and inner ear efferents (IEEs), including the CVAs in amniotes and the OENs in anamniotes, are through to reflect ancient evolutionary ones. As discussed to in Chapter 3, studies done on both CVAs and OENs have led many researchers to conclude that IEEs comprise a subset of the branchiomotor column that was re-routed to innervate the ear and lateral line [167, 65, 183]. This hypothesis explains the overwhelming molecular similarities between cranial BMNs and IEEs, common responsiveness to acetylcholine, and related projection pathways [166].

Indeed, recent experiments have provided evidence that all motoneurons, not just FBMNs, have the ability to re-route to mechanosensory hair cells such as those present in the inner ear and lateral line. Ectopic ears transplanted along the trunk of *X. laevis* were able to effectively re-route both somatomotor and visceromotor neurons of the spinal cord [51, 52]. My findings in Chapter 2 support this conclusion, suggesting that CENs were re-routed from a second motoneuron population within r5 much in the same way that RENs were re-routed

from the visceromotor FBMNs (nVII). Interestingly, in a comparison with other transplanted tissues, Elliot and colleagues note that the ear is uniquely able to be innervated by multiple types of motoneurons [52]. These results provide some insight into the developmental plasticity that may have allowed motoneurons to acquire novel targets over the course of evolutionary time.

However, very little is known about the mechanisms that allow motoneurons to re-route to mechanosensory hair cells. Is there an attractive cue to which they respond? The re-routing of the FBMNs to the inner ear is fairly intuitive in this context, given the placement of the ear alongside the root of the facial nerve. However, in cases where the acquired target is farther away from the efferent nucleus providing innervation, why do some motoneurons respond preferentially over others? The re-routing of cranial motoneurons to the lateral line raises such questions, given that the complex, branching axonal arbors of the OENs often reach targets located at substantial distances from the brainstem. Some insights could perhaps be gained from observing the timing of OEN outgrowth relative to afferent fiber development. In their transplants, Elliot and colleagues note that afferent fibers from ectopic ears can project to novel areas of the brain, often fasciculating with the nearest cranial nerves [52]. Conversely, the ablation of inner ear afferent fibers in mouse causes IEEs to project with the FBMNs rather than into the ear [117]. In the zebrafish, the ganglia of the lateral line lie alongside the hindbrain, and our incrosses of the transgenic lines *Tg(en.crest1-hsp70l:mKaede)* and *TgBAC(neurod:EGFP)nl1*, discussed in Chapter 3, show that CEN axons route through the PLL ganglion after exiting the brain, confirming the careful reconstructions of OEN projection patterns made by Metcalfe and colleagues [132]. From there, CENs may grow down afferent fibers to reach the hair cells of the posterior lateral line. Some insights into the signaling pathways responsible for their pathfinding behaviors might be gleaned from the sequencing experiments described above; regardless, these broad questions about developmental recruitment of motoneurons to novel targets have the

potential to shed light on possible mechanisms underlying the evolution of CVAs and OENs.

4.2.5 Effective implementation of single-plane illumination microscopy (SPIM) in the zebrafish

Lineage reconstruction via single-plane illumination microscopy (SPIM) is a powerful technique that allows for the examination of cell populations that 1) may not have a cell type specific marker or 2) may comprise multiple cell types labeled with the same marker. As opposed to standard confocal imaging, SPIM can rapidly acquire large volumes, allowing for greater temporal resolution. Additionally, by scanning a narrow light path through the plane of interest, it allows for high quality optical sectioning without photobleaching. As such, it is ideal for capturing rapid cell dynamics over long developmental timescales.

SPIM has been used in a variety of organisms to date, including the zebrafish. However, many zebrafish studies have focused on global dynamics of cells in the early embryo [34] or superficial cell types such as the lateral plate mesoderm [163]. As discussed in Chapter 2, the applicability of SPIM to ventral cell populations in the zebrafish is complicated by multiple factors, including 1) scatter of the excitation illumination upon reaching the opaque zebrafish yolk, which reduces the amount of light reaching ventral fluorophores and 2) refraction of emitted light through biological tissue before reaching the detection objective. The latter is also an issue in confocal imaging, but use of a pinhole blocks collection of most out-of-focus light. For these purposes, optical sectioning of ventral structures in the confocal microscope is still superior, especially in cases where temporal resolution is not a limiting factor.

In cases where high temporal resolution is needed, these optical issues present significant hurdles to the accurate tracking of ventral cell populations in SPIM datasets. Thinner excitation sheets tend to provide better optical sectioning [67], but in our hands these modifications still failed to adequately resolve individual nuclei in densely packed tissues such as the zebrafish neuroepithelium. Researchers building their own systems can take advantage

of newer microscope designs that combine two-photon illumination with SPIM to provide vastly improved imaging of deep tissues [118, 199]. However, for those limited to a standard commercial lightsheet microscope, a combination of clever experimental design and advances in image processing techniques offers a way forward.

First, scatter-labeling cells of interest rather than using a ubiquitously expressed transgene will decrease the density of fluorescent nuclei and allow for more accurate reconstruction of cell movements. Injection of single cells with a fluoresent marker at the 16-32 cell stage should decrease label density sufficiently. This could be accomplished by injection of mRNA encoding a nuclear-targeted fluorophore, although this will generate a non-renewable supply of protein that may degrade or photobleach before the end of the experiment. Conversely, injection of a Tol2 construct encoding a similar fluorophore would allow for continuous production of protein, but the efficiency of its uptake may vary between specimens. Scatter-labeling does present complications for the tracking of rare cell types, which may not be adequately sampled with a stochastic labeling method. In this case, use of a multi-color transgenic label such as Brainbow may offer a way forward [146], although the ability of a given system to handle multi-color imaging will vary.

Second, newer methods in deconvolution, including techniques adapted from medical image analysis [83, 225], are making deconvolution more tractable for larger datasets. Deconvolution attempts to mathematically restore out of focus light to its point of origin based on the optical aberrations generated by a particular imaging system [176]. Traditionally, deconvolution is a computationally intensive task requiring iterative processing of a given image, making it difficult to scale up to large, multi-terabyte datasets such as those generated through SPIM [34, 220]. Newer techniques have dramatically reduced the number of iterations needed to accurately deconvolve microscope data, making it easier to apply these methods to SPIM [83]. Importantly, these techniques provide a way to deblur out of focus light near the zebrafish yolk, aiding in the tracking of ventral cell types.

Importantly, the combination of scatter-labeling and deconvolution may provide enough separation between labeled cells that applying automated tracking methods becomes more feasible in zebrafish. Several methods of automated tracking have been developed to date, using either nuclear or membrane labels to segment cells and track them through time [6, 7, 186, 109, 33]. I tested one of these automated tracking methods on the data shown in Chapter 2 [6]. However, I was unable to successfully apply this technique to our system. This was an unsurprising finding, given the difficulty of manual cell tracking and the number of informed decisions I needed to make to accurately reconstruct cell trajectories (detailed Chapter 2, Box 1). While some of these decisions could be trained into a machine learning algorithm, this option will not circumvent the need for cleaner data. As such, a combined workflow that includes scatter-labeling, adequately sampled images, and post-processing via deconvolution is most likely to lead to success with automated lineage reconstruction in the zebrafish. These kinds of combined biological and computational approaches have the potential to answer a wide range of questions about cell behaviors during morphogenesis, particularly over long developmental timescales. However, much work remains to be done in testing their tractability for the end user and ensuring their adoption broadly within the field.

References

[1] Suzan Abu-Abed, Pascal Dollé, Daniel Metzger, Barbara Beckett, Pierre Chambon, and Martin Petkovich. The retinoic acid-metabolizing enzyme, CYP26A1, is essential for normal hindbrain patterning, vertebral identity, and development of posterior structures. *Genes and Development*, 15(2):226–240, 1 2001.

[2] Xian Adiconis, Diego Borges-Rivera, Rahul Satija, David S. Deluca, Michele A. Busby, Aaron M. Berlin, Andrey Sivachenko, Dawn Anne Thompson, Alec Wysoker, Timothy Fennell, Andreas Gnirke, Nathalie Pochet, Aviv Regev, and Joshua Z. Levin. Comparative analysis of RNA sequencing methods for degraded or low-input samples. *Nature Methods*, 10(7):623–629, 7 2013.

[3] Raphal Aguillon, Julie Batut, Arul Subramanian, Romain Madelaine, Pascale Dufourcq, Thomas F. Schilling, and Patrick Blader. Cell-type heterogeneity in the early zebrafish olfactory epithelium is generated from progenitors within preplacodal ectoderm. *eLife*, 7, 1 2018.

[4] Amir Al Oustah, Cathy Danesin, Nagham Khouri-Farah, Marie Amlie Farreny, Nathalie Escalas, Philippe Cochard, Bruno Glise, and Cathy Soula. Dynamics of Sonic hedgehog signaling in the ventral spinal cord are controlled by intrinsic changes in source cells requiring Sulfatase 1. *Development (Cambridge)*, 141(6):1392–1403, 3 2014.

[5] Paula Alexandre, Alexander M. Reugels, David Barker, Eric Blanc, and Jonathan D.W. Clarke. Neurons derive from the more apical daughter in asymmetric divisions in the zebrafish neural tube. *Nature Neuroscience*, 13(6):673–679, 6 2010.

[6] Fernando Amat, Burkhard Höckendorf, Yinan Wan, William C. Lemon, Katie McDole, and Philipp J. Keller. Efficient processing and analysis of large-scale light-sheet microscopy data. *Nature Protocols*, 2015.

[7] Fernando Amat, William Lemon, Daniel P. Mossing, Katie McDole, Yinan Wan, Kristin Branson, Eugene W. Myers, and Philipp J. Keller. Fast, accurate reconstruction of cell lineages from large-scale fluorescence microscopy data. *Nature Methods*, 2014.

[8] Angel Amores, Allan Force, Yi Lin Yan, Lucille Joly, Chris Amemiya, Andreas Fritz, Robert K. Ho, James Langeland, Victoria Prince, Yan Ling Wang, Monte Westerfield, Marc Ekker, and John H. Postlethwait. Zebrafish hox clusters and vertebrate genome evolution. *Science*, 282(5394):1711–1714, 11 1998.

[9] Ryoko Ando, Hiroshi Hama, Miki Yamamoto-Hino, Hideaki Mizuno, and Atsushi Miyawaki. An optical marker based on the UV-induced green-to-red photoconversion of a fluorescent protein. *Proceedings of the National Academy of Sciences of the United States of America*, 99(20):12651–12656, 10 2002.

[10] Bruce Appel. Zebrafish neural induction and patterning. *Developmental Dynamics*, 219(2):155–168, 10 2000.

[11] Yoko Arai and Elena Taverna. Neural Progenitor Cell Polarity and Cortical Development. *Frontiers in cellular neuroscience*, 11:384, 2017.

[12] Claudio Araya, Hanna Maria Häkkinen, Luis Carcamo, Mauricio Cerda, Thierry Savy, Christopher Rookyard, Nadine Peyriéras, and Jonathan D.W. Clarke. Cdh2 coordinates Myosin-II dependent internalisation of the zebrafish neural plate. *Scientific Reports*, 9(1), 12 2019.

[13] Benjamin R. Arenkiel, Petr Tvrdik, Gary O. Gaufo, and Mario R. Capecchi. Hoxb1 functions in both motoneurons and in tissues of the periphery to establish and maintain the proper neuronal circuitry. *Genes and Development*, 18(13):1539–1552, 7 2004.

[14] Nikolaos Balaskas, Ana Ribeiro, Jasmina Panovska, Eric Dessaud, Noriaki Sasai, Karen M. Page, James Briscoe, and Vanessa Ribes. Gene regulatory logic for reading the sonic hedgehog signaling gradient in the vertebrate neural tube. *Cell*, 148(1-2):273–284, 1 2012.

[15] Beier Bao, Yingzi He, Dongmei Tang, Wenyan Li, and Huawei Li. Inhibition of H3K27me3 histone demethylase activity prevents the proliferative regeneration of Zebrafish lateral line neuromasts. *Frontiers in Molecular Neuroscience*, 10, 3 2017.

[16] Christine E Beattie, Kohei Hatta, Marnie E Halpern, Hongbo Liu, Judith S Eisen, and Charles B Kimmel. Temporal separation in the specification of primary and secondary motoneurons in zebrafish. *Developmental Biology*, 187(2):171–182, 1997.

[17] Curtis C. Bell. Central distribution of octavolateral afferents and efferents in a teleost (mormyridae). *Journal of Comparative Neurology*, 195(3):391–414, 1 1981.

[18] Esther Bell, Richard J.T. Wingate, and Andrew Lumsden. Homeotic transformation of rhombomere identity after localized Hoxb1 misexpression. *Science*, 284(5423):2168–2171, 6 1999.

[19] S Bingham, A Nasevicius, S C Ekker, and A Chandrasekhar. Sonic hedgehog and tiggy-winkle hedgehog cooperatively induce zebrafish branchiomotor neurons. *Genesis (New York, N.Y. : 2000)*, 30(3):170–4, 7 2001.

[20] J. H. S. Blaxter. Structure and Development of the Lateral Line. *Biological Reviews*, 62(4):471–514, 11 1987.

[21] H. Bleckmann, U. Niemann, and B. Fritzsch. Peripheral and central aspects of the acoustic and lateral line system of a bottom dwelling catfish, Ancistrus sp. *Journal of Comparative Neurology*, 314(3):452–466, 12 1991.

[22] Philip Brennecke, Simon Anders, Jong Kyoung Kim, Aleksandra A Kołodziejczyk, Xiuwei Zhang, Valentina Proserpio, Bianka Baying, Vladimir Benes, Sarah A Teichmann, John C Marioni, and Marcus G Heisler. Accounting for technical noise in single-cell RNA-seq experiments. *Nature Methods*, 10(11):1093–1098, 11 2013.

[23] Olivier Bricaud, Vicky Chaar, Christine Dambly-Chaudire, and Alain Ghysen. Early efferent innervation of the zebrafish lateral line. *Journal of Comparative Neurology*, 434(3):253–261, 6 2001.

[24] James Briscoe and Johan Ericson. Specification of neuronal fates in the ventral neural tube, 2001.

[25] L L Bruce, J Kingsley, D H Nichols, and B Fritzsch. The Development of Vestibulocochlear Efferents and Cochlear Afferents in Mice. Technical Report 5, 1997.

[26] Clare E Buckley, Xiaoyun Ren, Laura C Ward, Gemma C Girdler, Claudio Araya, Mary J Green, Brian S Clark, Brian A Link, and Jonathan D W Clarke. Mirror-symmetric microtubule assembly and cell interactions drive lumen formation in the zebrafish neural rod. *The EMBO Journal*, 32(1):30–44, 11 2012.

[27] Boris P. Chagnaud, Jacob Engelmann, Bernd Fritzsch, Joel C. Glover, and Hans Straka. Sensing External and Self-Motion with Hair Cells: A Comparison of the Lateral Line and Vestibular Systems from a Developmental and Evolutionary Perspective. *Brain, Behavior and Evolution*, 2017.

[28] Anand Chandrasekhar. Turning Heads: Development of Vertebrate Branchiomotor Neurons. *Developmental Dynamics*, 229(1):143–161, 2004.

[29] Anand Chandrasekhar, Charles Kimmel, and John Y Kuwada. Development of branchiomotor neurons in zebrafish. 1997.

[30] Anand Chandrasekhar, James T. Warren, Kana Takahashi, Heike E. Schauerte, Fredericus J.M. Van Eeden, Pascal Haffter, and John Y. Kuwada. Role of sonic hedgehog in branchiomotor neuron induction in zebrafish. *Mechanisms of Development*, 76(1-2):101–115, 8 1998.

[31] Prisca Chapouton and Laure Bally-Cuif. Neurogenesis. volume 76, pages 163–206. Academic Press, 1 2004.

[32] Sarah E. Cheesman, Michael J. Layden, Tonia Von Ohlen, Chris Q. Doe, and Judith S. Eisen. Zebrafish and fly Nkx6 proteins have similar CNS expression patterns and regulate motoneuron formation. *Development*, 131(21):5221–5232, 11 2004.

[33] Xiaowei Chen, Xiaobo Zhou, and Stephen T.C. Wong. Automated segmentation, classification, and tracking of cancer cell nuclei in time-lapse microscopy. *IEEE Transactions on Biomedical Engineering*, 53(4):762–766, 4 2006.

[34] Raghav K. Chhetri, Fernando Amat, Yinan Wan, Burkhard Höckendorf, William C. Lemon, and Philipp J. Keller. Whole-animal functional and developmental imaging with isotropic spatial resolution. *Nature Methods*, 12(12):1171–1178, 12 2015.

[35] Victor V. Chizhikov and Kathleen J. Millen. Roof plate-dependent patterning of the vertebrate dorsal central nervous system, 1 2005.

[36] Seong Kyu Choe, Nikolaos Vlachakis, and Charles G. Sagerström. Meis family proteins are required for hindbrain development in the zebrafish. *Development*, 2002.

[37] Brian Ciruna, Andreas Jenny, Diana Lee, Marek Mlodzik, and Alexander F. Schier. Planar cell polarity signalling couples cell division and morphogenesis during neurulation. *Nature*, 439(7073):220–224, 1 2006.

[38] Jon Clarke. Role of polarized cell divisions in zebrafish neural tube formation. *Current Opinion in Neurobiology*, 19(2):134–138, 2009.

[39] Julie E. Cooke, Hilary A. Kemp, and Cecilia B. Moens. EphA4 is required for cell adhesion and rhombomere-boundary formation in the zebrafish. *Current Biology*, 15(6):536–542, 3 2005.

[40] F. Coumailleau, M. Fürthauer, J. A. Knoblich, and M. González-Gaitán. Directional Delta and Notch trafficking in Sara endosomes during asymmetric cell division. *Nature*, 2009.

[41] Nicolas Cubedo, Emmanuel Cerdan, Dora Sapede, and Mireille Rossel. CXCR4 and CXCR7 cooperate during tangential migration of facial motoneurons. *Molecular and Cellular Neuroscience*, 40(4):474–484, 2009.

[42] Marc Davenne, Mark K Maconochie, Rdiger Neun, Alexandre Pattyn, Pierre Chambon, Robb Krumlauf, and Filippo M Rijli. Hoxa2 and Hoxb2 Control Dorsoventral Patterns of Neuronal Development in the Rostral Hindbrain. *Ericson Laboratory of Developmental Neurobiology et al*, 22:677–691, 1999.

[43] E. M. De Robertis. Spemann's organizer and the self-regulation of embryonic fields, 12 2009.

[44] Eric Dessaud, Andrew P McMahon, and James Briscoe. Pattern formation in the vertebrate neural tube: A sonic hedgehog morphogen-regulated transcriptional network, 8 2008.

[45] Eric Dessaud, Vanessa Ribes, Nikolaos Balaskas, Lin Lin Yang, Alessandra Pierani, Anna Kicheva, Bennett G. Novitch, James Briscoe, and Noriaki Sasai. Dynamic assignment and maintenance of positional identity in the ventral neural tube by the morphogen sonic hedgehog. *PLoS Biology*, 8(6), 6 2010.

[46] Maria Di Bonito, Yuichi Narita, Bice Avallone, Luigi Sequino, Marta Mancuso, Gennaro Andolfi, Anna Maria Franzè, Luis Puelles, Filippo M. Rijli, and Michle Studer. Assembly of the Auditory Circuitry by a Hox Genetic Network in the Mouse Brainstem. *PLoS Genetics*, 9(2):e1003249, 2 2013.

[47] V. Dubreuil, M. R. Hirsch, A. Pattyn, J. F. Brunet, and C. Goridis. The Phox2b transcription factor coordinately regulates neuronal cell cycle exit and identity. *Development*, 127(23):5191–5201, 2000.

[48] Vronique Dubreuil, Marie Rose Hirsch, Caroline Jouve, Jean Franois Brunet, and Christo Goridis. The role of Phox2b in synchronizing pan-neuronal and type-specific aspects of neurogenesis, 2002.

[49] Lori Dulabon, Eric C. Olson, Mary G. Taglienti, Scott Eisenhuth, Barbara McGrath, Christopher A. Walsh, Jordan A. Kreidberg, and E. S. Anton. Reelin binds $\alpha 3\beta 1$ integrin and inhibits neuronal migration. *Neuron*, 27(1):33–44, 2000.

[50] V. Dupé and A. Lumsden. Hindbrain patterning involves graded responses to retinoic acid signalling. *Development*, 128(12):2199–2208, 2001.

[51] Karen L. Elliott and Bernd Fritzsch. Transplantation of Xenopus laevis ears reveals the ability to form afferent and efferent connections with the spinal cord. *The International Journal of Developmental Biology*, 54(10):1443–1451, 2010.

[52] Karen L. Elliott, Douglas W. Houston, and Bernd Fritzsch. Transplantation of Xenopus laevis Tissues to Determine the Ability of Motor Neurons to Acquire a Novel Target. *PLoS ONE*, 8(2):e55541, 2 2013.

[53] Gina E. Elsen, Louis Y. Choi, Victoria E. Prince, and Robert K. Ho. The autism susceptibility gene met regulates zebrafish cerebellar development and facial motor neuron migration. *Developmental Biology*, 335(1):78–92, 11 2009.

[54] Yumi Emoto, Hironori Wada, Hitoshi Okamoto, Akira Kudo, and Yoshiyuki Imai. Retinoic acid-metabolizing enzyme Cyp26a1 is essential for determining territories of hindbrain and spinal cord in zebrafish. *Developmental Biology*, 278(2):415–427, 2 2005.

[55] Timothy Erickson, Laura M. Pillay, and Andrew J. Waskiewicz. Zebrafish Tshz3b negatively regulates hox function in the developing hindbrain. *Genesis*, 49(9):725–742, 9 2011.

[56] J Ericson, P Rashbass, A Schedl, S Brenner-Morton, A Kawakami, V. Van Heyningen, T. M. Jessell, and J Briscoe. Pax6 controls progenitor cell identity and neuronal fate in response to graded Shh signaling. *Cell*, 90(1):169–180, 7 1997.

[57] Johan Ericson, Susan Morton, Atsushi Kawakami, Henk Roelink, and Thomas M Jessell. Two critical periods of Sonic Hedgehog signaling required for the specification of motor neuron identity. *Cell*, 87(4):661–673, 11 1996.

[58] Johan Ericson, Stefan Thor, Thomas Edlund, Thomas M. Jessell, and Toshiya Yamada. Early stages of motor neuron differentiation revealed by expression of homeobox gene Islet-1. *Science*, 256(5063):1555–1560, 1992.

[59] Simone A. Fietz and Wieland B. Huttner. Cortical progenitor expansion, self-renewal and neurogenesis-a polarized perspective, 2 2011.

[60] Ake Flock and Jan Wersgll. A study of the orientation of the sensory hairs of the receptor cells in the lateral line organ of fish, with special reference to the function of the receptors. *Journal of Cell Biology*, 1962.

[61] Marta Florio and Wieland B. Huttner. Neural progenitors, neurogenesis and the evolution of the neocortex, 6 2014.

[62] B. Fritzsch and D. H. Nichols. DiI reveals a prenatal arrival of efferents at the differentiating otocyst of mice. *Hearing Research*, 65(1-2):51–60, 2 1993.

[63] B Fritzsch, U Pirvola, J Ylikoski, Bernd Fritzsch, Ulla Pirvola, and Jukka Ylikoski. Making and breaking the innervation of the ear: neurotrophic support during ear development and its clinical implications. Technical report, 1999.

[64] Bernd Fritzsch. Development of the Labyrinthine Efferent System. *Annals of the New York Academy of Sciences*, 781(1 Lipids and Sy):21–33, 6 1996.

[65] Bernd Fritzsch and Karen L. Elliott. Evolution and development of the inner ear efferent system: Transforming a motor neuron population to connect to the most unusual motor protein via ancient nicotinic receptors. *Frontiers in Cellular Neuroscience*, 11, 4 2017.

[66] Deni S. Galileo, John Majors, Alan F. Horwitz, and Joshua R. Sanes. Retrovirally introduced antisense integrin RNA inhibits neuroblast migration in vivo. *Neuron*, 9(6):1117–1131, 1992.

[67] Liang Gao. Optimization of the excitation light sheet in selective plane illumination microscopy. *Biomedical Optics Express*, 6(3):881, 3 2015.

[68] G O Gaufo, P Flodby, and M R Capecchi. Hoxb1 controls effectors of sonic hedgehog and Mash1 signaling pathways. *Development*, 127:5343–5354, 2000.

[69] Gary O. Gaufo, Kirk R. Thomas, and Mario R. Capecchi. Hox3 genes coordinate mechanisms of genetic suppression and activation in the generation of branchial and somatic motoneurons. 2003.

[70] Anthony Gavalas. ArRAnging the hindbrain, 2002.

[71] Anthony Gavalas, Marc Davenne, Andrew Lumsden, Pierre Chambon, and Filippo M. Rijli. Role of Hoxa-2 in axon pathfinding and rostral hindbrain patterning. *Development*, 124(19):3693–3702, 1997.

[72] Anthony Gavalas, Christiana Ruhrberg, Jean Livet, Christopher E. Henderson, and Robb Krumlauf. Neuronal defects in the hindbrain of Hoxa1, Hoxb1 and Hoxb2 mutants reflect regulatory interactions among these Hox genes. 2003.

[73] Elisabeth Georges-Labouesse, Manuel Mark, Nadia Messaddeq, and Anne Gansmüller. Essential role of α6 integrins in cortical and retinal lamination. *Current Biology*, 8(17):983–986, 8 1998.

[74] Alain Ghysen and Christine Dambly-Chaudière. Development of the zebrafish lateral line, 2004.

[75] James M. Gilchrist. Seventh cranial neuropathy, 2 2009.

[76] Edwin Gilland and R. Baker. Conservation of neuroepithelial and mesodermal segments in the embryonic vertebrate head. *Cells Tissues Organs*, 148(2-3):110–123, 1993.

[77] Joel C. Glover, Jean Sbastien Renaud, and Filippo M. Rijli. Retinoic acid and hindbrain patterning, 6 2006.

[78] Judy M. Goddard, Mireille Rossel, Nancy R. Manley, and Mario R. Capecchi. Mice with targeted disruption of Hoxb-1 fail to form the motor nucleus of the VIIth nerve. 1996.

[79] Judy M. Goddard, Mireille Rossel, Nancy R. Manley, and Mario R. Capecchi. Mice with targeted disruption of Hoxb-1 fail to form the motor nucleus of the VIIth nerve. *Development*, 122(10):3217–3228, 1996.

[80] Paul K Grant and Cecilia B Moens. The neuroepithelial basement membrane serves as a boundary and a substrate for neuron migration in the zebrafish hindbrain. *Neural Development*, 5(1):9, 3 2010.

[81] Michelle Gray, Cecilia B. Moens, Sharon L. Amacher, Judith S. Eisen, and Christine E. Beattie. Zebrafish deadly seven functions in neurogenesis. *Developmental Biology*, 237(2):306–323, 9 2001.

[82] Sonia Guidato, Fabrice Prin, and Sarah Guthrie. Somatic motoneurone specification in the hindbrain: The influence of somite-derived signals, retinoic acid Hoxa3. *Development*, 130(13):2981–2996, 7 2003.

[83] Min Guo, Yue Li, Yijun Su, Talley Lambert, Damian Dalle Nogare, Mark W. Moyle, Leighton H. Duncan, Richard Ikegami, Anthony Santella, Ivan Rey-Suarez, Daniel Green, Jiji Chen, Harshad Vishwasrao, Sundar Ganesan, Jennifer C. Waters, Christina M. Annunziata, Markus Hafner, William A Mohler, Ajay B Chitnis, Arpita Upadhyaya, Ted B Usdin, Zhirong Bao, Daniel Colón-Ramos, Patrick La Riviere, Huafeng Liu, Yicong Wu, Hari Shroff, Min Guo, Yue Li, Yijun Su, Talley Lambert,

Damian Dalle Nogare, Mark W. Moyle, Leighton H. Duncan, Richard Ikegami, Anthony Santella, Ivan Rey-Suarez, Daniel Green, Jiji Chen, Harshad Vishwasrao, Sundar Ganesan, Jennifer C. Waters, Christina M. Annunziata, Markus Hafner, William A Mohler, Ajay B Chitnis, Arpita Upadhyaya, Ted B Usdin, Zhirong Bao, Daniel Colón-Ramos, Patrick La Riviere, Huafeng Liu, Yicong Wu, and Hari Shroff. Accelerating iterative deconvolution and multiview fusion by orders of magnitude. *bioRxiv*, page 647370, 5 2019.

[84] Su Guo, Jennifer Brush, Hiroki Teraoka, Audrey Goddard, Stephen W. Wilson, Mary C. Mullins, and Arnon Rosenthal. Development of noradrenergic neurons in the zebrafish hindbrain requires BMP, FGF8, and the homeodomain protein soulless/Phox2a. *Neuron*, 24(3):555–566, 11 1999.

[85] Sarah Guthrie and Andrew Lumsden. Formation and regeneration of rhombomere boundaries in the developing chick hindbrain. Technical report, 1991.

[86] Michael J. Harrington, Kavita Chalasani, and Rachel Brewster. Cellular mechanisms of posterior neural tube morphogenesis in the zebrafish. *Developmental Dynamics*, 239(3):747–762, 3 2010.

[87] Mary E. Hatten. Central nervous system neuronal migration. *Annual Review of Neuroscience*, 22(1):511–539, 3 1999.

[88] B. Hellniann and B. Fritzsch. Neuroanatomical and histochemical evidence for the presence of common lateral line and inner ear efferents and of efferents to the basilar papilla in a frog, xenopus laevis. *Brain, Behavior and Evolution*, 47(4):185–194, 1 1996.

[89] Rafael E. Hernandez, Aaron P. Putzke, Jonathan P. Myers, Lilyana Margaretha, and Cecillia B. Moens. Cyp26 enzymes generate the retinoic acid response pattern necessary for hindbrain development. *Development*, 134(1):177–187, 1 2007.

[90] Shin Ichi Higashijima, Yoshiki Hotta, and Hitoshi Okamoto. Visualization of cranial motor neurons in live transgenic zebrafish expressing green fluorescent protein under the control of the Islet-1 promoter/enhancer. *Journal of Neuroscience*, 20(1):206–218, 1 2000.

[91] Tom W. Hiscock, Joel B. Miesfeld, Kishore R. Mosaliganti, Brian A. Link, and Sean G. Megason. Feedback between tissue packing and neurogenesis in the zebrafish neural tube. *Development (Cambridge)*, 145(9), 5 2018.

[92] Benjamin M. Hogan, Michael P. Hunter, Andrew C. Oates, Meredith O. Crowhurst, Nathan E. Hall, Joan K. Heath, Victoria E. Prince, and Graham J. Lieschke. Zebrafish gcm2 is required for gill filament budding from pharyngeal ectoderm. *Developmental Biology*, 276(2):508–522, 12 2004.

[93] Elim Hong and Rachel Brewster. N-cadherin is required for the polarized cell behaviors that drive neurulation in the zebrafish. *Development*, 133(19):3895–3905, 10 2006.

[94] C Irving and I Mason. Signalling by FGF8 from the isthmus patterns anterior hindbrain and establishes the anterior limit of Hox gene expression. *Development*, 127:177–188, 2000.

[95] William R Jackman, James A Langeland, and Charles B Kimmel. islet reveals segmentation in the amphioxus hindbrain homolog. *Developmental Biology*, 220(1):16–26, 2000.

[96] Linjia Jiang, Andres Romero-Carvajal, Jeff S. Haug, Christopher W. Seidel, and Tatjana Piotrowski. Gene-expression analysis of hair cell regeneration in the zebrafish lateral line. *Proceedings of the National Academy of Sciences of the United States of America*, 111(14), 2014.

[97] S Jungbluth, E Bell, and A Lumsden. Motor neuron identity and Hox genes. Technical report, 1999.

[98] Alar Karis, Illar Pata, J. Hikke Van Doorninck, Frank Grosveld, Chris I. De Zeeuw, Dominique De Caprona, and Bernd Fritzsch. Transcription factor GATA-3 alters pathway selection of olivocochlear neurons and affects morphogenesis of the ear. *Journal of Comparative Neurology*, 429(4):615–630, 1 2001.

[99] A. Kaufmann, M. Mickoleit, M. Weber, and J. Huisken. Multilayer mounting enables long-term imaging of zebrafish development in a light sheet microscope. *Development*, 139(17):3242–3247, 2012.

[100] Koichi Kawakami and Akihiro Shima. Identification of the Tol2 transposase of the medaka fish Oryzias latipes that catalyzes excision of a nonautonomous Tol2 element in zebrafish Danio rerio. *Gene*, 240(1):239–244, 11 1999.

[101] Charles B. Kimmel, William W. Ballard, Seth R. Kimmel, Bonnie Ullmann, and Thomas F. Schilling. Stages of embryonic development of the zebrafish. *Developmental Dynamics*, 203(3):253–310, 7 1995.

[102] Jonathan S. Kniss, Linjia Jiang, and Tatjana Piotrowski. Insights into sensory hair cell regeneration from the zebrafish lateral line, 10 2016.

[103] F. O. Kok, A. Taibi, S. J. Wanner, X. Xie, C. E. Moravec, C. E. Love, V. E. Prince, J. S. Mumm, and H. I. Sirotkin. Zebrafish rest regulates developmental gene expression but not neurogenesis. *Development*, 139(20):3838–3848, 2012.

[104] Daijiro Konno, Go Shioi, Atsunori Shitamukai, Asako Mori, Hiroshi Kiyonari, Takaki Miyata, and Fumio Matsuzaki. Neuroepithelial progenitors undergo LGN-dependent planar divisions to maintain self-renewability during mammalian neurogenesis. *Nature Cell Biology*, 10(1):93–101, 1 2008.

[105] Yoichi Kosodo, Katja Röper, Wulf Haubensak, Anne Marie Marzesco, Denis Corbeil, and Wieland B. Huttner. Asymmetric distribution of the apical plasma membrane during neurogenic divisions of mamalian neuroepithelial cells. *EMBO Journal*, 23(11):2314–2324, 6 2004.

[106] Sabine Kressmann, Claudia Campos, Irinka Castanon, Maximilian Fürthauer, and Marcos González-Gaitán. Directional Notch trafficking in Sara endosomes during asymmetric cell division in the spinal cord. *Nature Cell Biology*, 2015.

[107] Maria K. Lehtinen, Mauro W. Zappaterra, Xi Chen, Yawei J. Yang, Anthony D. Hill, Melody Lun, Thomas Maynard, Dilenny Gonzalez, Seonhee Kim, Ping Ye, A. Joseph D'Ercole, Eric T. Wong, Anthony S. LaMantia, and Christopher A. Walsh. The Cerebrospinal Fluid Provides a Proliferative Niche for Neural Progenitor Cells. *Neuron*, 69(5):893–905, 3 2011.

[108] Christoph Leucht, Christian Stigloher, Andrea Wizenmann, Ruth Klafke, Anja Folchert, and Laure Bally-Cuif. MicroRNA-9 directs late organizer activity of the midbrain-hindbrain boundary. *Nature Neuroscience*, 11(6):641–648, 6 2008.

[109] Kang Li, Eric D. Miller, Mei Chen, Takeo Kanade, Lee E. Weiss, and Phil G. Campbell. Cell population tracking and lineage construction with spatiotemporal context. *Medical Image Analysis*, 12(5):546–566, 10 2008.

[110] Crystal E. Love and Victoria E. Prince. Rest represses maturation within migrating facial branchiomotor neurons. *Developmental Biology*, 401(2):220–235, 2015.

[111] Laura Anne Lowery and Hazel Sive. Strategies of vertebrate neurulation and a reevaluation of teleost neural tube formation, 10 2004.

[112] Andrew Lumsden. Closing in on rhombomere boundaries. *Nature Cell Biology*, 1(4):E83–E85, 1999.

[113] Andrew Lumsden and Roger Keynes. Segmental patterns of neuronal development in the chick hindbrain. *Nature*, 337(6206):424–428, 1989.

[114] Andrew Lumsden and Robb Krumlauf. Patterning the vertebrate neuraxis, 11 1996.

[115] David A. Lyons, Adam T. Guy, and Jonathan D.W. Clarke. Monitoring neural progenitor fate through multiple rounds of division in an intact vertebrate brain. *Development*, 130(15):3427–3436, 8 2003.

[116] Leung Hang Ma, Charlotte L. Grove, and Robert Baker. Development of oculomotor circuitry independent of hox3 genes. *Nature Communications*, 5:4221, 6 2014.

[117] Qiufu Ma, David J Anderson, and Bernd Fritzsch. Neurogenin 1 null mutant ears develop fewer, morphologically normal hair cells in smaller sensory epithelia devoid of innervation. *JARO - Journal of the Association for Research in Otolaryngology*, 1(2):129–143, 2000.

[118] Pierre Mahou, Julien Vermot, Emmanuel Beaurepaire, and Willy Supatto. Multicolor two-photon light-sheet microscopy, 5 2014.

[119] O. M. Mapp, G. S. Walsh, C. B. Moens, M. Tada, and V. E. Prince. Zebrafish Prickle1b mediates facial branchiomotor neuron migration via a farnesylation-dependent nuclear activity. *Development*, 138(10):2121–2132, 2011.

[120] Oni M. Mapp, Sarah J. Wanner, Monica R. Rohrschneider, and Victoria E. Prince. Prickle1b mediates interpretation of migratory cues during zebrafish facial branchiomotor neuron migration. *Developmental Dynamics*, 239(6):1596–1608, 6 2010.

[121] Giovanni Marchetti, Sarah Escuin, Arjan Van Der Flier, Adle De Arcangelis, Richard O. Hynes, and Elisabeth Georges-Labouesse. Integrin $\alpha5\beta1$ is necessary for regulation of radial migration of cortical neurons during mouse brain development. *European Journal of Neuroscience*, 31(3):399–409, 2 2010.

[122] O. Marín, A. Yaron, A. Bagri, M. Tessier-Lavigne, and J. L.R. Rubenstein. Sorting of striatal and cortical interneurons regulated by semaphorin-neuropilin interactions. *Science*, 293(5531):872–875, 8 2001.

[123] Heather Marshall, Michle Studer, Heike Pöpperl, Sam Aparicio, Atsushi Kuroiwa, Sydney Brenner, and Robb Krumlauf. A conserved retinoic acid response element required for early expression of the homeobox gene Hoxb-1. *Nature*, 370(6490):567–571, 1994.

[124] Heather A. Mason, Susumu Ito, and Gabriel Corfas. Extracellular signals that regulate the tangential migration of olfactory bulb neuronal precursors: Inducers, inhibitors, and repellents. *Journal of Neuroscience*, 21(19):7654–7663, 10 2001.

[125] Kimberly L. McArthur and Joseph R Fetcho. Key Features of Structural and Functional Organization of Zebrafish Facial Motor Neurons Are Resilient to Disruption of Neuronal Migration. *Current Biology*, 27(12):1746–1756, 2017.

[126] J M McClintock, M A Kheirbek, and V E Prince. Knockdown of duplicated zebrafish hoxb1 genes reveals distinct roles in hindbrain patterning and a novel mechanism of duplicate gene retention. *Development*, 129:2339–2354, 2002.

[127] James M. McClintock. Zebrafish paralogue group 1 Hox genes. *Development*, 128:2471–2484, 2001.

[128] Rebecca McIntosh, Joseph Norris, Jon D Clarke, and Paula Alexandre. Spatial distribution and characterization of non-apical progenitors in the zebrafish embryo central nervous system. *Open biology*, 7(2), 2017.

[129] Erik Meijering, Oleh Dzyubachyk, and Ihor Smal. Methods for Cell and Particle Tracking. Technical Report 9, 2012.

[130] G E Meredith and B L Roberts. Central organization of the efferent supply to the labyrinthine and lateral line receptors of the dogfish. *Neuroscience*, 17(1):225–233, 1986.

[131] G. E. Meredith and B. L. Roberts. Distribution and morphological characteristics of efferent neurons innervating end organs in the ear and lateral line of the european eel. *Journal of Comparative Neurology*, 265(4):494–506, 11 1987.

[132] Walter K Metcalfe, Charles B Kimmel, and Eric Schabtach. Anatomy of the posterior lateral line system in young larvae of the zebrafish. *Journal of Comparative Neurology*, 233(3):377–389, 1985.

[133] Takaki Miyata, Mayumi Okamoto, Tomoyasu Shinoda, and Ayano Kawaguchi. Interkinetic nuclear migration generates and opposes ventricular-zone crowding: Insight into tissue mechanics, 1 2015.

[134] Cecilia Moens. valentino: a zebrafish gene required for normal hindbrain segmentation. *Development*, 1996.

[135] Cecilia B. Moens and Victoria E. Prince. Constructing the hindbrain: Insights from the zebrafish, 5 2002.

[136] Chrystelle Montagne and Marcos Gonzalez-Gaitan. Sara endosomes and the asymmetric division of intestinal stem cells. *Development (Cambridge)*, 141(10):2014–2023, 5 2014.

[137] Paul Z Myers, Judith S Eisen, and Monte Westerfield. Development and Axonal Outgrowth of Identified Motoneurons in the Zebrafish. *Journal of Neuroscience*, 6:2278–2269, 1986.

[138] Bagirathy Nadarajah, Janice E. Brunstrom, Jaime Grutzendler, Rachel O.L. Wong, and Alan L. Pearlman. Two modes of radial migration in early development of the cerebral cortex. *Nature Neuroscience*, 4(2):143–150, 2001.

[139] Yuichi Narita and Filippo M Rijli. Chapter 5 Hox Genes in Neural Patterning and Circuit Formation in the Mouse Hindbrain, 2009.

[140] Kwan L. Ng, Jia Da Li, Michelle Y. Cheng, Frances M. Leslie, Alex C. Lee, and Qun Yong Zhou. Neuroscience: Dependence of olfactory bulb neurogenesis on prokineticin 2 signaling. *Science*, 308(5730):1923–1927, 6 2005.

[141] Karen Niederreither, Julien Vermot, Brigitte Schuhbaur, Pierre Chambon, and Pascal Dollé. Retinoic acid synthesis and hindbrain patterning in the mouse embryo. *Development*, 127(1):75–85, 2000.

[142] Nikolaus Obholzer, Sean Wolfson, Josef G. Trapani, Weike Mo, Alex Nechiporuk, Elisabeth Busch-Nentwich, Christoph Seiler, Samuel Sidi, Christian Söllner, Robert N.

Duncan, Andrea Boehland, and Teresa Nicolson. Vesicular glutamate transporter 3 is required for synaptic transmission in zebrafish hair cells. *Journal of Neuroscience*, 28(9):2110–2118, 2 2008.

[143] Toshihiko Ogura and Ronald M. Evans. A retinoic acid-triggered cascade of HOXB1 gene activation. *Proceedings of the National Academy of Sciences of the United States of America*, 92(2):387–391, 1995.

[144] Toshihiko Ogura and Ronald M Evans. Evidence for two distinct retinoic acid response pathways for HOXB1 gene regulation. *Proceedings of the National Academy of Sciences of the United States of America*, 92(2):392–396, 1995.

[145] Nancy A. O'Rourke. Neuronal chain gangs: Homotypic contacts support migration into the olfactory bulb, 6 1996.

[146] Y. Albert Pan, Jean Livet, Joshua R. Sanes, Jeff W. Lichtman, and Alexander F. Schier. Multicolor brainbow imaging in Zebrafish. *Cold Spring Harbor Protocols*, 6(1):pdb.prot5546, 1 2011.

[147] Cyrus Papan and Jos A. Campos-Ortega. On the formation of the neural keel and neural tube in the zebrafish Danio (Brachydanio) rerio. *Roux's Archives of Developmental Biology*, 203(4):178–186, 1 1994.

[148] Swati Parekh, Christoph Ziegenhain, Beate Vieth, Wolfgang Enard, and Ines Hellmann. The impact of amplification on differential expression analyses by RNA-seq. *Scientific Reports*, 6(1):25533, 7 2016.

[149] Judith TML Paridaen and Wieland B Huttner. Neurogenesis during development of the vertebrate central nervous system. *EMBO reports*, 15(4):351–364, 4 2014.

[150] Hae Chul Park, Amit Mehta, Joanna S. Richardson, and Bruce Appel. olig2 is required for zebrafish primary motor neuron and oligodendrocyte development. *Developmental Biology*, 248(2):356–368, 2002.

[151] Hugo J. Parker and Robb Krumlauf. Segmental arithmetic: summing up the Hox gene regulatory network for hindbrain development in chordates. *Wiley Interdisciplinary Reviews: Developmental Biology*, 6(6), 2017.

[152] Illar Pata, Michele Studer, J. Hikke van Doorninck, James Briscoe, Sulev Kuuse, J. Douglas Engel, Frank Grosveld, and Alar Karis. The transcription factor GATA3 is a downstream effector of Hoxb1 specification in rhombomere 4 . 1999.

[153] Alexandre Pattyn, Marie Rose Hirsch, Christo Goridis, and Jean Franois Brunet. Control of hindbrain motor neuron differentiation by the homeobox gene Phox2b. *Development*, 127(7):1349–1358, 2000.

[154] Alexandre Pattyn, Xavier Morin, Harold Cremer, Christo Goridis, and Jean-Franois Brunet. Expression and interactions of the two closely related homeobox genes Phox2a and Phox2b during neurogenesis. 1997.

[155] Stefan Pauls, Benedikt Geldmacher-Voss, and Jos A. Campos-Ortega. A zebrafish histone variant H2A.F/Z and a transgenic H2A.F/Z:GFP fusion protein for in vivo studies of embryonic development. *Development Genes and Evolution*, 211(12):603–610, 2001.

[156] Polyxeni Philippidou and Jeremy S. Dasen. Hox Genes: Choreographers in Neural Development, Architects of Circuit Organization, 10 2013.

[157] Simone Picelli, sa K. Björklund, Omid R. Faridani, Sven Sagasser, Gsta Winberg, and Rickard Sandberg. Smart-seq2 for sensitive full-length transcriptome profiling in single cells. *Nature Methods*, 2013.

[158] Simone Picelli, Omid R. Faridani, sa K. Björklund, Gsta Winberg, Sven Sagasser, and Rickard Sandberg. Full-length RNA-seq from single cells using Smart-seq2. *Nature Protocols*, 2014.

[159] Heike Pöpperl, Holly Rikhof, Heather Cheng, Pascal Haffter, Charles B. Kimmel, and Cecilia B. Moens. Iazarus is a novel pbx gene that globally mediates hox gene function in zebrafish. *Molecular Cell*, 6(2):255–267, 8 2000.

[160] Victoria E. Prince. The Hox paradox: More complex(es) than imagined. *Developmental Biology*, 249(1):1–15, 9 2002.

[161] Victoria E Prince, Lucille Joly, Marc Ekker, and Robert K. Ho. Zebrafish hox genes: Genomic organization and modified colinear expression patterns in the trunk. *Development*, 125(3):407–420, 1998.

[162] Victoria E Prince, Cecilia B Moens, Charles B Kimmel, and Robert K Ho. Zebrafish hox genes: Expression in the hindbrain region of wild-type and mutants of the segmentation gene, valentino. *Development*, 125(3):393–406, 1998.

[163] Karin Dorien Prummel, Christopher Hess, Eline Brombacher, Anastasia Felker, and Christian Mosimann. Charting cell migration dynamics during lateral plate mesoderm patterning in zebrafish using lightsheet microscopy. *Mechanisms of Development*, 145:S79–S80, 7 2017.

[164] Shenfeng Qiu, Shujun Luo, Oleg Evgrafov, Robin Li, Gary P. Schroth, Pat Levitt, James A. Knowles, and Kai Wang. Single-neuron RNA-Seq: Technical feasibility and reproducibility. *Frontiers in Genetics*, 3(JUL):124, 7 2012.

[165] Jane K. Rebman, Kathryn E. Kirchoff, and Gregory S. Walsh. Cadherin-2 Is Required Cell Autonomously for Collective Migration of Facial Branchiomotor Neurons. *PLOS ONE*, 11(10):e0164433, 10 2016.

[166] Barry L. Roberts and Gloria E. Meredith. The Efferent System. In *The Mechanosensory Lateral Line*, pages 445–459. Springer New York, 1989.

[167] Barry L. Roberts and Gloria E. Meredith. The Efferent Innervation of the Ear: Variations on an Enigma. In *The Evolutionary Biology of Hearing*, pages 185–210. Springer New York, 1992.

[168] L Rodella, R Rezzani, M. Gioia, and R Bianchi. Immunohistochemical Study of the Neurons Projecting to the Flocculus in the Abducens Nucleus of the Rat: A Double-Labelling Study. *Journal of Anatomy*, 152(4):262–262, 1995.

[169] Monica R. Rohrschneider, Gina E. Elsen, and Victoria E. Prince. Zebrafish Hoxb1a regulates multiple downstream genes including prickle1b. *Developmental Biology*, 309(2):358–372, 9 2007.

[170] Mireille Rossel and Mario R. Capecchi. Mice mutant for both Hoxa1 and Hoxb1 show extensive remodeling of the hindbrain and defects in craniofacial development. *Development*, 126(22):5027–5040, 1999.

[171] Yavuz Sahin, Olcay Güngör, Akif Ayaz, Glay Güngör, Bedia Sahin, Kursad Yaykasli, and Serdar Ceylaner. A novel homozygous HOXB1 mutation in a Turkish family with hereditary congenital facial paresis. *Brain and Development*, 39(2):166–170, 2017.

[172] Antoine Emmanuel Saliba, Alexander J. Westermann, Stanislaw A. Gorski, and Jrg Vogel. Single-cell RNA-seq: Advances and future challenges. *Nucleic Acids Research*, 42(14):8845–8860, 2014.

[173] Omar Abdel Samad, Marc J. Geisen, Giuliana Caronia, Isabelle Varlet, Vincenzo Zappavigna, Johan Ericson, Christo Goridis, and Filippo M. Rijli. Integration of anteroposterior and dorsoventral regulation of Phox2b transcription in cranial motoneuron progenitors by homeodomain proteins. *Development*, 131(16):4071–4083, 2004.

[174] Peter A. Santi. Light sheet fluorescence microscopy: A review. *Journal of Histochemistry and Cytochemistry*, 59(2):129–138, 2011.

[175] Dora Sapède, Mireille Rossel, Christine Dambly-Chaudière, and Alain Ghysen. Role of SDF1 chemokine in the development of lateral line efferent and facial motor neurons. *Proceedings of the National Academy of Sciences of the United States of America*, 102(5):1714–1718, 2 2005.

[176] Pinaki Sarder and Arye Nehorai. Deconvolution methods for 3-D fluorescence microscopy images, 2006.

[177] H E Schauerte, Fredericus J. M. van Eeden, Cornelia Fricke, Jrg Odenthal, Uwe Strähle, and Pascal Haffter. Sonic hedgehog is not required for the induction of medial floor plate cells in the zebrafish. *Development*, 1998.

[178] Judith Schenk, Michaela Wilsch-Bräuninger, Federico Calegari, and Wieland B. Huttner. Myosin II is required for interkinetic nuclear migration of neural progenitors. *Proceedings of the National Academy of Sciences of the United States of America*, 106(38):16487–16492, 9 2009.

[179] Quenten Schwarz, Chenghua Gu, Hajime Fujisawa, Kimberly Sabelko, Marina Gertsenstein, Andras Nagy, Masahiko Taniguchi, Alex L. Kolodkin, David D. Ginty, David T. Shima, and Christiana Ruhrberg. Vascular endothelial growth factor controls neuronal migration and cooperates with SemaSA to pattern distinct compartments of the facial nerve. *Genes and Development*, 18(22):2822–2834, 11 2004.

[180] Atsunori Shitamukai, Daijiro Konno, and Fumio Matsuzaki. Oblique radial glial divisions in the developing mouse neocortex induce self-renewing progenitors outside the germinal zone that resemble primate outer subventricular zone progenitors. *Journal of Neuroscience*, 31(10):3683–3695, 3 2011.

[181] Atsunori Shitamukai and Fumio Matsuzaki. Control of asymmetric cell division of mammalian neural progenitors, 4 2012.

[182] Julie A. Siegenthaler, Amir M. Ashique, Konstantinos Zarbalis, Katelin P. Patterson, Jonathan H. Hecht, Maureen A. Kane, Alexandra E. Folias, Youngshik Choe, Scott R. May, Tsutomu Kume, Joseph L. Napoli, Andrew S. Peterson, and Samuel J. Pleasure. Retinoic Acid from the Meninges Regulates Cortical Neuron Generation. *Cell*, 139(3):597–609, 10 2009.

[183] Ulrike J. Sienknecht, Christine Köppl, and Bernd Fritzsch. Evolution and development of hair cell polarity and efferent function in the inner ear. *Brain, Behavior and Evolution*, 83(2):150–161, 2014.

[184] Dwayne D Simmons. Development of the inner ear efferent system across vertebrate species, 2002.

[185] Horst Simon and Andrew Lumsden. Rhombomere-specific origin of the contralateral vestibulo-acoustic efferent neurons and their migration across the embryonic midline. *Neuron*, 11(2):209–220, 1993.

[186] Johannes Stegmaier, Fernando Amat, William C. Lemon, Katie McDole, Yinan Wan, George Teodoro, Ralf Mikut, and Philipp J. Keller. Real-Time Three-Dimensional Cell Segmentation in Large-Scale Microscopy Data of Developing Embryos. *Developmental Cell*, 36(2):225–240, 2016.

[187] Petra Stockinger, Jean Lon Maître, and Carl Philipp Heisenberg. Defective neuroepithelial cell cohesion affects tangential branchiomotor neuron migration in the zebrafish neural tube. *Development*, 138(21):4673–4683, 2011.

[188] M Studer. Initiation of facial motoneurone migration is dependent on rhombomeres 5 and 6. *Development*, 128:3707–3716, 2001.

[189] Michle Studer, Anthony Gavalas, Heather Marshall, Linda Ariza-McNaughton, Filippo M. Rijli, Pierre Chambon, and Robb Krumlauf. Genetic interactions between Hoxa1 and Hoxb1 reveal new roles in regulation of early hindbrain patterning. *Development*, 125(6):1025–1036, 1998.

[190] Michle Studer, Andrew Lumsden, Linda Ariza-McNaughton, Allan Bradley, and Robb Krumlauf. Altered segmental identity and abnormal migration of motor neurons in mice lacking Hoxb-1. *Nature*, 384(6610):630–634, 1996.

[191] Michle Studer, Heike Pöpperl, Heather Marshall, Atsushi Kuroiwa, and Robb Krumlauf. Role of a conserved retinoic acid response element in rhombomere restriction of Hoxb-1. *Science*, 265(5179):1728–1732, 1994.

[192] Elena Taverna and Wieland B. Huttner. Neural progenitor nuclei IN motion, 2010.

[193] Marcel Tawk, Claudio Araya, Dave A. Lyons, Alexander M. Reugels, Gemma C. Girdler, Philippa R. Bayley, David R. Hyde, Masazumi Tada, and Jonathan D W Clarke. A mirror-symmetric cell division that orchestrates neuroepithelial morphogenesis. *Nature*, 446(7137):797–800, 2007.

[194] Marcel Tawk, Claudio Araya, Dave A. Lyons, Alexander M. Reugels, Gemma C. Girdler, Philippa R. Bayley, David R. Hyde, Masazumi Tada, and Jonathan D.W. Clarke. A mirror-symmetric cell division that orchestrates neuroepithelial morphogenesis. *Nature*, 446(7137):797–800, 4 2007.

[195] Julia K. Terzis and Katerina Anesti. Developmental facial paralysis: A review. *Journal of Plastic, Reconstructive and Aesthetic Surgery*, 64(10):1318–1333, 10 2011.

[196] Pflumio S. Furthauer M. Loppin B. Heyer V. Degrave A. Woehl R. Lux A. Steffan T. Charbonnier X. et al. Thisse, B. Expression of the zebrafish genome during embryogenesis., 2001.

[197] M. C. Tiveron, A. Pattyn, M. R. Hirsch, and J. F. Brunet. Role of Phox2b and Mash1 in the generation of the vestibular efferent nucleus. *Developmental Biology*, 260(1):46–57, 8 2003.

[198] Marie Catherine Tiveron and Harold Cremer. CXCL12/CXCR4 signalling in neuronal cell migration, 6 2008.

[199] Thai V. Truong, Willy Supatto, David S. Koos, John M. Choi, and Scott E. Fraser. Deep and fast live imaging with two-photon scanned light-sheet microscopy. *Nature Methods*, 8(9):757–762, 9 2011.

[200] Yuji Tsunekawa, Joanne M Britto, Masanori Takahashi, Franck Polleux, Seong-Seng Tan, and Noriko Osumi. Cyclin D2 in the basal process of neural progenitors is linked to non-equivalent cell fates. *The EMBO Journal*, 31(8):1879–1892, 4 2012.

[201] Osamu Uemura, Yohei Okada, Hideki Ando, Mickael Guedj, Shin Ichi Higashijima, Takuya Shimazaki, Naoichi Chino, Hideyuki Okano, and Hitoshi Okamoto. Comparative functional genomics revealed conservation and diversification of three enhancers of the isl1 gene for motor and sensory neuron-specific expression. *Developmental Biology*, 278(2):587–606, 2 2005.

[202] Mohammad Yahya Vahidi Mehrjardi, Reza Maroofian, Seyed M. Kalantar, Mojtaba Jaafarinia, John Chilton, and Mohammadreza Dehghani. A Novel Loss-of-Function Mutation in HOXB1 Associated with Autosomal Recessive Hereditary Congenital Facial Palsy in a Large Iranian Family. *Molecular Syndromology*, 8(5):261–265, 2017.

[203] Gary Vanderlaan, Oksana V. Tyurina, Rolf O. Karlstrom, and Anand Chandrasekhar. Gli function is essential for motor neuron induction in zebrafish. *Developmental Biology*, 282(2):550–570, 6 2005.

[204] N. Vlachakis, S. K. Choe, and C. G. Sagerström. Meis3 synergizes with Pbx4 and Hoxb1b in promoting hindbrain fates in the zebrafish. *Development*, 2001.

[205] Markus Vogel, Eunike Velleuer, Leon F. Schmidt-Jiménez, Ertan Mayatepek, Arndt Borkhardt, Malik Alawi, Kerstin Kutsche, and Fanny Kortüm. Homozygous HOXB1 loss-of-function mutation in a large family with hereditary congenital facial paresis. *American Journal of Medical Genetics, Part A*, 170(7):1813–1819, 2016.

[206] Adri Voltes, Covadonga F. Hevia, Carolyn Engel-Pizcueta, Chaitanya Dingare, Simone Calzolari, Javier Terriente, Caren Norden, Virginie Lecaudey, and Cristina Pujades. Yap/Taz-TEAD activity links mechanical cues to progenitor cell behavior during zebrafish hindbrain segmentation. *Development (Cambridge, England)*, 146(14), 7 2019.

[207] Gregory S. Walsh, Paul K. Grant, John A. Morgan, and Cecilia B. Moens. Planar polarity pathway and Nance-Horan syndrome-like 1b have essential cell-autonomous functions in neuronal migration. *Development*, 138(14):3033–3042, 7 2011.

[208] S. J. Wanner and V. E. Prince. Axon tracts guide zebrafish facial branchiomotor neuron migration through the hindbrain. *Development*, 140(4):906–915, 2013.

[209] Sarah J. Wanner, Ivan Saeger, Sarah Guthrie, and Victoria E. Prince. Facial motor neuron migration advances. *Current Opinion in Neurobiology*, 23(6):943–950, 2013.

[210] Mark E. Warchol. Sensory regeneration in the vertebrate inner ear: Differences at the levels of cells and species. *Hearing Research*, 273(1-2):72–79, 3 2011.

[211] James T. Warren, Anand Chandrasekhar, John P. Kanki, Radha Rangarajan, Andrew J. Furley, and John Y. Kuwada. Molecular cloning and developmental expression of a zebrafish axonal glycoprotein similar to TAG-1. *Mechanisms of Development*, 80(2):197–201, 2 1999.

[212] A. J. Waskiewicz, H. A. Rikhof, R. E. Hernandez, and C. B. Moens. Zebrafish Meis functions to stabilize Pbx proteins and regulate hindbrain patterning. *Development*, 2001.

[213] Andrew Jan Waskiewicz, Holly A. Rikhof, and Cecilia B. Moens. Eliminating zebrafish Pbx proteins reveals a hindbrain ground state. *Developmental Cell*, 3(5):723–733, 11 2002.

[214] Michel A. Wassef, Diane Chomette, Marie Pouilhe, Aline Stedman, Emmanuelle Havis, Carole Desmarquet Trin Dinh, Sylvie Schneider-Maunoury, Pascale Gilardi-Hebenstreit, Patrick Charnay, and Julien Ghislain. Rostral hindbrain patterning involves the direct activation of a Krox20 transcriptional enhancer by Hox/Pbx and Meis factors. *Development*, 135(20):3369–3378, 2008.

[215] Natsuko Watari, Yoko Kameda, Masatoshi Takeichi, and Osamu Chisaka. Hoxa3 regulates integration of glossopharyngeal nerve precursor cells. *Developmental Biology*, 240(1):15–31, 12 2001.

[216] Natsuko Watari-Goshima and Osamu Chisaka. Chicken HOXA3 gene: Its expression pattern and role in branchial nerve precursor cell Migration. *International Journal of Biological Sciences*, 7(1):87–101, 2011.

[217] Richard J. White, Qing Nie, Arthur D. Lander, and Thomas F. Schilling. Complex regulation of cyp26a1 creates a robust retinoic acid gradient in the zebrafish embryo. *PLoS Biology*, 5(11):2522–2533, 11 2007.

[218] Hynek Wichterle, Jose Manuel García-Verdugo, and Arturo Alvarez-Buylla. Direct evidence for homotypic, glia-independent neuronal migration. *Neuron*, 18(5):779–791, 5 1997.

[219] Elaine Y.M. Wong, Xing An Wang, Siu Shan Mak, Jearn Jang Sae-Pang, Kam Wing Ling, Bernd Fritzsch, and Mai Har Sham. Hoxb3 negatively regulates Hoxb1 expression in mouse hindbrain patterning. *Developmental Biology*, 352(2):382–392, 2011.

[220] Yicong Wu, Abhishek Kumar, Corey Smith, Evan Ardiel, Panagiotis Chandris, Ryan Christensen, Ivan Rey-Suarez, Min Guo, Harshad D. Vishwasrao, Jiji Chen, Jianyong Tang, Arpita Upadhyaya, Patrick J. La Riviere, and Hari Shroff. Reflective imaging improves spatiotemporal resolution and collection efficiency in light sheet microscopy. *Nature Communications*, 8(1):1–12, 12 2017.

[221] Tian Yang, Alexander G. Bassuk, Sigmar Stricker, and Bernd Fritzsch. Prickle1 is necessary for the caudal migration of murine facial branchiomotor neurons. *Cell and Tissue Research*, 357(3):549–561, 6 2014.

[222] Xiaojun Yang, Jian Zou, David R. Hyde, Lance A. Davidson, and Xiangyun Wei. Stepwise maturation of apicobasal polarity of the neuroepithelium is essential for vertebrate neurulation. *Journal of Neuroscience*, 29(37):11426–11440, 9 2009.

[223] Sana Zakaria, Yaopan Mao, Anna Kuta, Catia Ferreira De Sousa, Gary O. Gaufo, Helen McNeill, Robert Hindges, Sarah Guthrie, Kenneth D. Irvine, and Philippa H. Francis-West. Regulation of neuronal migration by Dchs1-Fat4 planar cell polarity. *Current Biology*, 24(14):1620–1627, 2014.

[224] Denise A. Zannino and Bruce Appel. Olig2 + precursors produce abducens motor neurons and oligodendrocytes in the zebrafish hindbrain. *Journal of Neuroscience*, 29(8):2322–2333, 2 2009.

[225] Gengsheng L. Zeng and Grant T. Gullberg. Unmatched projector/backprojector pairs in an iterative reconstruction algorithm. *IEEE Transactions on Medical Imaging*, 19(5):548–555, 5 2000.

[226] Christoph Ziegenhain, Beate Vieth, Swati Parekh, Bjrn Reinius, Amy Guillaumet-Adkins, Martha Smets, Heinrich Leonhardt, Holger Heyn, Ines Hellmann, and Wolfgang Enard. Comparative Analysis of Single-Cell RNA Sequencing Methods. *Molecular Cell*, 65(4):631–643, 2 2017.